

Copyright
by
Runhua Chen
2007

The Dissertation Committee for Runhua Chen
certifies that this is the approved version of the following dissertation:

**Multiuser MIMO Systems in Single-cell and Multi-Cell Wireless
Communication**

Committee:

Jeffrey G. Andrews, Supervisor

Robert W. Heath, Jr., Supervisor

Edward J. Powers

Sriram Vishwanath

Sanjay Shakkottai

Arunabha Ghosh

**Multiuser MIMO Systems in Single-cell and Multi-Cell Wireless
Communication**

by

Runhua Chen, B.S.; M.Phil.

DISSERTATION

Presented to the Faculty of the Graduate School of
The University of Texas at Austin
in Partial Fulfillment
of the Requirements
for the Degree of

DOCTOR OF PHILOSOPHY

THE UNIVERSITY OF TEXAS AT AUSTIN

May 2007

Dedicated to my family.

Acknowledgments

I would like to express my sincere gratitude to my supervisors Prof. Jeffrey G. Andrews and Prof. Robert W. Heath, Jr., for their invaluable guidance. Their knowledge, creativity, never-ending energy and encouragement have been fundamental to my technical growth during my research at UT.

I am also greatly thankful to my family for their years of support. They are the most valuable treasure in my life.

My gratitude also goes to to my colleagues and friends from WNCG, for the fruitful discussion and collaboration during my Ph.D. study.

Multiuser MIMO Systems in Single-cell and Multi-Cell Wireless Communication

Publication No. _____

Runhua Chen, Ph.D.

The University of Texas at Austin, 2007

Supervisors: Jeffrey G. Andrews
Robert W. Heath, Jr.

MIMO technology improves the capacity and link robustness of wireless communication by deploying multiple transmit and receive antennas. A multiuser MIMO communication system involves multiple mobile stations (MS) and potentially multiple base transceiver stations (BTS). These systems are fundamentally limited by interference, and require new treatment of both the capacity characteristics and physical layer algorithm design. In this dissertation, multiuser MIMO systems in both single-cell and multi-cell environments are studied. A single-cell MIMO broadcast channel is defined by a central BTS transmitting to multiple MSs simultaneously over the same spectrum. A multi-cell MIMO system consists of multiple BTSs transmitting to MSs in different cells.

For a single-cell MIMO broadcast channel, block diagonalization is a transmit precoding technique that multiplexes multiple users in the spatial domain and pre-cancels inter-user interference. Precoder can be adaptively designed based on the size of transmit/receive antenna arrays and the number of users. In the case where the BTS has more antennas or radio frequency (RF) units than strictly required for interference cancellation, this dissertation proposes novel downlink precoder with enhanced transmit selection diversity. Eigenmode selection and transmit antenna selection are derived to optimize a symbol

error rate upper bound and improve the diversity performance. When there are a large number of users in the system, a subset of users and receive antennas may be selected to maximize the sum capacity under the block diagonalization signaling. The optimum joint user and antenna selection involves brute-force search, therefore is prohibitively complicated. In this dissertation, two low-complexity sub-optimal selection algorithms are proposed to significantly reduce the selection complexity.

Conventional single-user MIMO techniques suffer significant performance loss in an interference-limited multi-cell network. Interference on a MIMO system is more severe than in a single-antenna cellular network, as each antenna element acts as a unique interferer. In this dissertation, power control is investigated as an interference management tool to properly determine the transmit power of MIMO array under a pre-determined SNR constraint. Two uplink MIMO power control techniques are proposed. The first equal allocation algorithm enforces each antenna element of a MIMO array to transmit at the same power, resulting in a closed-form but suboptimal solution. The second algorithm adaptively distributes power on a MIMO antenna array to exploit the channel selectivity, hence substantially reduces the transmit power and interference, and creates far better cell coverage.

Finally, block diagonalization precoding in the single-cell scenario is generalized to the multi-cell environment as a coordinated MIMO transmission technique. Multiple BTSs cooperate with each other to design the downlink signal, thereby eliminating interference and improving the spectral efficiency. An improved precoding scheme is proposed to address the per base station power constraint in the cellular environment. Future research topics for cellular block diagonalization precoding are discussed.

Table of Contents

Acknowledgments	v
Abstract	vi
List of Tables	xii
List of Figures	xiii
Chapter 1. Introduction	1
1.1 Overview of MIMO Communication Systems	1
1.2 Multiuser MIMO Communication	2
1.2.1 Single-Cell MIMO Systems	2
1.2.2 Multi-Cell MIMO Systems	5
1.3 Summary of Contributions	7
1.4 Organization of Dissertation	10
Chapter 2. Transmit Selection Diversity for Multiuser MIMO	11
2.1 Introduction	12
2.1.1 Overview of Multiuser MIMO Broadcast Systems	12
2.1.2 Overview of MU-MIMO Precoding with Single-Antenna per MS . . .	13
2.1.3 Overview of MU-MIMO Precoding with Multi-Antenna per MS . . .	14
2.1.4 Contributions of the Proposed Work	15
2.2 Preliminaries and System Model	16
2.2.1 Notation	17
2.2.2 Channel Model	17
2.2.3 Signal Model	18
2.3 Transmit Precoding for Interference Cancellation	20
2.3.1 BD for Interference Cancellation	20
2.3.2 Multiuser Downlink Precoder	21
2.3.3 Complexity Analysis	22
2.4 Transmit Precoding with Eigenmode Selection	23
2.4.1 Problem Formulation	23
2.4.2 Eigenmode Selection	25

2.4.3	SER Performance Analysis	27
2.4.4	Sum Rate Capacity Analysis	28
2.4.5	Numerical Results	29
2.5	Transmit Antenna Selection	30
2.5.1	Single-user Antenna Selection	31
2.5.2	Proposed Multiuser Antenna Selection	31
2.5.2.1	Brute-Force Search	32
2.5.2.2	Low-Complexity Antenna Selection	35
2.5.3	Numerical Results	37
2.6	Antenna Selection vs. Eigenmode Selection	40
2.7	Performance in Correlated and Imperfect CSI Condition	41
2.7.1	i.i.d. Gaussian Channel with Imperfect Channel Knowledge	42
2.7.2	Correlated MIMO Channel with Perfect Channel Knowledge	43
2.8	Conclusions	46

Chapter 3. Joint User and Receive Antenna Selection for MIMO Broadcast Transmission **48**

3.1	Introduction	49
3.1.1	Background on Multi-mode Transmission	49
3.1.2	Background on Multiuser Scheduling	49
3.1.3	Joint User and Receive Antenna Selection	50
3.2	System and Signal Model	51
3.3	User, Mode and Antenna Selection with BD	53
3.3.1	User and Mode Selection for BD	53
3.3.2	User and Antenna Selection with BD	54
3.4	Low-Complexity Joint User/Antenna Selection Algorithms	56
3.4.1	Effective Energy Based User/Antenna Selection Algorithm	56
3.4.2	Throughput-based User/Antenna Selection Algorithm	59
3.4.3	Numerical Results	60
3.4.4	Effects of Channel Correlations	64
3.5	Computational Complexity Analysis	64
3.5.1	Complexity of Exhaustive User/Antenna Selection	64
3.5.2	Complexity of Throughput-based Low-Complexity Algorithm	65
3.5.3	Complexity of Energy-based Low-Complexity Algorithm	66
3.6	Conclusions	68

Chapter 4. Uplink Power Control in Multi-Cell MIMO Networks	69
4.1 Introduction	69
4.1.1 Single-Antenna Power Control	70
4.1.2 Multi-Antenna Power Control	71
4.2 System Model	72
4.2.1 Signal Model	72
4.2.2 Multiple Mobiles per Cell	74
4.3 Overview of Power Control	75
4.3.1 SISO Power Control with Fixed SINR Target	75
4.3.2 Power Control with Fixed Capacity Target	76
4.3.3 Power Control for Utility Maximization	76
4.4 MIMO Power Control with Equal Power Allocation and Full-CSI	77
4.4.1 Signal Model	77
4.4.2 Problem Formulation	78
4.4.3 Optimal Solution	80
4.4.4 Standard Power Control Algorithm	81
4.4.5 Low Complexity Iterative Power Control	82
4.5 MIMO Power Control with Equal Power Allocation and Self-CSI	83
4.5.1 Problem Formulation	83
4.5.2 Standard Power Control Algorithm	84
4.5.3 Discussion on Synchronization	85
4.5.4 Numerical Results	85
4.6 MIMO Power Control with Adaptive Power Allocation	86
4.6.1 Signal Model	87
4.6.2 Iterative Algorithm for Adaptive Power Allocation	88
4.6.3 Convergence of Adaptive Power Allocation	90
4.7 Numerical Results	93
4.7.1 Adaptive vs Equal Allocation Power Control	93
4.7.2 Cell Coverage Evaluation	95
4.7.3 Power Control vs Iterative Waterfilling	96
4.8 Conclusions	98

Chapter 5. Coordinated Multi-cell MIMO with Cellular Block Diagonalization (CBD)	99
5.1 Background of Coordinated Multi-cell MIMO	99
5.2 Multi-Cell BD	100
5.2.1 Problem Formulation	100
5.2.2 Signal Model	101
5.3 Precoder Design for Multi-cell BD	103
5.4 Future Work with Multi-Cell BD	105
5.4.1 Joint and Disjoint Processing at Transmitter	106
5.4.2 Multiuser Scheduling	107
5.4.3 Multi-mode Switching	108
5.5 Conclusions	109
Chapter 6. Conclusions	110
Appendix	113
Bibliography	115
Vita	125

List of Tables

2.1	Summary of notations	28
-----	--------------------------------	----

List of Figures

2.1	Block diagram of the MUSM system with precoding: perfect feedback is assumed with $\{\mathbf{H}_k\}_{k=1}^K$ exactly known at the transmitter for precoder design.	18
2.2	CCDF of the NMSE with ZF receiver	25
2.3	SER comparison of single user and multiuser spatial multiplexing system with 3 antennas, 2 substreams per user, using ZF and V-BLAST receivers. .	30
2.4	SER performance of antenna selection with 2 users, 2 receive antennas and 2 data substreams per user, using ZF receiver.	34
2.5	SER performance of exhaustive and low-complexity antenna selection with 2 users, 2 receive antennas and 2 data substreams per user, using 4QAM modulation and MMSE receiver per MS.	38
2.6	SER performance of exhaustive and low-complexity antenna selection with 2 users, 4 receive antennas and 4 data substreams per user, using 4QAM modulation and MMSE receiver per MS	39
2.7	Sum rate capacity of exhaustive and low-complexity antenna selection with 2 users, 2 receive antennas per user.	39
2.8	Sum rate capacity of exhaustive and low-complexity antenna selection with 2 users, 4 receive antennas per user.	40
2.9	SER comparison of antenna selection and eigenmode selection with 2 users, 3 receive antennas and 2 data substreams per user, using ZF receiver. . . .	41
2.10	SER comparison with channel estimation error for two-user system with 3 receive antennas, 2 substreams per user.	42
2.11	SER of antenna selection with channel estimation error for two-user system with 2 receive antennas, 2 substreams per user.	43
2.12	Performance of eigenmode selection in correlated channel for two-user system with 3 receive antennas, 2 substreams per user, 1 extra BTS antenna. . . .	45
2.13	Performance of antenna selection in correlated channel for two-user system with 2 receive antennas, 2 substreams per user, 1 extra BTS antenna for selection.	46
3.1	Block diagram of the proposed low-complexity user/antenna selection algorithm, with $\{k : \mathcal{S}_k\}$ denotes user k and its selected antenna set \mathcal{S}_k . For example, in stage 1, antenna 1 of user 1 is selected. In stage 2, antenna 2 of user 3 is selected.	57
3.2	Sum throughput for $N_t = 12$, $N_r = 4$, and different number of users \tilde{K} . . .	63
3.3	Sum throughput for $N_t = 10$, $N_r = 2$, and different number of users \tilde{K} . . .	63
3.4	Upper bound of the complexity ratio of the proposed low-complexity method and the brute-force search.	68

4.1	Histogram of the normalized approximation error x	79
4.2	Convergence of the 1-bit power control algorithm with equal power allocation and different step size δ : $K = 7$, $\sigma_n^2 = 0.01$, $N_t = 4$, $N_r = 6$, $\Gamma = 6$ dB.	86
4.3	Convergence of the iterative algorithm given that the channel provides a feasible solution: $\Gamma = 6$ dB, $\sigma_n^2 = 0.01$	93
4.4	Probability of infeasibility with equal power allocation and adaptive power allocation: $K = 19$, $\sigma_n^2 = 0.01$	94
4.5	Average ratio of sum transmit power between adaptive power allocation and equal power allocation power control: $\sigma_n^2 = 0.01$	94
4.6	Cell coverage comparison of equal and adaptive PC with $K = 19$, $N_t = 4$, $N_r = 6$, $\sigma_n^2 = 0.01$	95
4.7	Throughput and outage probability comparison of proposed power control and the iterative waterfilling algorithm: $K = 7$, $\sigma_n^2 = 0.01$	97
5.1	Example of the clustered cellular network: cluster size $B = 7$	101

Chapter 1

Introduction

1.1 Overview of MIMO Communication Systems

Wireless communication have rapidly developed in the past few decades. Compared to wireline communication, wireless communication provides the advantage of mobility and is easier to deploy at a lower cost. The interest in future broadband wireless communication has created an increased demand for ubiquitous high quality and high speed wireless access. Data rates provided by current wireless systems, however, are still far below what wireline competitors can offer. This gap can be attributed to limited spectrum, low transmit power, and signal fluctuation in hostile wireless environments. As a result, novel techniques for increasing data rates and link reliability are highly desirable.

Multiple-input multiple-output (MIMO) techniques can provide significant capacity and link reliability improvement for wireless communication. A MIMO system is created by deploying multiple antennas at both the transmitter and receiver ends of a communication link. Because these antennas are physically separated, the deployment of MIMO creates additional degrees of freedom in the spatial domain which are unavailable in single antenna system. With intelligently designed transceiver and signal processing algorithms, the spatial degrees of freedom due to MIMO can be exploited to significantly improve the spectral efficiency, suppress interference, and combat channel fading of wireless communication. The benefits of MIMO are characterized by multiplexing and diversity gains. MIMO spatial multiplexing systems transmit multiple data streams simultaneously over the same spectrum [33], thereby increasing the achievable data rates. MIMO diversity techniques improve signal quality and link reliability by sending multiple encoded versions of a single data

stream across different antennas and time slots, achieving diversity gain [4, 91, 92]. The fundamental diversity and multiplexing tradeoff (DMT) has been investigated in [70, 109], while practical signaling algorithms are proposed to adaptively switch between multiplexing and diversity modes [32, 56, 68, 70].

Due to its capability to improve wireless system performance without additional bandwidth and power, MIMO technology has been playing a critical role and is expected to become mandatory in many wireless standards, including 802.11n for local area networks (WLAN), 802.16e/WiMAX fixed broadband wireless system (WLAN), and 3GPP long term evolution (LTE) for cellular networks. In our joint research with AT&T Laboratories on 802.16e/WiMAX wireless metropolitan area networks (WMAN), it is found that MIMO techniques can achieve a spectral efficiency of 4-5 bps/Hz with two transmit antennas, two to three times higher than the achievable rate of a single antenna system [35].

1.2 Multiuser MIMO Communication

MIMO techniques have been well understood in a point-to-point, single-user link. An increasing amount of interest in multiuser MIMO communication has been observed in recent years. A multi-user MIMO system involves multiple mobile terminals and potentially multiple centralized controllers. In this dissertation, a multiuser system with a single centralized controller is referred to as a single-cell system (e.g. a WLAN with a single access point), and a network with multiple centralized controllers is defined as a multi-cell system (e.g. a cellular network with multiple base stations).

1.2.1 Single-Cell MIMO Systems

For a single-cell multiuser system, two typical scenarios are the downlink broadcast (BC) channel and the uplink multi-access channel (MAC). The uplink MAC channel has been extensively investigated by previous researchers and well understood.

In a downlink BC system, one centralized BTS transmits to multiple mobile users over the same spectrum. As multiple users are simultaneously supported, MIMO-BC systems greatly increase the sum capacity over that of conventional TDMA systems [50, 83]. It is generally assumed that receiver processing is distributed, i.e., MSs do not cooperate with each other to decode the received signals. On the other hand, channel station information is typically assumed available at the BTS, through feedback or channel reciprocity. Dirty paper coding (DPC) is the capacity optimal approach for MIMO BC systems [12, 28, 94, 95, 97, 104]; however, it is not practical due to the complicated non-causal successive encoding. A more practical MIMO-BC transmission technique is multiuser precoding, which is a transmitter-based process that multiplexes users in the spatial domain. Various precoding schemes have been proposed in the literature, for example, the *zero-forcing precoding* [12, 102] (also named as channel inversion), *regularized channel inversion* [45, 66], *block diagonalization* [22, 89, 98]. The common purpose of these techniques is to use the BTS antenna array to orthogonalize the downlink signals of different users, and eliminate inter-user interference at the BTS side. Hence, MS can apply low complexity single-user MIMO receiver.

Among various existing multiuser precoding techniques, block diagonalization (BD) is a more general scheme that accommodates multiple receive antennas at each mobile terminal. The BD precoder is a function of the downlink channel, the number of BTS and MS antennas, as well as the number of users in the system. As these parameters vary, BD precoder needs to be adaptively designed to optimize the system performance. One premise of this dissertation is to investigate the precoder design and user scheduling based on the antenna and user configurations.

A necessary condition for BD is that the number of transmit antennas is larger than the total number of receive antennas. If there is a large BTS array and a small group of users, the BTS has more antennas than the minimum required for interference cancellation. These

excess transmit resources need to be efficiently exploited to optimize the system performance according to a certain performance metric. Conventional BD precoding techniques aim at capacity maximization [89] or mean square error minimization [98]. The diversity gain which is critical to ensure the link level performance, however, is not adequately studied. This dissertation will derive novel linear precoder design for optimizing the diversity gain of a MIMO BC system, when extra antennas or radio frequency (RF) units are available at the BTS. In contrast to the capacity optimization in the previous work, this dissertation addresses precoder design from the link-level error rate optimization perspective with a fixed number of substreams, since it is an important factor in a practical system besides Shannon capacity.

When there is a small BTS antenna array and a large number of users, the total number of receive antennas exceeds the number of transmit antennas. As a result, the BTS cannot support all users simultaneously, and a subset of users may be selected to meet the antenna constraint. Multiuser scheduling has been shown to improve the capacity significantly by exploiting the channel selectivity. This capacity improvement is usually referred to as multiuser diversity. This dissertation will propose novel BD design solutions and multiuser scheduling algorithm in the presence of many mobile users.

MIMO is capable of transmitting multiple data streams in the spatial domain. The number of data streams can be dynamically adjusted by *multi-mode switching* to suit the channel realization. switching between single-stream diversity mode and multi-stream multiplexing mode. Multi-mode switching has been carefully investigated for single-user MIMO systems, and demonstrates significantly performance gain thanks to multi-mode switching gain [32, 56, 68, 70]. For a multiuser MIMO-BC channel, the optimal multi-mode switching involves an exhaustive search over all possible mode and user combinations. This exhaustive search, however, possesses a very high complexity and is impractical. A sub-optimal multi-mode switching technique is proposed in [85], where a subset of receive antennas are

chosen for each selected user. This scheme, unfortunately, still requires an exhaustive search over all user/antenna subsets and is prohibitively complicated. To reduce the complexity, this dissertation proposes two low-complexity joint user/antenna selection algorithms as a suboptimal multi-mode switching solution. Both algorithms aim to find the optimal user and antenna subset with the highest sum capacity with BD signaling, while avoiding the prohibitive complexity associated with exhaustive search.

1.2.2 Multi-Cell MIMO Systems

A multipoint-to-multipoint network consists of multiple transmitters and mobile receivers, e.g. a cellular network. The conventional single-user MIMO techniques suffer serious performance loss in multi-cell environment, because a cellular network is fundamentally limited by co-channel interference (CCI) and typically operates in a low SNR range (i.e. below 10 dB [5, 93]). Although the problem of CCI has existed in cellular systems for many years, its effect on MIMO systems is far more severe because each MIMO array element acts as a unique interfering source. Interference has to be properly dealt with to ensure the success of MIMO in cellular networks.

The capacity of a cellular system is achieved by coordinating multiple base stations to perform joint processing. Capacity results with Monte Carlo simulation are provided in [13]. A model by Wyner [99] is adopted by some researchers to allow for a tractable analysis of the cellular system capacity. The Wyner model is highly simplified where cells are ordered in either an infinite linear or circular array fashion, such that each cell receives interference only from (one or two) adjacent cells. For the uplink MAC channel, capacity under the Wyner model is investigated in [41, 80, 81, 86, 88]. For the downlink channel, capacity under the Wyner model is studied in [82] with a *sum power constraint* over all BTSs, and more generally in [88] with *per base station power constraint*. For more general cellular system without the Wyner model, transmit optimization to maximize the downlink

sum rate is studied by Jafar et al. in [49] with *per base station power constraint*. A capacity bound is derived in [23] by applying DPC across multiple base stations.

In a practical cellular system, interference needs to be properly cancelled to ensure successful decoding. It is more desirable to perform interference mitigation at the base stations which are less power and computationally limited. The general idea is to coordinate multiple BTSs as a “super transmitter”, and design the downlink signal with block diagonalization as in the single-cell environment. Hence, the multiuser channel is decomposed into parallel single-user channels, thus interference is pre-cancelled. The per base station power constraint is solved by using linear scaling in [108] and by using convex optimization in [52]. Advanced mobile receiver design has been proposed to mitigate interference by Dai et al. [29, 30] but these techniques require highly complicated receiver impractical for a commercial system.

The aforementioned works assume that users’ data and channel state information are fully exchanged among base stations. This assumption, however, is quite difficult to implement. It is easier to exchange channel information via a high speed backbone network, especially in a low-mobility environment. Information data to users, however, changes much more rapidly and is much more difficult to share across cells, particularly for real-time wireless services. This dissertation will propose to use power control as an interference management tool for the uplink MIMO cellular systems. This technique only requires channel to be shared across different cells, while the data to users are not required to be shared.

In a power controlled cellular network, transmit power of different users are adjusted based on instantaneous channel realization. The objective is to satisfy a given QoS specification while reducing transmit power, mitigating interference and increasing cell coverage. Various solutions can be found in literature for the single-input single-output (SISO) systems, in the single-carrier [1, 101] and multi-carrier systems [58, 105]. Cellular MIMO

power control, however, is more complicated because it is necessary to determine not only the sum power, but also the power on each antenna element. More importantly, the effective interference is strongly dependent on the MIMO receiver and usually non-linear of the interfering antenna's power. In this dissertation, it is shown that multi-dimensional MIMO power control is different from single antenna power control due to the MIMO receiver, thereby requiring novel treatment to fit the multi-antenna environment. This dissertation will propose two power control solutions for the cellular MIMO system, where a transmitter's power is equally or adaptively distributed to its antenna array. Different scenarios are investigated where channel information is fully shared across all cells (e.g., full-CSI), or only within the same cell (e.g., self-CSI).

1.3 Summary of Contributions

Multiuser MIMO communication in the downlink broadcast and cellular environments are studied. The premises of this dissertation are novel physical layer MIMO transmission techniques in broadcast and multi-cell environments as a means to improve the spectral efficiency and signal quality of future wireless networks. The main contributions presented in this dissertation are listed as follows:

- **Transmit precoder design for multiuser MIMO-BC channel**

Transmit precoding is investigated to improve the diversity performance of the single-cell MIMO broadcast systems [17, 18]. Advanced transmit selection diversity techniques are proposed to use extra transmit antennas, beyond the minimum required for interference cancellation, to improve the diversity gain. Two scenarios are investigated. In the first case, there are an equal number of radio frequency (RF) units and transmit antennas, both of which exceed the minimum for interference cancellation. First, a two-step unitary precoding design in the Stiefel manifold is proposed to exploit *eigenmode selection diversity*, which includes both interference cancellation and

symbol error performance enhancement. The first step is to identify a group of unitary downlink precoding to perfectly cancel inter-user interference with QR decomposition, while the second step involves the minimization of a symbol error rate (SER) upper bound. For the second case, a limited number of RF units are available and the BTS transmits over a subset of the available antennas. Transmit antenna selection is proposed to identify the optimum set of antennas to maximize the sum throughput, or to minimize a SER upper bound. Because exhaustive antenna selection has a very high complexity, two efficient algorithms are proposed with substantially lower complexity than the brute-force search. The proposed techniques can lead to significant diversity gain and error performance improvements.

- **Joint user and antenna selection for multiuser broadcast channel**

The number of data streams in a MIMO system can be dynamically adjusted by multi-mode switching to suit the wireless channel. In this dissertation, joint user and antenna selection is investigated as a multi-user multi-mode switching technique [19, 20]. The objective is to select a subset of users and receive antennas to maximize the sum throughput, using instantaneous channel information. To avoid the computational complexity of the exhaustive search, two low-complexity user/antenna selection algorithms are proposed. The first algorithm aims to maximize the effective channel energy, derived as a lower bound of the sum throughput, while the second algorithm directly maximizes the sum throughput. Following a greedy search method, the proposed algorithms activate one receive antenna at a time, associated with the best user, until no more active receive antenna can be added to the system. The complexity of the proposed algorithms is significantly lower than that of the optimal brute-force search, while simulation results demonstrate that most of the throughput gain is achieved with the proposed low-complexity solutions.

- **Power control for uplink cellular MIMO spatial multiplexing systems**

Power control is proposed as an interference management tool for the uplink of cellular MIMO systems, to minimize the transmit power and mutual interference [15, 16]. It is shown that that power control for MIMO cellular system is fundamentally different from the single-antenna power control counterpart. Two power control techniques are then proposed. In the first method, a user's power is equally distributed on its transmit antennas. A lower bound on the post-processing SINR with a linear MMSE receiver is derived, expressed in terms of an eigenvalue approximation of both the desired and interfering users' channel. Using this bound, the MIMO power control problem is formulated in a similar framework in the SISO scenario, to derive closed-form optimal (in terms of the SINR bound) and low-complexity sub-optimal solutions. To reduce the infeasibility probability, a second algorithm is proposed that adaptively distributes the transmit power on the transmit antennas, which effectively exploits the variation of antenna array response and substantially outperforms the equal allocation approach in terms of the infeasibility probability, sum power and cell coverage.

- **Ongoing and future work on cooperative MIMO cellular system with multi-cell block-diagonalization.**

In a coordinated MIMO cellular network, multiple BTSs cooperate with each other in the downlink transmission. By sharing information across BTSs and designing the downlink signal coordinately, signals from other cells may be used to assist the transmission of the desired cell instead of acting as interference. This dissertation will investigate block diagonalization precoding in the cellular channel as a cooperative MIMO transmission scheme. The idea in the context of coordinated MIMO is to apply the concept of BD across multiple cells. An improved BD precoding scheme is proposed to address the per base station power constraint in the multi-cell environment. Future topics on cooperative base station transmission for MIMO cellular systems are discussed under the cellular BD model, such as precoder design with

different level of information sharing across base stations, user scheduling schemes.

The proposed multiuser MIMO algorithms can be applied in future broadband wireless communication systems that are currently in the standardization process, such as IEEE 802.16/WiMAX [35] and 3GPP LTE.

1.4 Organization of Dissertation

In Chapter 2, transmit selection diversity with eigenmode selection and antenna selection are proposed. Various efficient transmit antenna selection algorithms with reduced complexity are proposed and analyzed. In Chapter 3, joint user and receive antenna selection for MIMO broadcast channel is investigated. Low-complexity algorithms based on channel energy and based on throughput are proposed. In Chapter 4, power control for the uplink cellular MIMO systems is studied. Solutions with adaptive or equal power allocation, with full or partial channel information are studied. In Chapter 5, cooperative MIMO cellular system based on multi-cell BD is proposed, with novel precoder design in the multi-cell infrastructure. Finally the dissertation is concluded in Chapter 6.

Chapter 2

Transmit Selection Diversity for Multiuser MIMO

In the downlink of a multiuser spatial multiplexing system, a base transceiver station (BTS) transmits to multiple MSs at the same time over the same frequency band. Data to multiple MSs are transmitted simultaneously in the same spectrum, therefore inter-user interference is the major performance impairment that needs to be properly dealt with. It is typically assumed that receiver processing is distributed, i.e., MSs do not cooperate with each other in processing the received signals.

The non-linear DPC required to achieve the sum capacity of MIMO broadcast channel is very difficult to implement in practice. Linear transmit precoding is a practical technique for combating inter-user interference in a downlink MU-MIMO system. In general, the objective is to find channel-dependent transmit precoders to suppress inter-user interference while maximizing the system performance (e.g., capacity, mean square error). Block diagonalization (BD) has been proposed as an effective precoding scheme, which decomposes the multiuser MIMO channel into parallel non-interfering single-user MIMO channels, therefore interference is perfectly eliminated at the BTS side. By doing this, simple single-user MIMO receiver can be applied at the mobile terminal ends, resulting in a compact, lower-power mobile design. Most existing BD design focus on the capacity maximization, mean square error minimization. The diversity gain which is critical for the link-level error performance, was not adequately addressed. In this chapter, transmit precoding with enhanced selection diversity is proposed to improve the link robustness of MU-MIMO systems. Particularly, the scenario where the BTS has more transmit resources (e.g., antennas, RF units) than strictly required for interference cancellation will be studied. Novel precoding design will

be proposed in this chapter to efficiently utilize the excess transmit resources to improve the diversity gain of the MU-MIMO system.

2.1 Introduction

In this section, downlink multiuser MIMO broadcast system is first introduced. An overview of various existing precoding techniques is presented. Transmit selection diversity will then be motivated as a diversity improvement approach to enhance the communication robustness, which will be addressed in this chapter.

2.1.1 Overview of Multiuser MIMO Broadcast Systems

Downlink MU-MIMO broadcast communication [3, 7, 12, 22, 64, 94, 96, 98, 102] involves a single BTS transmitting to multiple MSs at the same time over the same frequency band, where multiple antennas are applied at both the transmitter and receiver ends. Because multiple mobiles are served at the same time by spatial division multiplexing (SDMA), MU-MIMO system can significantly improve the channel capacity than conventional TDMA-based system [50, 83], and can potentially reduce the latency for each mobile.

A MIMO broadcast system with single-antenna BTS and single-antenna MS has been well understood in the literature. The channel is degraded in nature where the capacity optimum strategy is to transmit to a single user with the highest channel gain, at any time instant. For a MU-MIMO system with multiple BTS antennas and multiple antennas per MS, however, the transmission strategy to achieve the maximum sum capacity has been remaining an unsolved problem for a long time, because the channel is non-degraded. In recent years, lots of ground-breaking results have been found in terms of both its theoretical capacity characteristics, the capacity achieving strategy as well as various practical signaling schemes. Pioneering work on MIMO-BC capacity included [12, 103] which investigated the

special case of a single receive antenna per user, and [94, 96, 104] where multiple antennas are employed at each mobile. The optimal technique for achieving the sum rate capacity of MIMO-BC channel is the so-called “dirty-paper coding” (DPC) approach [28], by which multiuser interference is non-causally canceled at the transmitter. It has also been proven that the capacity region of DPC is the same with that of a MIMO broadcast system [97], therefore the capacity characteristics of MIMO-BC channel is completely solved.

Despite its significance from the information theoretical point of view, DPC is not considered practical due to its high complexity. Practical techniques are therefore required to achieve the capacity gain promised by MU-MIMO while providing a satisfactory link-level performance. The primary concern is how to balance the interference and the desire of high received signal power for each user. Prior research on interference cancellation of multiuser MIMO systems has primarily focused on the uplink [62, 90] since complex receivers are really only viable at the BTS. In reality, mobile devices must avoid complicated processing to maintain compact and power efficient. This motivates the precoding approach, in which the BTS assists in the interference cancellation process so that simple linear receivers are viable at the mobile units.

2.1.2 Overview of MU-MIMO Precoding with Single-Antenna per MS

Due to the low-complexity realization at mobile unit, and the large diversity gain, precoding for MIMO systems - also referred to as “closed-loop” MIMO where CSI is known at the transmitter - has been a subject of much recent interest.

Extensive results are available for single-user precoder design, e.g. [42, 72, 76, 77]. Relatively fewer results exist on multiuser MIMO precoding. One category of multiuser precoders allow some inter-user interference and apply beamforming to support multiple users [7]. The iterative nature of such algorithms, however, usually results in huge complexity, and the residual co-channel interference (CCI) still needs to be canceled to ensure

satisfactory error performance. Perfect interference cancellation requires more transmit antennas and is generally suboptimal in terms of sum capacity [102], but it enables simpler precoder design and allows for low-complexity mobile device [22, 89, 98], which is attractive for practical systems.

Existing precoding techniques with single-antenna MS are summarized as follows.

- **Channel Inversion** - This is also referred to as “zero-forcing” (ZF) beamforming precoding [12, 102]. As a dual problem of the zero-forcing receiver, ZF precoding applies a channel inverter at the BTS side, which pre-inverts the channel and removes the interference. One problem associated with the channel inversion is the signal quality attenuation, especially as the channel is rank-deficient. The capacity of MU-MIMO with channel inversion does not scale linear with the number of users, in contrast to DPC [66].
- **Regularized Channel Inversion** - Just as the MMSE receiver avoids the noise enhancement of ZF receiver by applying a regularization vector, regularized channel inversion adds a regularization vector to the ZF beamforming matrix, to reduce the channel attenuation problem. The regularization vector is heuristically determined to obtain a good tradeoff of the numerical condition of the channel inversion and the amount of residual interference. Regularized channel inversion leads to linear capacity growth with the number of users, in contrast to the channel inversion scheme.

2.1.3 Overview of MU-MIMO Precoding with Multi-Antenna per MS

MU-MIMO precoding with single-antenna per MS aims to eliminate interference across each single receive antenna. On the other hand, MU-MIMO precoding with multi-antenna per MS only aims to eliminate the interference across different users, but not across the antennas associated with the same user. As a result, MU-MIMO precoding aims

to diagonalize the multiuser MIMO channel into a set of non-interfering single-user MIMO channels.

In [98], an iterative joint channel diagonalization (JCD) approach was proposed to avoid the CCI, but only the necessary condition for the existence of channel diagonalization was provided, and the complicated iterative algorithm was not theoretically proved to converge universally. Another CCI cancellation approach is the block diagonalization (BD) method in [89], which diagonalizes the multiuser MIMO channel non-iteratively, followed by a conventional water-filling module to maximize the sum capacity. The BTS must have a minimum number of antennas to ensure complete interference cancellation. These works aimed to achieve the sum capacity, subject to zero-interference constraint achieved by different interference cancellation approaches. The diversity gain which is critical for combating fading and link-level error performance, was not addressed.

2.1.4 Contributions of the Proposed Work

In this chapter, linear precoders for multiuser MIMO is proposed for the special scenario where the BTS has more antennas than strictly required for interference avoidance. In contrast to the capacity optimization in the previous work, this work studies the precoder design from the link-level error rate optimization perspective with a fixed number of substreams, since it is an important performance measure in practical system besides the Shannon capacity. Two cases are studied, where (1) there are the same number of RF (radio-frequency) units as antenna elements; (2) a limited number of RFs are available and the BTS transmits over a subset of the available antennas. For the first case, a two-step unitary precoder design in the Stiefel manifold framework is proposed, which includes both interference cancellation and symbol error performance enhancement by selection diversity. The first step is to identify a group of unitary downlink precoding matrices at the BTS that perfectly avoid interference at mobile terminals. A QR decomposition based method is pro-

posed to meet the zero-interference constraint, which has lower computational complexity than existing approaches. In the second step, an enhanced space-time precoder with eigenmode selection is proposed to minimize a symbol error rate (SER) upper bound. Based on the signal-to-noise ratio (SNR) bounds in [63, 71], eigenmode selection is proposed to optimally bound the SER of each user by performing a secondary singular value decomposition (SVD) and allocating data to the optimal set of eigenmodes.

The advantages of MUSM over time division multiple access (TDMA) in terms of asymptotic capacity have been addressed by Sharif *et al.* in [83], Jindal *et al.* in [50], and Yoo *et al.* in [102] and noting that zero-forcing beamforming is a special case of MUSM with single-antenna terminals. In addition, the precoded MUSM system provides a natural framework for multiuser diversity, in which extra users are present and the best subset of users for transmission are scheduled optimally [67, 102]. The user and antenna scheduling issue in the presence of a large number of mobile users is discussed in the next chapter.

An alternative to the optimal eigenmode selection procedure is to switch appropriately chosen antenna elements from the array to the available RF chains, when a limited number of RF units are available due to cost constraints. Since antenna elements are much cheaper than RF amplifiers, performing antenna selection will substantially decrease the system cost. Prior work on antenna selection has focused on single-user systems. In this chapter, antenna selection technique is proposed in the context of unitary precoding. Two selection criteria are proposed, which minimize the SER and maximize the sum capacity, respectively. To avoid the computational complexity of brute-force search, low-complexity selection algorithms are developed.

2.2 Preliminaries and System Model

In this section, the notation and the narrow-band channel model are introduced. All vectors and matrices are in boldface, with matrices capitalized.

2.2.1 Notation

- Let Φ denote a complex matrix, and Φ^T , Φ^H and Φ^\dagger denote the transpose, conjugate transpose and Moore-Penrose pseudo-inverse of Φ , respectively.
- $\Phi^{(i,j)}$ denotes the $(i,j)^{th}$ element of matrix Φ .
- W_Φ denotes the vector space spanned by the columns of Φ and W_Φ^\perp denotes the complementary subspace of W_Φ .
- $\text{vec}(\Phi)$ denotes the vector produced by stacking the columns of Φ .
- $\text{diag}\{\phi_1, \phi_2, \dots, \phi_n\}$ denotes a $n \times n$ diagonal matrix with $\text{diag}\{\phi_1, \phi_2, \dots, \phi_n\}^{(i,i)} = \phi_i$.
- \mathcal{E}_s denotes expectation with respect to random variable s .
- The trace of a $m \times m$ square matrix Φ is expressed as $\text{tr}(\Phi) = \sum_{i=1}^m \Phi^{(i,i)}$.
- The Frobenius norm of a $m \times n$ matrix Φ is $\|\Phi\|_F^2 = \text{tr}(\Phi\Phi^H) = \sum_{i=1}^r |\lambda_i(\Phi)|^2$, where $r = \text{rank}(\Phi) \leq \min(m, n)$ and $\{\lambda_i(\Phi)\}_{i=1}^r$ are the singular values of Φ .
- The singular values $\{\lambda_i(\Phi)\}_{i=1}^n$ are non-negative for arbitrary complex matrix Φ , as shown in [37].
- $\mathbb{U}(n, k)$ is the collection of $n \times k$ complex matrices with unit-norm orthogonal columns, which is commonly known as the Stiefel manifold.

2.2.2 Channel Model

Consider the MU-MIMO system illustrated in Fig. 2.1 with M_T' transmit antennas, M_T RF chains at the BTS, and K mobile users where the k^{th} user has $M_{R,k}$ receive antennas, $k = 1, 2, \dots, K$. A narrow-band flat-fading channel is assumed. The channel transfer matrix from the BTS to the k^{th} mobile station (MS) is given as $\mathbf{H}_k \in \mathbb{C}^{M_{R,k} \times M_T}$, where $\mathbf{H}_k^{(i,j)}$ denotes the channel fading coefficient from the j^{th} transmit antenna to the i^{th}

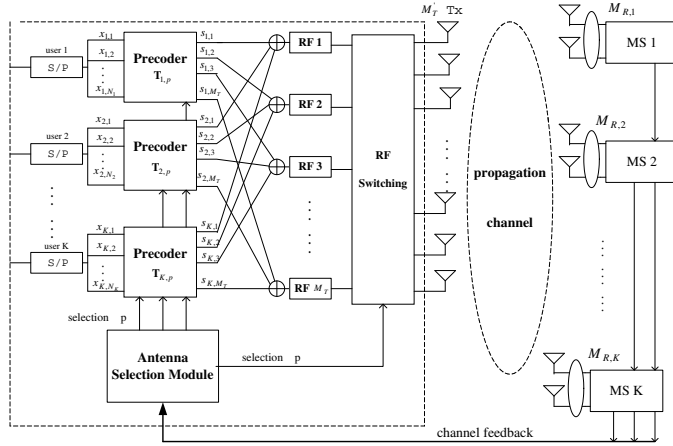


Figure 2.1: Block diagram of the MUSM system with precoding: perfect feedback is assumed with $\{\mathbf{H}_k\}_{k=1}^K$ exactly known at the transmitter for precoder design.

receive antenna of user k . It is assumed that both the BTS and MSs experience sufficient local scattering, thus the entries of \mathbf{H}_k are samples of an i.i.d. (independent identically distributed) zero-mean complex Gaussian process with distribution $\mathcal{CN}(0, 1)$. Channel degeneracy due to keyhole channel [21], or extreme correlations are not considered, and \mathbf{H}_k has full rank (i.e. $\text{rank}(\mathbf{H}_k) = \min(M_{R,k}, M_T)$) with probability one. In addition, it is assumed that the channels $\{\mathbf{H}_k\}_{k=1}^K$ are independent, therefore the composite channel matrix $\mathbf{H} = [\mathbf{H}_1^H \quad \mathbf{H}_2^H \quad \dots \quad \mathbf{H}_K^H]^H$ has full rank.

2.2.3 Signal Model

The BTS broadcasts data to all K users simultaneously over the same frequency band. The data from the k^{th} user is demultiplexed into $N_k \leq M_{R,k}$ data substreams, where $M_{R,k}$ upper bounds the maximum number of substreams that can be detected with a linear receiver. At a discrete time instant (the temporal index is dropped for simplicity), the spatial multiplexer of the k^{th} data branch generates a N_k -dimensional vector symbol $\mathbf{x}_k = [x_{k,1}, x_{k,2}, \dots, x_{k,N_k}]^T$, where symbols $x_{k,i}$ ($k = 1, \dots, K; i = 1, \dots, N_k$) are chosen from the same constellation set \mathcal{S} . For convenience it is assumed no error correction coding and a uniform allocation of power across the substreams for each user, i.e. $\mathbf{R}_{\mathbf{x}_k} = \mathcal{E}_{\mathbf{x}}\{\mathbf{x}_k \mathbf{x}_k^H\} =$

$\frac{E_{s,k}}{N_k} \mathbf{I}$, where E_s is the sum power, $E_{s,k} = \frac{N_k}{\sum_{j=1}^K N_j} E_s$ is the power allocated to the k^{th} user. As will be shown in the next section, the proposed precoder decomposes the multiuser MIMO channel into multiple parallel single-user MIMO channels, therefore a separate power allocation/bit loading module can be concatenated to the proposed precoder as an outer block for each user.

At the BTS, the symbol vector for the k^{th} user is multiplied by a $M_T \times N_k$ precoding matrix \mathbf{T}_k and summed with the precoded signals from the other users to produce the composite transmitted vector $\sum_{k=1}^K \mathbf{T}_k \mathbf{x}_k$. Each precoding matrix in $\{\mathbf{T}_k\}_{k=1}^K$ are chosen from the Stiefel manifold $\mathbb{U}(M_T, N_k)$. This implies that $\mathbf{T}_k^H \mathbf{T}_k = \mathbf{I}_{N_k}, \forall k$, i.e., \mathbf{T}_k has orthonormal columns, which was also used in [22, 89]. The unitary property forces the power per stream to be a constant thus does not alter the uniform power allocation strategy. As discussed above, adaptive power allocation can be achieved by concatenating a power adaptation module to the proposed precoder. In that case, the unitary constraint is generalized to the sum power constraint in [42, 76].

Neglecting symbol timing errors and frequency offsets, the $M_{R,k}$ -dimensional received signal \mathbf{r}_k at the k^{th} terminal is a superposition of the K signal branches distorted by channel fading plus additive white Gaussian noise (AWGN)

$$\mathbf{r}_k = \mathbf{H}_k \mathbf{T}_k \mathbf{x}_k + \mathbf{H}_k \sum_{j=1, j \neq k}^K \mathbf{T}_j \mathbf{x}_j + \mathbf{n}_k = \mathbf{H}_k \mathbf{T}_k \mathbf{x}_k + \mathbf{z}_k + \mathbf{n}_k. \quad (2.1)$$

The AWGN noise on the k^{th} user's receive antenna array is given by \mathbf{n}_k , which follows the complex i.i.d. Gaussian distribution of $\mathcal{CN}(0, N_o \mathbf{I})$. The CCI component on the k^{th} user is represented as \mathbf{z}_k .

It is assumed $\{\mathbf{H}_k\}_{k=1}^K$ is perfectly known at the transmitter to design the precoding matrices and perform antenna selection. It is assumed that each receiver only has knowledge of its own channel. The assumption of perfect CSI has been widely used in many existing literature in MIMO precoding [9, 42, 72, 76–78] and multiuser MIMO system [12, 28, 94, 96,

102–104]. It can be fulfilled by channel estimation in time-division-duplex (TDD) systems (e.g. IEEE 802.16, [35]), or feedback in frequency-division-duplex (FDD) systems.

2.3 Transmit Precoding for Interference Cancellation

The goal of multiuser MIMO downlink transmission is to achieve high data rates by using SDMA to serve multiple users at the same time. Since the data to multiple users are simultaneously transmitted and the spatial channels are not exactly orthogonal, CCI constitutes the major performance impairment. Recent information theoretic results reveal that when the interference is non-causally known at the transmitter, DPC is able to achieve the sum rate capacity of the MIMO-BC channel, at the expense of a very complicated binning strategy which has to be realized using nested codes [107]. Tomlinson-Harashima precoding (THP), which was originally developed for inter-symbol interference pre-cancellation, has been shown able to achieve capacity close to DPC, but it suffers from several shaping and power losses [103]. A combined beamforming and coding technique for known interference to achieve sum data rate of MIMO-BC channel was proposed in [2]. Several transmitter-based CCI pre-cancellation techniques have also been proposed recently, e.g., the BD [89], the JCD [98], and the transmitter pre-processing [22]. The basic idea behind these techniques is to use a large number of transmit antennas to orthogonalize the signal, followed by water-filling to optimize the capacity.

2.3.1 BD for Interference Cancellation

The BD approach seeks to find the precoding matrices $\{\mathbf{T}_k\}_{k=1}^K$ such that $\mathbf{H}_k \mathbf{T}_j = \mathbf{0}, \forall j \neq k$. Denote $\bar{\mathbf{H}}_k = [\mathbf{H}_1^H \ \cdots \ \mathbf{H}_{k-1}^H \ \mathbf{H}_{k+1}^H \ \cdots \ \mathbf{H}_K^H]^H$. The zero-interference constraint is re-expressed as

$$\bar{\mathbf{H}}_k \mathbf{T}_k = \mathbf{0}, \quad \forall k = 1, \dots, K. \quad (2.2)$$

Denote the SVD of $\bar{\mathbf{H}}_k$ as $\bar{\mathbf{H}}_k = \bar{\mathbf{U}}_k (\bar{\boldsymbol{\Sigma}}_k \ \mathbf{0}) (\bar{\mathbf{V}}_k^1 \ \bar{\mathbf{V}}_k^0)^H$, where $\bar{\mathbf{V}}_k = (\bar{\mathbf{V}}_k^1 \ \bar{\mathbf{V}}_k^0) \in$

$\mathbb{U}(M_T, M_T)$, $\bar{\mathbf{\Sigma}}_k$ is the $\bar{r}_k \times \bar{r}_k$ diagonal matrix containing the \bar{r}_k non-zero singular values of $\bar{\mathbf{H}}_k$, $\bar{r}_k = M_T - \sum_{j \neq k} M_{R,j}$, and $\bar{\mathbf{V}}_k^0$ contains the singular vectors corresponding to the zero singular values. Since the columns of $\bar{\mathbf{V}}_k^0$ span the null space of $\bar{\mathbf{H}}_k$, constructing \mathbf{T}_k with N_k columns of $\bar{\mathbf{V}}_k^0$ will automatically satisfy the zero-interference constraints. Assuming that the matrix channel is full rank, which occurs with enough scattering with probability one, N_k such singular vectors exist provided that the transmit array size satisfies $M_T \geq \sum_{j=1, j \neq k}^K M_{R,j} + N_k$. In case the channels are not full rank, the transmit array constraint will be in terms of channel ranks and is in fact less restrictive. Since this occurs much less frequently, this condition is not elaborated on. For future reference note that such precoding matrices are not unique, because right multiplication by an arbitrary unitary matrix will also satisfy (2.2).

2.3.2 Multiuser Downlink Precoder

The interference cancellation step of the proposed precoder is implemented by enforcing the orthogonality in the matrix channel of each user, i.e., by projecting the interfering data branches onto the complementary subspace spanned by the desired users' channel \mathbf{H}_k . This projection method has also been followed in [22, 89] with SVD approach. In this dissertation, it is proposed to use standard QR decomposition to allow for a quicker solution for interference cancellation.

Note that for a $n \times m$ matrix $\mathbf{\Phi}$ where $n \leq m$, it follows $\mathbf{\Phi}(\mathbf{I} - \mathbf{\Phi}^\dagger \mathbf{\Phi}) = \mathbf{0}$. Hence, \mathbf{T}_k can be constructed as a linear combination of the column basis vectors of $(\mathbf{I} - \bar{\mathbf{H}}_k^\dagger \bar{\mathbf{H}}_k)$, which can be obtained by the Gram-Schmidt Orthogonalization (GSO), or the standard QR decomposition which has several numerically stable solutions. Write the QR decomposition of $\mathbf{I} - \bar{\mathbf{H}}_k^\dagger \bar{\mathbf{H}}_k$ as

$$\mathbf{I} - \bar{\mathbf{H}}_k^\dagger \bar{\mathbf{H}}_k = \mathbf{Q}_k \mathbf{R}_k = \begin{pmatrix} \mathbf{Q}_k & \bar{\mathbf{Q}}_k \end{pmatrix} \begin{pmatrix} \mathbf{R}_k \\ \mathbf{0} \end{pmatrix}, \quad (2.3)$$

where $\mathbf{Q}_k \in \mathbb{U}(M_T, M_T - \sum_{j=1, j \neq k}^K M_{R,j})$ contains the basis of the complimentary sub-

space of $W_{\mathbf{H}_k}^\perp$. \mathbf{R}_k is an upper triangular matrix of dimension $(M_T - \sum_{j=1, j \neq k}^K M_{R,j}) \times M_T$. To reflect the fact that right multiplication of unitary matrices preserve both the orthogonalization and unitary properties, write the precoder as

$$\mathbf{T}_k = \mathbf{Q}_k \mathbf{D}_k, \quad (2.4)$$

where $\mathbf{D}_k \in \mathbb{U}(M_T - \sum_{j=1, j \neq k}^K M_{R,j}, N_k)$, $\forall k = 1, \dots, K$ are unitary eigenmode selection matrices.

When (2.2) is satisfied, the interference at mobile receiver k is perfectly avoided. Substituting (2.4) into (2.1) (for every user $k = 1, \dots, K$), the received signal at the k^{th} user is obtained as

$$\mathbf{r}_k = \mathbf{H}_k \mathbf{T}_k \mathbf{x}_k + \mathbf{H}_k \sum_{j=1, j \neq k}^K \mathbf{T}_j \mathbf{x}_j + \mathbf{n}_k = \tilde{\mathbf{H}}_k \mathbf{x}_k + \mathbf{n}_k, \quad (2.5)$$

where the $M_{R,k} \times N_k$ matrix $\tilde{\mathbf{H}}_k = \mathbf{H}_k \mathbf{T}_k$ is the equivalent channel transfer matrix to terminal k . Note that the multiuser MIMO channel is decoupled into K parallel non-interfering single-user MIMO links. Each user operates in its corresponding single-user link independently without affecting other links.

2.3.3 Complexity Analysis

The complexity of the previously proposed precoder design [89] is based on the SVD of $\bar{\mathbf{H}}_k$, which has a complexity of $\mathcal{O}(\max(p^2q, pq^2, q^3))$ (see pp. 254, [37]), where $p = M_T$ and $q = \sum_{j=1, j \neq k}^K M_{R,j}$. To completely cancel the interference, the system must satisfy $M_T \geq \max_k(\sum_{j=1, j \neq k}^K M_{R,j})$ (see [89]), hence the computational complexity turns out to be $\mathcal{O}(M_T^2 \max_k(\sum_{j=1, j \neq k}^K M_{R,j}))$.

The complexity of the proposed precoder is mainly determined by the Moore-Penrose pseudo-inverse $\bar{\mathbf{H}}_k^\dagger = \bar{\mathbf{H}}_k (\bar{\mathbf{H}}_k \bar{\mathbf{H}}_k^H)^{-1}$, and the QR decomposition of $\mathbf{I} - \bar{\mathbf{H}}_k^\dagger \bar{\mathbf{H}}_k$. The complexity of the most efficient pseudo-inverse operation follows $\mathcal{O}((\max_k \sum_{j=1, j \neq k}^K M_{R,j})^\omega)$ where $2 < \omega < 3$ [27]. The complexity of QR decomposition of $\mathbf{I} - \bar{\mathbf{H}}_k^\dagger \bar{\mathbf{H}}_k$ is lower than

$\mathcal{O}\left(\left(\max_k \sum_{j=1, j \neq k}^K M_{R,j}\right)^3\right)$ by a factor of 1.3-1.4 [43]. Since $M_T \geq \max_k \left(\sum_{j=1, j \neq k}^K M_{R,j}\right)$, the proposed algorithm has slightly lower computational complexity than the SVD-based approach. In addition, the QR-based method is generally much more stable and accurate numerically [37, 47].

The approach in [98] follows an iterative SVD operation of a smaller size interfering matrix, so the computational complexity cannot be directly compared to the proposed approach.

2.4 Transmit Precoding with Eigenmode Selection

In this section, it is shown how to improve the error rate by selecting the proper spatial eigenmodes when extra transmit antennas are available. Note that after interference pre-cancellation, each user operates in a single-user MIMO link, where the effective channel of user k is $\mathbf{H}_k \mathbf{Q}_k \mathbf{D}_k$ and \mathbf{Q}_k contains the null space basis of $\bar{\mathbf{H}}_k$. As a result, conventional single user MIMO techniques can be applied as a baseline to the multiuser problem, concatenated with the interference cancellation module in Section III, to optimize the SER. Increasing M_T will increase the spatial redundancy due to two reasons: a larger number of transmit antenna in \mathbf{H}_k , and an increased number of available null space basis for \mathbf{Q}_k to choose from. In contrast to single user MIMO optimization where only the user's channel \mathbf{H}_k is exploited, in a multiuser channel such a redundancy in spatial eigenmodes must be exploited with a joint consideration of \mathbf{H}_k and $\mathbf{Q}_k = f(\mathbf{H}_1, \dots, \mathbf{H}_{k-1}, \mathbf{H}_{k+1}, \dots, \mathbf{H}_K)$. This optimization is performed via optimizing the eigenmode selection matrix \mathbf{D}_k , subject to the zero-interference constraint.

2.4.1 Problem Formulation

It was shown in [63, 71] that the SNR of single-user spatial multiplexing systems with linear receivers is lower bounded by a monotonically increasing function of the minimum

singular value of the equivalent channel. This bound is specified as

$$SNR_{min} \geq \frac{E_{s,k}}{N_k N_o} \lambda_{\min}^2(\mathbf{H}_k \mathbf{T}_k), \quad (2.6)$$

for zero-forcing (ZF) receiver and

$$SNR_{min} \geq \frac{E_{s,k}}{N_k N_o} \left(\lambda_{\min}(\mathbf{H}_k \mathbf{T}_k) + \sqrt{\frac{N_k N_o}{E_{s,k}}} \right)^2 - 1, \quad (2.7)$$

for MMSE receiver.

To evaluate the tightness of this bound, 100,000 i.i.d. complex Gaussian channel realizations are randomly generated to evaluate the normalized mean square error (NMSE) of a ZF receiver

$$\mathbf{NMSE} = \frac{\|SNR_{bound} - SNR_{true}\|^2}{\|SNR_{true}\|^2}, \quad (2.8)$$

where SNR_{bound} is given in (2.6) and the true minimum SNR is

$$SNR_{true} = \frac{E_s}{N_o N_t} \frac{1}{\max_{i=1, \dots, N_t} \left((\mathbf{H}'\mathbf{H})^{-1} \right)^{(i,i)}}. \quad (2.9)$$

Fig. 2.2 demonstrates the complementary cumulative distribution function (CCDF) of the NMSE

$$F_{NMSE}(x) = Prob(NMSE > x). \quad (2.10)$$

It can be confirmed in Fig. 2.2 that this bound is reasonably tight. For example, only 1% of the channel realizations have NMSE larger than 20%, with $N_t = 2$, $N_r = 2$ or 4.

A similar bound exists for the non-linear successive interference cancellation (SIC) based receivers, e.g. V-BLAST [33], where the substreams are detected and subtracted sequentially to assist the decoding of subsequent substreams, therefore the performance is primarily dependent on the first substream. As a result, the objective of eigenmode optimization is to find

$$\mathbf{T}_{k,opt} = \arg \max_{\mathbf{T}_k \in \mathcal{U}(M_T, N_k), \bar{\mathbf{H}}_k \mathbf{T}_k = \mathbf{0}} \lambda_{\min}(\mathbf{H}_k \mathbf{T}_k). \quad (2.11)$$

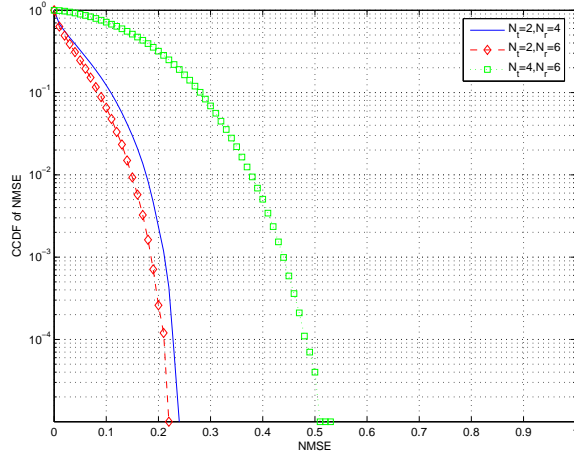


Figure 2.2: CCDF of the NMSE with ZF receiver

2.4.2 Eigenmode Selection

Since $\mathbf{T}_k = \mathbf{Q}_k \mathbf{D}_k$ and \mathbf{Q}_k is fixed, the above optimization problem is equivalent to selecting $\mathbf{D}_{k,opt}$. This relates to how the right multiplication of a tall matrix with unit-norm orthogonal columns will affect the minimum singular value of matrix, where the following theorem will prove useful:

Theorem 2.4.1. (*Horn & Johnson [47]*) Let \mathbf{A}_n be $n \times n$ Hermitian matrix, and $r \leq n$ be a given integer. Let $\mathbf{U} = [\mathbf{u}_1 \cdots \mathbf{u}_r] \in \mathbb{U}(n, r)$ and $\mathbf{B}_r = \mathbf{U}^H \mathbf{A}_n \mathbf{U} \in \mathbb{C}^{r \times r}$. Arranging the eigenvalues of \mathbf{A}_n and \mathbf{B}_r in decreasing order, then it follows

$$\mu_k(\mathbf{A}_n) \geq \mu_k(\mathbf{B}_r) \geq \mu_{k+n-r}(\mathbf{A}_n), \quad k = 1, 2, \dots, r. \quad (2.12)$$

The detailed proof is given in [47]. An extension of this theorem is derived in the following corollary.

Corollary 2.4.2. Let Φ be a $n \times m$ matrix where $n \leq m$, and $r \leq n$ be a given integer. Let $\mathbf{U} = [\mathbf{u}_1 \cdots \mathbf{u}_r] \in \mathbb{U}(m, r)$ be arbitrary unitary matrix and $\tilde{\Phi} = \Phi \mathbf{U} \in \mathbb{C}^{n \times r}$. Arranging the singular values of Φ and $\tilde{\Phi}$ in decreasing order yields

$$\lambda_k(\Phi) \geq \lambda_k(\tilde{\Phi}) \geq \lambda_{k+n-r}(\Phi), \quad k = 1, 2, \dots, r. \quad (2.13)$$

Proof: The corollary is proven by denoting $\mathbf{A} = \mathbf{\Phi}^H \mathbf{\Phi}$ and substituting $\mu_k(\mathbf{A}) = \lambda_k^2(\mathbf{\Phi})$, $\mu_k(\mathbf{U}^H \mathbf{A} \mathbf{U}) = \lambda_k^2(\mathbf{\Phi} \mathbf{U})$ into the above theorem, recalling the non-negativity of singular values. \square

The benefits of choosing the optimal $\mathbf{D}_{k,opt}$ is similar to the single user scenario. With excess transmit antennas, the equivalent channel generates $r_k = \text{rank}(\mathbf{H}_k \mathbf{Q}_k)$ spatial eigenmodes, more than the number of substreams N_k . According to Corollary 1, selecting the first N_k eigenmodes achieves the upper bound for $\lambda_{min}(\mathbf{H}_k \mathbf{Q}_k \mathbf{D}_k)$ and therefore minimizes the SER upper bound. It is interesting to note that the selection of the optimum set of eigenmodes was also developed in [89], whereas for capacity optimization goal. The number of selected eigenmodes in [89] is a variable determined by water-filling, while N_k is fixed in this dissertation to consider the SER optimization.

The benefits of eigenmode selection depend on the number of spatial eigenmodes, which is a function of the system antenna configuration.

Lemma 2.4.3. *The k^{th} user has*

$$r_k = \text{rank}(\mathbf{H}_k \mathbf{Q}_k) = \min \left(M_{R,k}, M_T - \sum_{i=1, i \neq k}^K M_{R,i} \right) \quad (2.14)$$

spatial eigenmodes to transmit its N_k data substreams.

Proof: $(\mathbf{I} - \bar{\mathbf{H}}_k^\dagger \bar{\mathbf{H}}_k)$ is a projection matrix with rank $(M_T - \sum_{i=1, i \neq k}^K M_{R,i})$, therefore its QR decomposition \mathbf{Q}_k also has rank $(M_T - \sum_{i=1, i \neq k}^K M_{R,i})$. Because \mathbf{Q}_k is a function of $\bar{\mathbf{H}}_k$ and independent of \mathbf{H}_k , the rank of $\mathbf{H}_k \mathbf{Q}_k$ satisfies the condition specified above. \square

Denote $\mathbf{H}_k \mathbf{Q}_k = \mathbf{U}_k \mathbf{\Sigma}_k \mathbf{V}_k^H$, where $\mathbf{U}_k \in \mathbb{U}(M_{R,k}, r_k)$, $\mathbf{V}_k \in \mathbb{U}(M_T - \sum_{j=1, j \neq k}^K M_{R,j}, r_k)$, rank r_k is given in (2.14), and $\mathbf{\Sigma}_k = \text{diag}\{\lambda_{k,1}, \lambda_{k,2}, \dots, \lambda_{k,r_k}\}$ is the diagonal matrix consisting of all the singular values in descending order. According to Corollary 1, $\lambda_{min}(\mathbf{H}_k \mathbf{Q}_k \mathbf{D}_k) \leq \lambda_{k,N_k}$ where equality holds with the optimum eigenmode selection matrix given as

$$\mathbf{D}_{k,opt} = \arg \max_{\mathbf{D}_k \in \mathbb{U}(r_k, N_k)} \lambda_{min}(\mathbf{H}_k \mathbf{Q}_k \mathbf{D}_k) = \mathbf{V}_{k,[1:N_k]}, \quad (2.15)$$

where $\mathbf{V}_{k,[1:N_k]}$ denotes the first N_k columns of \mathbf{V}_k . Recall that the precoding matrix is not unique since performance is invariant to right multiplication by a unitary matrix, hence (2.15) is only one of the possible solutions.

Lemma 2.4.4. *The necessary condition for eigenmode selection is*

$$M_{R,k} > N_k, \quad (2.16)$$

$$M_T - \sum_{i=1, i \neq k}^K M_{R,i} > N_k. \quad (2.17)$$

Proof: Proof is straightforward as this specification ensures more eigenmodes than data streams. \square

So far it is assumed that the BTS has perfect knowledge of $\{\mathbf{H}_k\}_{k=1}^K$. When the transmitter has imperfect knowledge of the channel matrices, the precoding matrices cannot perfectly cancel interference, while the mismatch of the precoder and the eigenvectors of the effective channel will lead to further performance loss. In [47], imperfect CSI for a *space-time block coded* multiuser MIMO system has been analytically investigated, where a SER and BER lower bound is derived under imperfect CSI. This approach can be similarly applied to the multiuser spatial multiplexing system.

2.4.3 SER Performance Analysis

Lemma 2.4.5. *If the MIMO channel \mathbf{H}_k follows i.i.d. complex Gaussian distribution $\mathcal{CN}(0, 1)$, then the equivalent MIMO channel $\tilde{\mathbf{H}}_k$ after unitary precoding is also i.i.d. Gaussian distributed $\mathcal{CN}(0, 1)$, if eigenmode selection is not performed.*

Proof: After downlink precoding, each mobile user is effectively in a single-user MIMO channel with equivalent channel $\tilde{\mathbf{H}}_k = \mathbf{H}_k \mathbf{T}_k$. Without eigenmode selection, \mathbf{T}_k is a function of \mathbf{H}_j , $j \neq k$ and therefore independent of \mathbf{H}_k . Since \mathbf{H}_k has i.i.d complex Gaussian entries of zero mean and unit variance, and because linear operations of Gaussian

Table 2.1: Summary of notations

\mathbf{H}	$(\mathbf{H}_1^H \mathbf{H}_2^H \dots \mathbf{H}_K^H)^H$
$\tilde{\mathbf{H}}_k$	$(\mathbf{H}_1^H \dots \mathbf{H}_{k-1}^H \mathbf{H}_{k+1}^H \dots \mathbf{H}_K^H)^H$
$\tilde{\mathbf{H}}_k$	$\tilde{\mathbf{H}}_k = \mathbf{H}_k \mathbf{T}_k = \mathbf{H}_k \mathbf{Q}_k \mathbf{D}_k$
\mathbf{Q}_k	QR decomposition result of $\mathbf{I} - \tilde{\mathbf{H}}_k^\dagger \tilde{\mathbf{H}}_k$
$\mathbf{D}_{k,opt}$	$\mathbf{V}_{k,[1:N_k]}$
\mathbf{V}_k	right singular vector matrix of $\mathbf{H}_k \mathbf{Q}_k$

random variables are still Gaussian, $\tilde{\mathbf{H}}_k$ conditioning on \mathbf{T}_k is also i.i.d. Gaussian with zero-mean and unit variance, independent of \mathbf{T}_k . Hence it is easy to see that the unconditional distribution of $\tilde{\mathbf{H}}_k$ is still i.i.d. Gaussian.

The error performance of each user can be obtained through existing spatial multiplexing performance analysis methodologies for single-user spatial multiplexing system [46, 110]. With eigenmode selection, however, the error performance of each user is dependent on the joint statistical distribution of the selected subset of eigenmodes and is more difficult to solve.

Note that for the same number of eigenchannels, water-filling is suboptimal in terms of SER to equal power allocation, because water-filling allocates less power to eigenchannels with lower gain, and the SER is a convex function of SNR. Therefore if the water-filling technique selects $n \geq N_k$ eigenchannels, the proposed eigenmode selection outperforms in SER. If $n < N_k$, it is unknown which scheme is better because the water-filling does not provide a closed-form power distribution over the substreams. Also note that adaptively distributing transmit power to the eigenmodes can further reduce the SER. This improvement, however, is independent of the proposed eigenmode selection and can be concatenated as an outer module.

2.4.4 Sum Rate Capacity Analysis

Assuming that the transmitted data streams are independently encoded and independently decoded, the sum rate capacity of the multiuser system is simply the summation

of each user's individual channel capacity. The optimum capacity is achieved by water-filling performed over the eigenchannels of all users, expressed as

$$C = \sum_{k=1}^K \sum_{i=1}^{N_k} \log_2 \left(1 + \frac{1}{N_k N_o} \left(\gamma - \frac{N_o}{|\lambda_{k,i}|^2} \right)_+ |\lambda_{k,i}|^2 \right), \quad (2.18)$$

where

$$(x)_+ = \begin{cases} 0 & x \leq 0 \\ x & x > 0 \end{cases} \quad (2.19)$$

and γ is the threshold determined by the sum power constraint

$$E_s = \sum_{k=1}^K \sum_{i=1}^{N_k} \left(\gamma - \frac{N_o}{|\lambda_{k,i}|^2} \right)_+. \quad (2.20)$$

In terms of sum capacity, the eigenmode selection chooses the best N_k eigenchannels out of the total r_k eigenchannels, while the number of used eigenchannels in approaches in [89] is a variable determined by the water-filling. Therefore the eigenmode selection is suboptimal in terms of sum capacity. This suboptimality, however, results from the deliberate restriction on the number of streams per user (N_k).

2.4.5 Numerical Results

Fig. 2.3 compares the SER performance of a single and multiuser system where each user has three antennas and receives 2 data substreams. The channel is assumed to be Gaussian distributed, which is perfectly known at the BTS. Three cases are studied: (a) single-user system with 2 transmit antennas, (b) two-user system with 5 transmit antennas, (c) two-user system with 6 transmit antennas and eigenmode selection. The horizontal axis represents the average SNR per branch (user) per receive antennas. The vertical axis represents the SER averaged among all users. In case (a) and (b), the number of BTS antennas is the minimum required for interference cancellation, so no eigenmode selection is performed. The multiuser system achieves the same per user performance with a single-user system, which obtains a diversity order of 2 with ZF receiver. By adding a single antenna to the BTS and utilizing eigenmode selection, however, a significant SNR reduction of 8 dB is

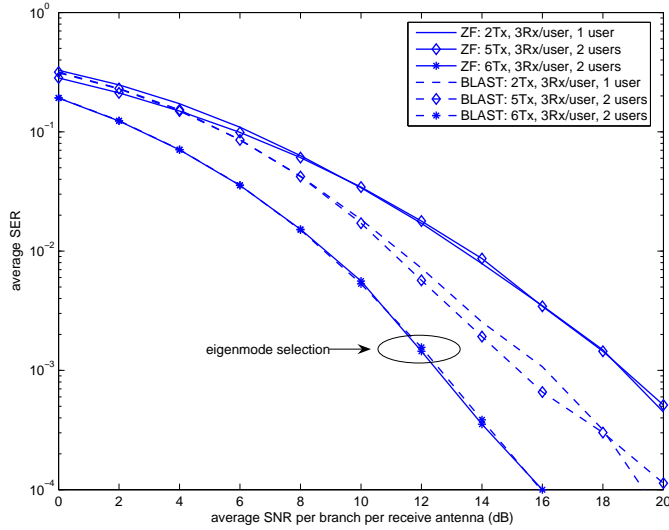


Figure 2.3: SER comparison of single user and multiuser spatial multiplexing system with 3 antennas, 2 substreams per user, using ZF and V-BLAST receivers.

achieved at $\text{SER}=10^{-4}$ for the ZF receiver. Similarly, a SNR reduction of 5 dB is achieved for V-BLAST receiver. The asymptotic slope of SER curve, which is the definition of diversity gain, is larger than scenarios without eigenmode selection. Clearly, the eigenmode selection achieves a higher diversity and this improvement becomes more significant as more antennas are added at the BTS.

2.5 Transmit Antenna Selection

The previous section proposed eigenmode selection as an effective transmit selection diversity technique when the number of BTS RF amplifiers and antennas both exceed the requirement for interference cancelation. One drawback of eigenmode selection is that it also requires M_T expensive RF chains to meet the channel rank requirement (2.14), which leads to a higher system cost. As an alternative, antenna selection can be used to provide transmit diversity at a relatively lower system cost with fewer RF chains, although naturally with some performance loss.

2.5.1 Single-user Antenna Selection

Antenna selection refers to choosing a subset of available antennas from the BTS antenna pool and switching them to the available RF units. Extensive research has been conducted on its application in a single-user MIMO system, at the transmitter or the receiver, using either instantaneous or statistical channel knowledge. In [39, 40], the authors studied receive antenna selection for spatial multiplexing systems, and proposed the optimal and suboptimal selection algorithms to maximize channel capacity. Transmit antenna selection for link-level error performance optimization of spatial multiplexing system was studied in [71]. For space-time coded MIMO systems, Gore *et al.* studied various selection algorithms [38] where the objective is to maximize post-processing SNR. A complete overview of MIMO antenna selection technique can be found in [61, 73].

Even though only a subset of antennas are used, analysis and simulation show a very interesting result: antenna selection over M_T antennas can achieve the same diversity performance as a full system where *all* M'_T antennas are simultaneously used [39, 61]. This implies that there may not be a large penalty for reducing the number of RF chains, as long as $M'_T > M_T$ antenna elements can be deployed.

2.5.2 Proposed Multiuser Antenna Selection

The system configuration is different in the context of antenna selection. Suppose there are only M_T RF chains which are exactly the minimum requirement for supporting multiuser downlink precoding, thus eigenmode selection is not feasible. Suppose there are $M'_T > M_T$ BTS antennas available, however, and for each transmission, a selected subset of M_T antennas is switched to the RF chains to transmit over the “preferred” antennas. The selected antenna set is indexed by $p \in P$ where P is the available $C_{M'_T}^{M_T}$ sets. The channel matrices $\{\mathbf{H}_k\}_{k=1}^K$ will be indexed by the antenna set p , i.e., $\{\mathbf{H}_{k,p}\}_{k=1}^K$.

Two antenna selection techniques will be proposed in this chapter.

- **Brute-force Exhaustive Search** - An exhaustive search is conducted over all possible $C_{M_T}^{M_T}$ antenna combinations, to find the set that optimizes the system performance in terms of a specific metric. Two selection algorithms will be proposed. The first algorithm aims to maximize the sum-rate capacity. The second algorithm aims to maximize a lower bound of the post-decoding SNR for all users, which is equivalent to minimizing the SER upper bound.
- **Low-Complexity Antenna Selection** - Because the brute-force method needs to search over all possible antenna combinations, the computational complexity is extremely high, especially as the total number of BTS antennas M_T' becomes large. To reduce the computational demand and make antenna selection practical in a commercial wireless system, two low-complexity selection algorithms will be proposed in this chapter. Both selection algorithms follow a greedy selection method, where the transmit antennas are one by one deactivated, until the number of remaining active antennas is equivalent to the number of RF units. The first algorithm aims to maximize the SNR lower bound, while the second algorithms aims to maximize sum Frobenius norm of the effective channel.

2.5.2.1 Brute-Force Search

In this section, exhaustive search is applied to find the optimum antenna subset that optimizes a given performance metric. A total of $C_{M_T}^{M_T}$ antenna combinations are exhaustively search over.

Antenna selection can be based on the optimization of SER or the channel capacity. Again, for reasons stated earlier, we first focus on the minimization of the maximum SER, which is an effective upper bound of the average SER. The equivalent channel matrix after unitary precoding depends on both the real channel $\mathbf{H}_{k,p}$ and the precoding matrices $\mathbf{T}_{k,p}$ which is a function of p . Recall (2.6)(2.7) and note that the maximum SER of user k is

upper bounded by a non-decreasing function of $\lambda_{\min}(\mathbf{H}_{k,p}\mathbf{T}_{k,p})$, therefore the maximum system SER is upper bounded by the user with the worst performance, which depends on the minimum of *all* users' minimum singular values. Therefore, one approach for antenna selection is to maximize the minimum of all users' singular values.

Algorithm 1. SER-based Exhaustive Search For every transmit antenna subset $p \in P$, compute $\tilde{\lambda}_{p,\min} = \min_{k=1,\dots,K} \lambda_{\min}(\mathbf{H}_{k,p}\mathbf{T}_{k,p})$ corresponding to p . To optimize the SER performance, select the antenna set p that maximizes the minimum singular value $\tilde{\lambda}_{p,\min}$

$$p_{opt} = \arg \max_{p \in P} \tilde{\lambda}_{p,\min}. \quad (2.21)$$

Antenna selection can also be implemented by choosing the performance metric as the sum rate capacity.

Algorithm 2. Norm-based Exhaustive Search For every subset of transmit antennas $p \in P$, compute the sum capacity in (2.18) and select the antenna set p that maximizes sum capacity

$$p_{opt} = \arg \max_{p \in P} R. \quad (2.22)$$

Selection according to a capacity criterion identifies the optimum antenna subset with the largest sum rate. This sum rate is only achieved when there is no restriction on the complexity and length of the coding scheme. Due to the complexity, delay, and modulation constellation constraints in practical system, the actual achievable data rate needs to consider a SNR-gap in the sum rate expression in (2.18). Particularly, the achievable data rate is expressed as

$$C = \sum_{k=1}^K \sum_{i=1}^{N_k} \log_2 \left(1 + \frac{E_{s,k}}{\Gamma N_k N_o} |\lambda_{k,i}|^2 \right) \quad (2.23)$$

for uniform power allocation scheme and

$$C = \sum_{k=1}^K \sum_{i=1}^{N_k} \log_2 \left(1 + \frac{1}{\Gamma N_k N_o} \left(\gamma - \frac{N_o}{|\lambda_{k,i}|^2} \right)_+ |\lambda_{k,i}|^2 \right) \quad (2.24)$$

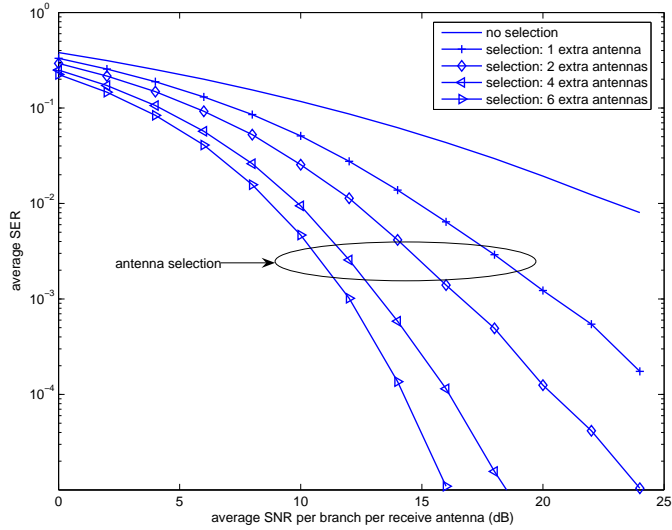


Figure 2.4: SER performance of antenna selection with 2 users, 2 receive antennas and 2 data substreams per user, using ZF receiver.

for the water-filling case. The SNR-gap Γ defines the gap between a practical coding and modulation scheme and the Shannon capacity.

The SER of antenna selection for a 2-user system with ZF receiver is given in Fig. 2.4. Each user has 2 receive antennas and receives 2 substreams. Eigenmode selection is not applicable because condition (2.16) is violated. The number of RF chains is $M_T = 4$, the minimum to support spatial multiplexing with linear receivers. The BTS has M'_T transmit antennas, where M'_T varies from 4 to 10. $M'_T = 4$ is the case without antenna selection, and $M'_T = 5, 6, 8, 10$ corresponds to the cases of 1, 2, 4, 6 extra antennas for selection. The SER-based exhaustive search is used. With only 1 extra antenna, a surprisingly large SNR gain of 10 dB is achieved at a SER of 10^{-3} . Adding another extra antenna brings a further SNR gain of 3 dB. The gain per antenna, naturally, decreases as more antennas are added so one or two extra antennas appears to be sufficient for most practical cases.

2.5.2.2 Low-Complexity Antenna Selection

One issue with the exhaustive-search based algorithms is the computational complexity. Because a total of $C_{M'_T}^{M_T}$ antenna combinations need to be searched over, the computational complexity grows linearly with $C_{M'_T}^{M_T}$. This complexity easily becomes intractably high for any commercial wireless network, especially as M'_T becomes large.

To reduce the computational complexity and exploit the antenna selection diversity in a practical system, two low-complexity algorithms are proposed in this section. The first algorithm aims to maximize a lower bound of the post-decoding SNR, and the second algorithm aims to maximize the aggregate Frobenius norm of the effective channel. Both algorithms follows a greedy antenna selection approach, where one BTS antenna is deactivated in each iteration, until the number of remaining antennas is equal to the number of RF units.

Algorithm 3. *SER-based Low-Complexity Algorithm*

1. Stage $s = 0$: Let all M'_T BTS antennas be active, and feedback the channel $\{\mathbf{H}_k\}_{k=1}^K$ to the BTS. Let $\mathcal{A} = \{1, 2, \dots, M'_T\}$ denote the set of active BTS antennas, and let $\mathcal{S} = \phi$ denote the set of inactive antennas.

2. Stage $s = s + 1$:

(a) For every antenna $i \in \mathcal{A}$, temporarily deactivate it by setting $\tilde{\mathcal{A}} = \mathcal{A} - \{i\}$, and calculate the post-decoding SNR lower bound by

$$\lambda_{i,min} = \min_{k=1,\dots,K} \lambda_{min} \left(\mathbf{H}_{k,\tilde{\mathcal{A}}} \mathbf{T}_{k,\tilde{\mathcal{A}}} \right) \quad (2.25)$$

where $\mathbf{H}_{k,\tilde{\mathcal{A}}}$ is the channel matrix of user k associated with the active BTS antenna set $\tilde{\mathcal{A}}$, and $\mathbf{T}_{k,\tilde{\mathcal{A}}}$ is the corresponding precoding matrices.

(b) Find the antenna that maximizes the SNR lower bound

$$i_{opt} = \arg \max_{i \in \mathcal{A}} \lambda_{i,min} \quad (2.26)$$

(c) Deactivate antenna i_{opt} by letting $\mathcal{A} = \mathcal{A} - \{i_{opt}\}$.

3. If $s < (M'_T - M_T)$, go to stage (2). Else, exit the iteration.

This algorithm is described as follows. The key idea is to greedily reduce the number of selected antennas, until the number of remaining active BTS antennas is equal to M_t . At the beginning, all transmit antennas are active. Then in each iteration, we select the antenna that will maximize the system performance if it is deactivated, and remove it from the BTS. The BTS keeps deactivating the transmit antennas, one at a time, until the optimum M_T antennas are finally selected. Therefore this algorithm needs to undergo a maximum of $M'_T - M_T$ iterations, where no more than $M'_T - s + 1$ antenna need to be searched over in the s^{th} iteration. As a result, the size of search space is upper bounded by

$$\sum_{s=1}^{M'_T - M_T} (M'_T - s + 1) = (M'_T + M_T + 1) \frac{M'_T - M_T}{2}, \quad (2.27)$$

which is greatly simplified than the exhaustive search method where $C_{M'_T}^{M_T}$ possible combinations have to be searched over.

Algorithm 4. Norm-based Low-Complexity Algorithm A second low-complexity antenna selection algorithm is proposed as follows, where the performance metric is the aggregate Frobenius norm of the effective channel. The Frobenius norm is chosen because it is closely related to the eigenvalues of the effective channel after precoding. Although the aggregate Frobenius norm cannot completely characterize the sum-rate capacity, it well reflects the overall energy of the channel, i.e., the sum of the eigenvalues of $\mathbf{H}\mathbf{H}^\dagger$ is equal to $\|\mathbf{H}\|_F^2$.

1. Stage $s = 0$: Let all M'_T BTS antennas be active, and collect the channel $\{\mathbf{H}_k\}_{k=1}^K$ at the BTS. Let $\mathcal{A} = \{1, 2, \dots, M'_T\}$ denote the set of active BTS antennas, and let $\mathcal{S} = \emptyset$ denote the set of inactive antennas.

2. Stage $s = s + 1$:

(a) For every antenna $i \in \mathcal{A}$, temporarily deactivate it by setting $\tilde{\mathcal{A}} = \mathcal{A} - \{i\}$. Use the channel $\mathbf{H}_{k,\tilde{\mathcal{A}}}$ to calculate the precoding matrices $\mathbf{T}_{k,\tilde{\mathcal{A}}}$. Calculate the aggregate Frobenius norm as

$$E_i = \sum_{k=1}^K \|\mathbf{H}_{k,\tilde{\mathcal{A}}} \mathbf{T}_{k,\tilde{\mathcal{A}}}\|_F^2 \quad (2.28)$$

(b) Find the antenna that maximizes the aggregate Frobenius norm

$$i_{opt} = \arg \max_{i \in \mathcal{A}} E_i \quad (2.29)$$

(c) Deactivate antenna i_{opt} by letting $\mathcal{A} = \mathcal{A} - \{i_{opt}\}$.

3. If $s < (M'_T - M_T)$, go to stage (2). Else, exit the iteration.

Similar to the SER-based low-complexity algorithm, the norm-based algorithm follows a greedy selection approach. In each iteration, the BTS selects the optimal antenna that generates the maximum Frobenius norm, supposing it is deactivated. The algorithm terminates when the number of active transmit antennas reaches M_T . The search size is

$$\sum_{s=1}^{M'_T - M_T} (M'_T - s + 1) = (M'_T + M_T + 1) \frac{M'_T - M_T}{2}, \quad (2.30)$$

which is much less complicated than the exhaustive search over $C_{M'_T}^{M_T}$ antenna subsets.

2.5.3 Numerical Results

SER Performance: Fig. 2.5 plots the SER performance of the exhaustive and the proposed SER-based low-complexity antenna selection algorithms, with 2 users, 2 receive antennas per user, 4QAM modulation and MMSE receiver. The performance of the

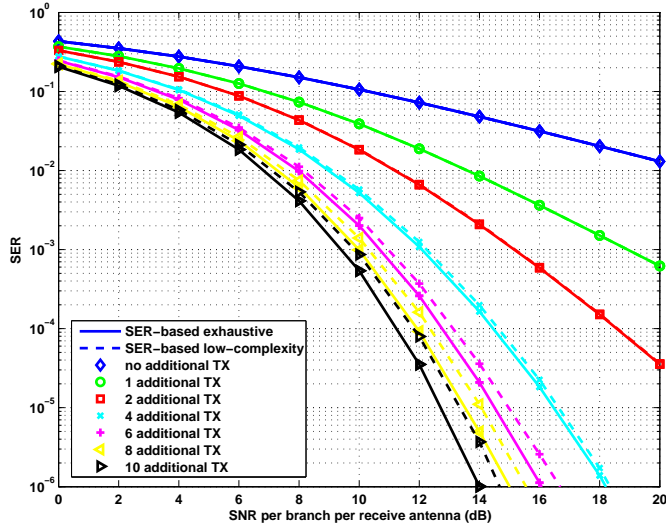


Figure 2.5: SER performance of exhaustive and low-complexity antenna selection with 2 users, 2 receive antennas and 2 data substreams per user, using 4QAM modulation and MMSE receiver per MS.

low-complexity algorithm is almost identical to that of the exhaustive search method, especially when the number of extra transmit antennas is fewer than 4, which is mostly likely the scenario in a practical system. Similarly, Fig. 2.6 compares the SER results with 2 users, 4 receive antennas per user, and 4QAM modulation. Again, the low-complexity algorithm performs almost the same as the exhaustive search method, with substantially lower complexity.

Capacity Performance: The sum rate capacity of the exhaustive and the Frobenius norm based low-complexity algorithms is compared in Fig. 2.7, with 2 users, 2 receive antennas per user. Again, it is confirmed that the capacity performance of these two algorithms are very close to each other. The capacity with 2 users, 4 receive antennas is compared in Fig. 2.8. The Frobenius norm based low-complexity algorithm achieves about 98% of the capacity of the capacity-based exhaustive search, with much less complexity.

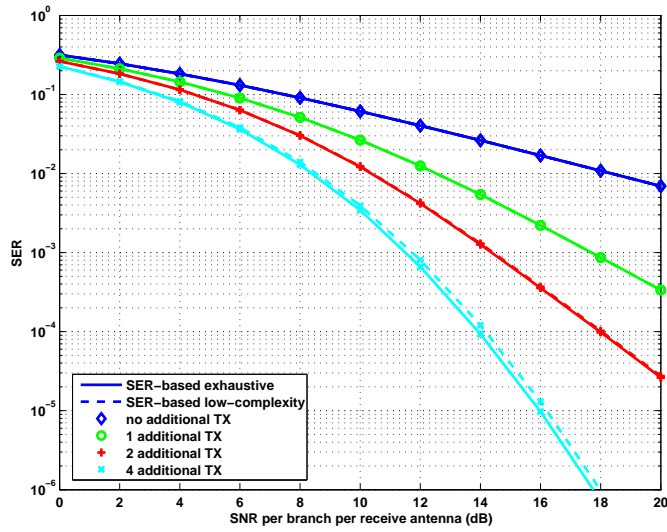


Figure 2.6: SER performance of exhaustive and low-complexity antenna selection with 2 users, 4 receive antennas and 4 data substreams per user, using 4QAM modulation and MMSE receiver per MS

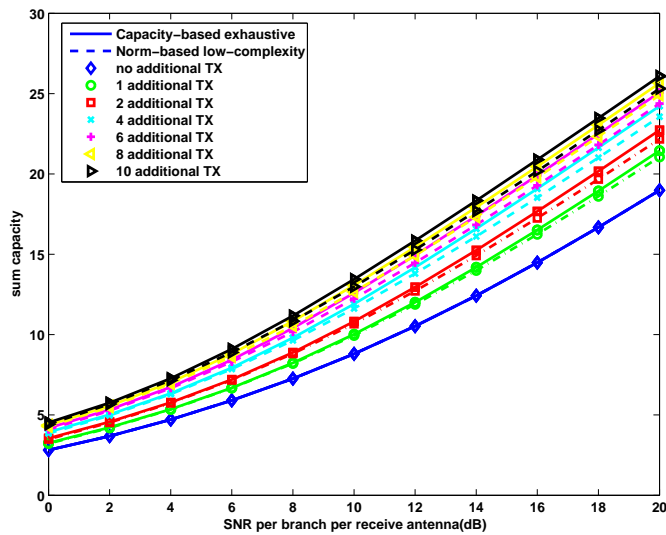


Figure 2.7: Sum rate capacity of exhaustive and low-complexity antenna selection with 2 users, 2 receive antennas per user.

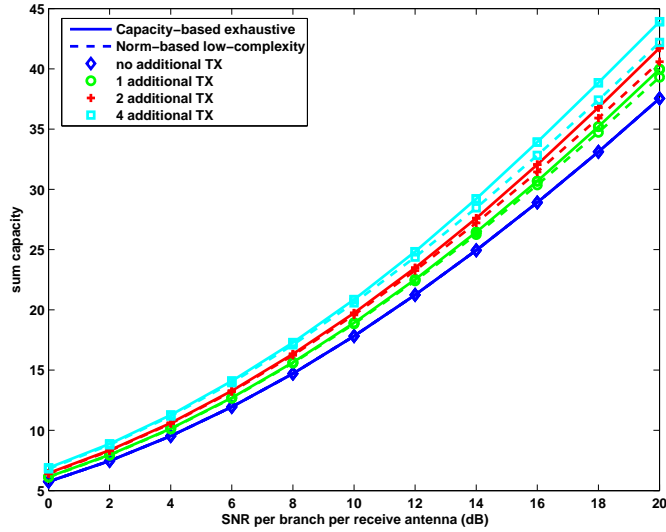


Figure 2.8: Sum rate capacity of exhaustive and low-complexity antenna selection with 2 users, 4 receive antennas per user.

2.6 Antenna Selection vs. Eigenmode Selection

Antenna selection and eigenmode selection are two diversity techniques to improve the communication link quality by utilizing excess transmit antennas at the BTS. The major differences between these techniques lie in two aspects.

First, eigenmode selection works for a system where the base station has more RF and antennas than strictly required for interference cancelation. Antenna selection, on the other hand, works for the case where the RF number is the minimum for interference cancelation, while there are additional antennas. Antenna selection requires fewer RF amplifiers than eigenmode selection and has a lower equipment cost, as RF amplifier is one of the most expensive components in a BTS. Although antenna selection naturally has suboptimal performance than eigenmode selection, it has the same diversity gain as a full system using *all* antennas. For example, Fig. 2.9 compares the average SER of eigenmode and antenna selection, in a 2-user system where each user has 3 receive antennas and receives 2 substreams. The BTS performs antenna selection if there are $M_T = 5$ RF chains, or eigenmode selection if there are $M_T \geq 6$ RF chains. There are 6 transmit antennas in either

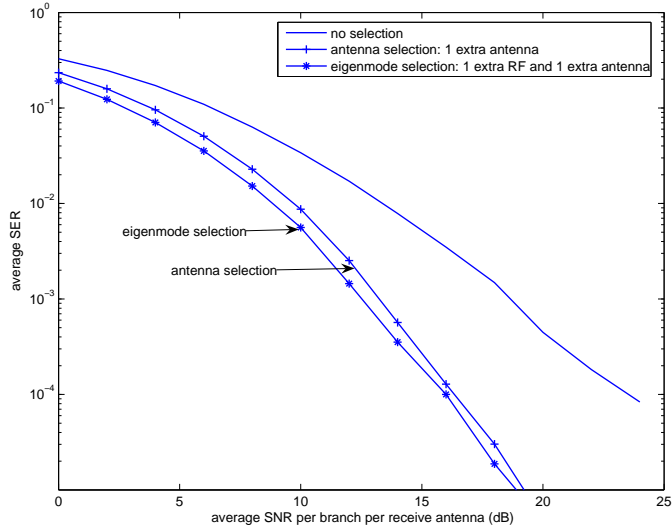


Figure 2.9: SER comparison of antenna selection and eigenmode selection with 2 users, 3 receive antennas and 2 data substreams per user, using ZF receiver.

case. The eigenmode selection method slightly outperforms antenna selection, while both methods achieve the same diversity gain and substantially outperform a system without any selection diversity. This indicates that from a financial point of view, with sufficiently spaced antennas switches are more valuable to system performance than RF chains.

Second, antenna selection has less strict system configuration requirements than the eigenmode selection. One of the necessary conditions to perform eigenmode selection is that the k^{th} user has more receive antenna than its data substreams, i.e. $N_k < M_{R,k}$. Antenna selection, however, is still feasible even if this requirement is not met, as long as the BTS antenna number M_T' is larger than the total number of receive antennas.

2.7 Performance in Correlated and Imperfect CSI Condition

In this section, the performance of the proposed selection diversity approaches is investigated with imperfect CSI at transmitter. Performance in correlated Rayleigh fading channel is also investigated.

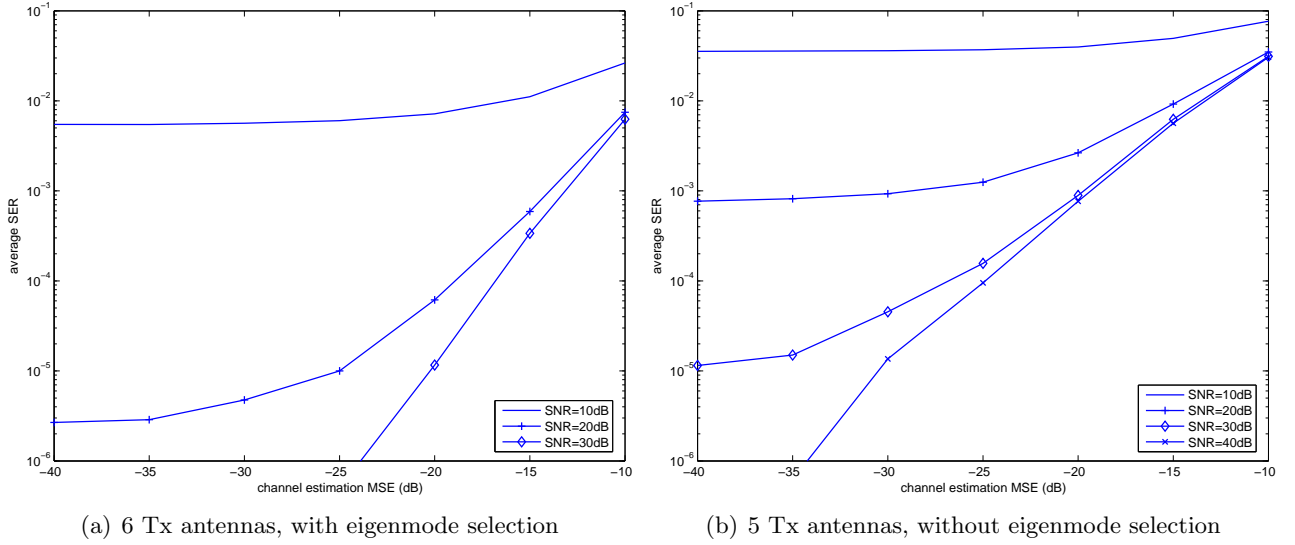


Figure 2.10: SER comparison with channel estimation error for two-user system with 3 receive antennas, 2 substreams per user.

2.7.1 i.i.d. Gaussian Channel with Imperfect Channel Knowledge

Perfect channel knowledge at the BTS is difficult to acquire, due to channel estimation/feedback error. This section provides numerical evaluation on the impact of imperfect channel knowledge on the proposed approaches. The channel estimation model in [14][48] is used, where the channel matrix known at the BTS $\check{\mathbf{H}}_k$ is given by $\check{\mathbf{H}}_k = \mathbf{H}_k + \mathbf{E}_k$, where \mathbf{H}_k is the true channel matrix and \mathbf{E}_k is the channel error. Entries of \mathbf{E}_k follows i.i.d. complex Gaussian distribution with zero mean and covariance $\sigma_{MSE}^2/2$ per real dimension. The channel knowledge error is denoted as $MSE = 10 \log_{10} \sigma_{MSE}^2$ dB.

Plotted in Fig. 2.10 are the curves of SER vs. channel mean square error (MSE) for a two-user system where each user has 3 antennas and receives 2 substreams. In (a), one extra antenna/RF chain is used for eigenmode selection. Intuitively, the SER deteriorates as channel error increases and results in larger channel mismatch. Performance is less sensitive to channel MSE when SNR is in low to moderate range, where channel noise dominates. As SNR increases, channel error plays a more important role and becomes the major per-

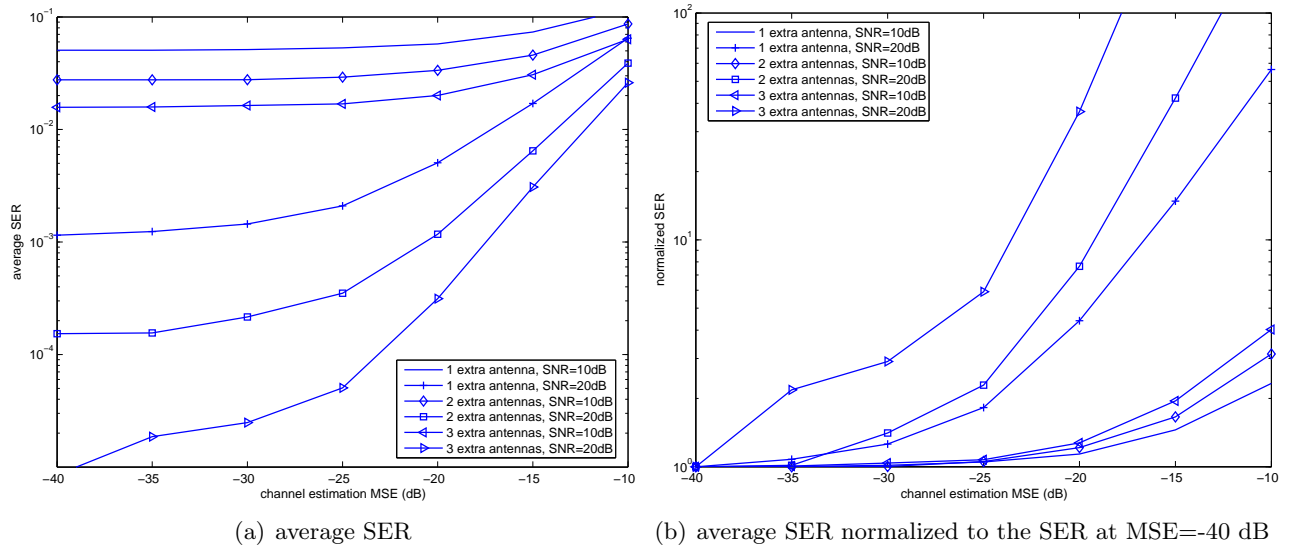


Figure 2.11: SER of antenna selection with channel estimation error for two-user system with 2 receive antennas, 2 substreams per user.

formance dominant factor. Similarly, Fig. 2.10 (b) shows the SER vs. channel MSE curves for the same system configuration, except that no eigenmode selection is performed.

The SER curves of antenna selection with channel knowledge error for a two-user system where each user has 2 antennas and receive 2 substreams is plotted in Fig. 2.11 (a). For comparison, the SER curves normalized to the SER at a MSE=-40 dB is plotted in Fig. 2.11. (b). It is observed that the performance is more sensitive to channel knowledge error when SNR is relatively high, and when more redundant antennas are used for selection.

2.7.2 Correlated MIMO Channel with Perfect Channel Knowledge

The proposed selection diversity techniques are performed with regard to an instantaneous channel realization. The channel information is collected and fed back to the BTS to determine the transmission strategy. The processing time at BTS is assumed smaller than the coherent time and hence the channel is quasi-static, which is true for most scenarios of interests. Because the proposed algorithm only deals with a particular channel realization, channel correlation does not directly impact the model of our algorithms.

Spatial correlation may negatively affect the numerical results of the proposed algorithms, due to its limits on the degrees of freedom available in the wireless link. In this section, the effects of channel correlation are numerically evaluated. The exponentially correlated model and IEEE 802.11N model are used for evaluation. It is assumed that correlation exists between all elements of the transmit antenna array, and between the elements of the receive antenna array of *each* mobile. Correlation between antennas of different users are omitted, due to their well separated geographic locations.

Exponentially Correlated MIMO Model: Denote a flat-faded MIMO channel matrix of user k as \mathbf{H}_k . The spatial correlation between the channel matrix elements is modeled as

$$\mathbf{R}_{\mathbf{H}_k} = \mathcal{E} \left(\text{vec}(\mathbf{H}_k) \text{vec}(\mathbf{H}_k)^H \right) = \mathbf{R}_{t,k}^T \otimes \mathbf{R}_{r,k}, \quad (2.31)$$

where \otimes represents the Kronecker product. The $M_T \times M_T$ transmit correlation matrix $\mathbf{R}_{t,k}$ and the $M_{R,k} \times M_{R,k}$ receive correlation matrix $\mathbf{R}_{r,k}$ denote the correlations of the rows and the columns of \mathbf{H}_k . The exponentially correlated channel has $\mathbf{R}_{t,k}$ given as $\mathbf{R}_{t,k}^{(i,j)} = \rho_t^{|i-j|}$, where $|\rho_t| \leq 1$. $\mathbf{R}_{r,k}$ follows the same model except that ρ_r replaces ρ_t . This model has been shown to be suitable for many channels [53][6].

IEEE 802.11N Channel Model: This model provides a deeper perception into the real MIMO channel by taking into account various factors such as the angle of arrival (AOA), angle of departure (AOD), antenna array fashion and angle spread (AS). A B-model is considered which captures a non-line-of-sight (NLOS) environment. Antenna element spacing is set to half wavelength in this simulation [31].

Fig. 2.12 gives the SER and sum rate capacity of a two-user system under exponentially correlated channel, where each user has 3 receive antennas, 2 substreams, one extra BTS antenna and performs eigenmode selection. Scenarios where correlation exists at the transmitter, at the receiver, and at both side of the link are investigated, with various ρ_t and ρ_r . Clearly, channel correlation degrades both the SER and capacity performance,

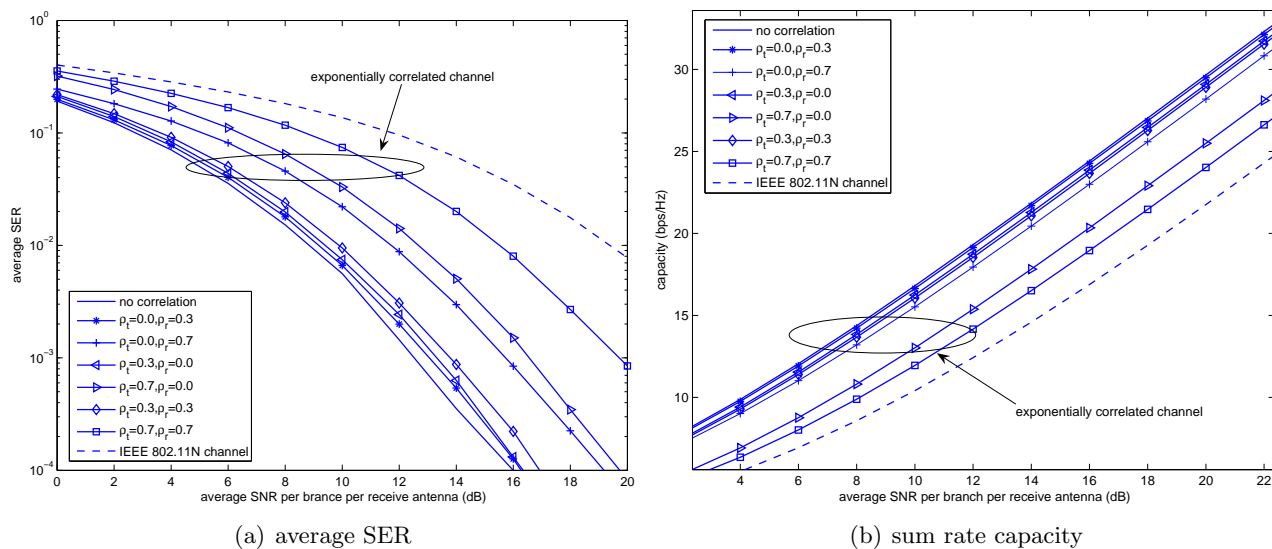


Figure 2.12: Performance of eigenmode selection in correlated channel for two-user system with 3 receive antennas, 2 substreams per user, 1 extra BTS antenna.

due the loss of spatial degrees of freedom. For example, given $\rho_t = \rho_r = 0.7$, the SER increases by a magnitude of 100, while the sum rate capacity is reduced by approximately 30% at a SNR=20 dB, compared with the uncorrelated channel. Performance degradation is more severe at the transmitter than at the receiver side (e.g, $\rho_t = 0.7, \rho_r = 0.0$ vs. $\rho_t = 0.0, \rho_r = 0.7$), which can be attributed to two facts. Firstly, spatial freedom loss due to correlation is more significant at the transmitter because it consists of more antennas. Secondly, the correlation at the transmitter will affect the performance of *all* users. The correlation at a *given* user, however, only decrease its own spatial degrees of freedom, while the degrees of freedom of other users remain unchanged or increased (e.g., see (2.3)).

The SER and sum rate capacity of antenna selection, in exponentially correlated MIMO channel for a two-user system, are shown in Fig. 2.13. Each user has 2 receive antennas, 2 substreams, while the BTS has one extra antenna. Similarly, correlation substantially degrades the performance, and such loss is more sensitive to correlation at transmitter.

For IEEE 802.11N model, the SER and capacity of eigenmode and antenna selection

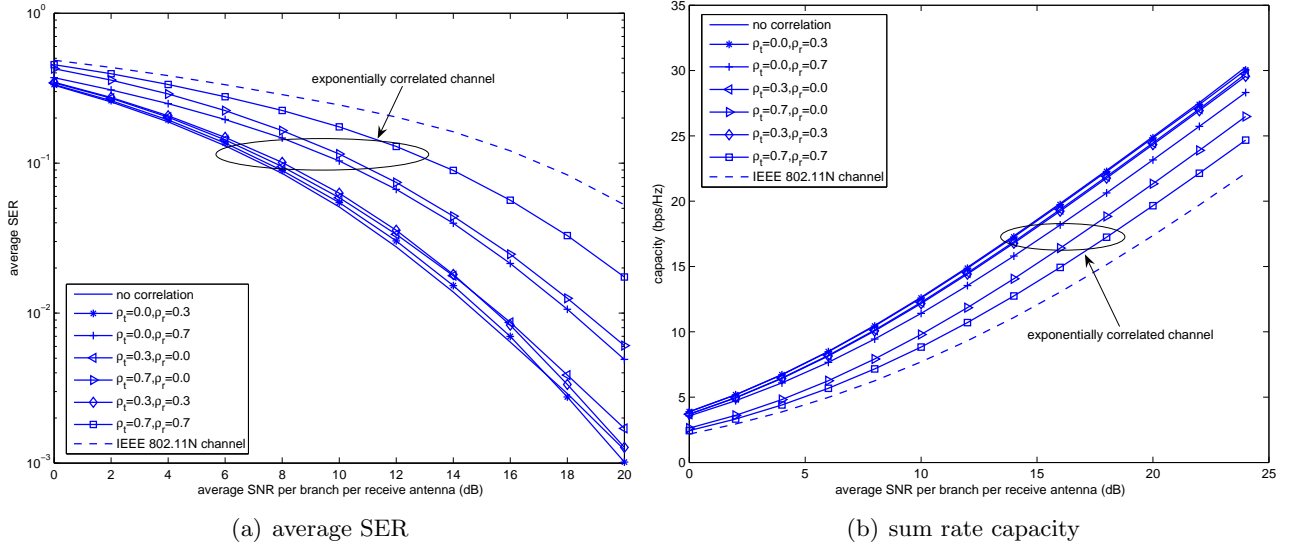


Figure 2.13: Performance of antenna selection in correlated channel for two-user system with 2 receive antennas, 2 substreams per user, 1 extra BTS antenna for selection.

are depicted in Fig. 2.12- Fig. 2.13. More SER degradation is observed compared to the exponential correlated channel model, in terms of both SER and sum rate capacity.

It is predicted that antenna selection experiences a smaller performance degradation than eigenmode selection in correlated channels. In the case of channel correlation, antenna selection may select a group of less correlated antennas, therefore the channel rank deficiency introduced by correlation is alleviated. Eigenmode selection involves all RFs and antennas in the transmission, and thus experiences more performance degradation when channel is correlated.

2.8 Conclusions

Multuser MIMO uses precoding to support multiple users in multi-antenna wireless channels. In this chapter, a novel unitary precoder design for multuser spatial multiplexing system is proposed, which uses additional antennas to improve the diversity advantage for all users simultaneously. Two specific designs are proposed: eigenmode selection and multi-user antenna selection. The principle of eigenmode selection is that every user sig-

nals on the best orthogonal basis, according to maximizing the minimum singular value of the effective channel or the sum capacity, and yet maintaining the zero inter-user interference constraint. Multi-user antenna selection operates similarly to eigenmode selection with the additional constraint that only a subset of the available transmit antennas are employed. Multi-user antenna selection requires fewer RF chains and suffers a slight performance penalty versus complete eigenmode selection. To avoid the complexity of optimum exhaustive transmit antenna search, low-complexity algorithms are proposed to reduce the computational demand.

Chapter 3

Joint User and Receive Antenna Selection for MIMO Broadcast Transmission

Multi-mode transmission is a MIMO link adaptation technique where the number of data streams, defined as mode, is adaptively adjusted to fit the wireless propagation channel. Multi-mode transmission switches between single-stream beamforming and multi-stream spatial multiplexing to exploit the channel selectively, substantially improving the spectral efficiency and error performance. Multi-mode transmission has been extensively studied for the point-to-point single-user system and offers significant performance gain [70]. In this chapter, multi-mode switching will be investigated for the downlink of a multiuser MIMO broadcast channel. Particularly, this chapter studies a sub-optimal scheme where a subset of receive antennas are selected for each user, which provides significant advantages in reducing the computational complexity and lowering the feedback requirement.

One necessary condition for BD is that the number of BTS antennas is larger than the number of data streams of all users, to completely eliminate interference. If there are a large number of mobiles, BTS cannot serve all of them simultaneously, hence a subset of users may be selected to satisfy the antenna constraint. In this chapter, users scheduling is jointly investigated with multi-mode switching. At each time instant, a subset of mobile users and receive antennas are selected to maximize the sum throughput under the BD structure. To avoid the computational complexity associated with the optimal brute-force search, two low-complexity algorithms will be proposed. The computational complexity will be analytically evaluated and compared to the exhaustive search.

3.1 Introduction

This section presents some background on multi-mode transmission of single and multiuser MIMO communication systems, then describes the multi-user scheduling problem under the BD signal structure.

3.1.1 Background on Multi-mode Transmission

Multi-mode transmission is a MIMO link adaptation technique that adaptively determines the number of data streams to suit the wireless propagation channel. The transmission mode is switched between single-stream beamforming and multi-stream spatial multiplexing to exploit the channel selectivity, offering significant performance gain [69]. Switching can be based on the error rate minimization [56, 70] or the capacity maximization [32, 57], with instantaneous channel information or channel statistical characteristics (e.g., channel correlation). Significant capacity and link robustness improvement can be achieved by exploiting the multi-mode diversity, for point-to-point single-user system [32, 56, 68, 69]

Multi-mode switching for multiuser MIMO broadcast system has not been adequately studied. Most existing multi-user literature assume a fixed transmission mode for every MS [64, 84, 89]. In this chapter, multi-mode switching for MU-MIMO system based on the BD signal structure will be studied.

3.1.2 Background on Multiuser Scheduling

In multiuser MIMO systems, transmit precoder is designed to apply the BTS antenna arrays to suppress inter-user interference. A necessary condition for BD is that the number of BTS antennas is larger than the number of data streams of all users. When there are a large number of users, the BTS cannot serve all of them simultaneously, hence a subset of users may be selected to meet the antenna constraint. The users with good channels conditions and less uncorrelated with each other will normally be selected to enhance the

sum spectral efficiency. Multi-user scheduling exploits the channel selectivity of different users and achieves multiuser diversity in scale of $\mathcal{O}(\log \log K)$ [67, 102], which greatly enhances the system performance. Brute-force search can be applied to exhaustively search over all possible user subsets, however the computational complexity is prohibitively high. Low-complexity multiuser scheduling algorithms based on BD has been studied in [84]. In [84], no multi-mode switching is considered. Each user receives a pre-determined number of data streams.

3.1.3 Joint User and Receive Antenna Selection

The throughput optimal multi-mode transmission for MU-MIMO involves exhaustively searching over all possible user and mode subsets. This brute-force search, however, has prohibitively high complexity. A suboptimal multi-mode scheme for MU-MIMO is to select a subset of users and a subset of receive antennas for each user, to maximize the sum throughput [85]. In other words, only antennas with good channel conditions are used while “bad” antennas in deep fades are disabled. In this way the spatial channel is dynamically shared among the users. Antenna selection can achieve spatial diversity gain and significantly boost the system performance, in addition to the multiuser diversity achieved with user scheduling [67, 84].

Previous work in [85] applies an exhaustive search to find the optimum user and antenna subset with the highest sum throughput. This approach, however, is still highly complicated because the number of possible user/antenna subsets increases polynomially with the number of users and the number of receive antennas per user. As a result, a low-complexity algorithm is crucial to achieve the capacity gain promised by multiuser and multi-mode diversity, while keeping the search complexity low.

In this chapter, two low-complexity joint user/antenna selection algorithms are proposed. Both algorithms aim to find the optimal user and antenna subset with the highest

sum rate capacity with the BD signal structure, which is a well approximation of the actual throughput with instantaneous link adaption under a certain error constraint [26, 36]. The first algorithm uses the effective channel energy as the selection metric, derived as a lower bound of the channel capacity, while the second algorithm greedily maximizes the sum rate capacity. Following a greedy search method, the proposed algorithms activate one receive antenna at a time, associated with the best user, until no more active receive antenna can be added to the system. The computational complexity of the proposed algorithms will be analytically evaluated and compared to that of the optimum exhaustive search method.

3.2 System and Signal Model

In this section, it is assumed that each MS applies all its receive antennas.

Consider a MU-MIMO system with K active users. A narrow-band frequency flat-fading channel is considered, with perfect CSI available at the BS [64, 89]. Denote the number of BS transmit antennas by N_t , and the number of receive antennas at user k by $N_{r,k}$. The transmit vector symbol of user k is denoted by a $L_k \times 1$ vector \mathbf{x}_k , where $\mathbf{Q}_k = E(\mathbf{x}_k \mathbf{x}_k^\dagger)$ is the transmit covariance matrix. Vector symbol \mathbf{x}_k is multiplied by a $N_t \times L_k$ precoding matrix \mathbf{T}_k and sent to the BS antenna array. At receiver k , a $L_k \times N_{r,k}$ equalizer matrix \mathbf{R}_k^\dagger is applied at the receive signal, and the post-processing signal is given as

$$\mathbf{y}_k = \mathbf{R}_k^\dagger \mathbf{H}_k \mathbf{T}_k \mathbf{x}_k + \mathbf{R}_k^\dagger \mathbf{H}_k \sum_{j=1, j \neq k}^K \mathbf{T}_j \mathbf{x}_j + \mathbf{R}_k^\dagger \mathbf{n}_k, \quad (3.1)$$

Assuming there is sufficient local scattering, \mathbf{H}_k has full rank, i.e. $\text{rank}(\mathbf{H}_k) = \min(N_{r,k}, N_t)$ with probability one.

Note that the model in (3.1) takes into account the equalizer \mathbf{R}_k explicitly. Therefore, the transmission mode L_k is explicitly reflected by the size of \mathbf{R}_k . Given the signal mode in (3.1), the zero-interference constraint with BD is to find $\mathbf{T}_k \in \mathbb{U}(N_t, L_k)$ and

equalizer matrix $\mathbf{R}_k \in \mathbb{U}(N_{r,k}, L_k)$, such that

$$\mathbf{R}_k^\dagger \mathbf{H}_k \mathbf{T}_j = \mathbf{0}, \quad \forall 1 \leq k \neq j \leq K. \quad (3.2)$$

If (3.2) is satisfied, then interuser interference is perfectly canceled and the received signal at MS k is

$$\mathbf{y}_k = \mathbf{R}_k^\dagger \mathbf{H}_k \mathbf{T}_k \mathbf{x}_k + \mathbf{R}_k^\dagger \mathbf{n}_k. \quad (3.3)$$

Let $\tilde{\mathbf{H}}_k = [\mathbf{H}_1^\dagger \mathbf{R}_1, \dots, \mathbf{H}_{k-1}^\dagger \mathbf{R}_{k-1}, \mathbf{H}_{k+1}^\dagger \mathbf{R}_{k+1}, \dots, \mathbf{H}_K^\dagger \mathbf{R}_K]^\dagger$. To satisfy the zero-interference constraint (3.2), a sufficient condition is that the precoder \mathbf{T}_k should lie in the null space of $\tilde{\mathbf{H}}_k$. Under this assumption, constraint (3.2) can be rewritten as

$$\tilde{\mathbf{H}}_k \mathbf{T}_k = \mathbf{0}, \quad 1 \leq k \leq K. \quad (3.4)$$

Denote the SVD of $\tilde{\mathbf{H}}_k$ as $\tilde{\mathbf{H}}_k = \tilde{\mathbf{U}}_k [\tilde{\mathbf{\Lambda}}_k, \mathbf{0}_{\tilde{L}_k \times (N_t - \tilde{L}_k)}] \times [\tilde{\mathbf{V}}_k^{(1)}, \tilde{\mathbf{V}}_k^{(0)}]^\dagger$ where $\tilde{L}_k = \min(\sum_{j=1, j \neq k}^K L_j, N_t)$ is the rank of $\tilde{\mathbf{H}}_k$, $\tilde{\mathbf{\Lambda}}_k = \text{diag}(\lambda_{1,k}, \dots, \lambda_{\tilde{L}_k,k})$ is the $\tilde{L}_k \times \tilde{L}_k$ diagonal matrix containing the singular values, $\tilde{\mathbf{V}}_k^{(1)}$ contains the first \tilde{L}_k right singular vectors, and $\tilde{\mathbf{V}}_k^{(0)}$ contains the last $N_t - \tilde{L}_k$ singular vectors. The columns of $\tilde{\mathbf{V}}_k^{(0)}$ form a null space basis of $\tilde{\mathbf{H}}_k$. As a result, any solution of (3.4) has columns that are linear combinations of the columns of $\tilde{\mathbf{V}}_k^{(0)}$.

Lemma 1. [64, 89] To ensure that the null space is not empty, a necessary condition to perform BD is $N_t \geq \sum_{j=1}^K L_j$. \square

Lemma 1 shows that the number of BS transmit antennas must be larger than the total number of data streams in the system. If each MS has L streams, then the maximum number of users supported simultaneously is upper bounded by $K = \lfloor \frac{N_t}{L} \rfloor$, where $\lfloor \cdot \rfloor$ is the floor operation. As a result, if there are $\tilde{K} > K$ users in the system, the BS cannot support all users at the same time. Therefore, an optimal subset of K users may be selected to maximize the sum throughput, where K is uniquely determined by N_t and $\{L_k\}_{k=1}^{\tilde{K}}$.

For simplicity, in this chapter it is assumed that $N_{r,t} = N_r$. The proposed algorithms can be easily extended to the scenario with different number of antennas per MS.

3.3 User, Mode and Antenna Selection with BD

In multi-mode transmission for MU-MIMO systems, the number of streams for each user is adaptively selected.

3.3.1 User and Mode Selection for BD

Conventional BD schemes assume a fixed number of data streams for each user, which is a suboptimal solution. Multi-mode transmission, where the number of data streams for each user is adaptively selected, can substantially improve the capacity and symbol error rate by exploiting the multi-mode diversity [56, 68]. The modes L_k denotes the size of the transmit covariance matrix \mathbf{Q}_k . For example, in the capacity optimizing problem, the number of modes are selected such that the sum capacity is maximized as

$$C_{\max} = \max_{L_k, \mathbf{T}_k, \mathbf{R}_k, \mathbf{Q}_k} \sum_{k=1}^{\tilde{K}} \log_2 \left| \mathbf{I} + \frac{1}{\sigma_n^2} \mathbf{R}_k^\dagger \mathbf{H}_k \mathbf{T}_k \mathbf{Q}_k \mathbf{T}_k^\dagger \mathbf{H}_k^\dagger \mathbf{R}_k \right|, \quad (3.5)$$

$$\text{where} \quad \sum_{k=1}^{\tilde{K}} L_k \leq N_t; \quad 0 \leq L_k \leq N_r, \quad \forall k; \quad \sum_{k=1}^{\tilde{K}} \text{trace}(\mathbf{Q}_k) \leq P, \quad (3.6)$$

and P is the sum transmit power. Note that in (3.5), MS k uses all its N_r receive antennas to receive L_k streams. Adaptively selecting the mode L_k can significantly increase the system performance by allowing a dynamic allocation of the transmission resources (i.e., up to N_t total data streams) among the users. Even though decreasing L_k for user k might reduce its own throughput, it frees up the transmission resource and benefits the other users in two aspects. First, as the null space dimension in (3.4) is increased, it is easier for the other users to satisfy the zero-interference constraint and increase their throughput. Secondly, potentially more users can be supported at the same time, thereby achieving a higher sum

throughput.

Brute-force methods can be used to exhaustively search over all possible user and mode sets in (3.5) to find the optimal one with the highest throughput. This is extremely complicated, however, due to two reasons.

- **Search Size:** The brute-force method needs to search over $\sum_{l=1}^{N_t} C_{\tilde{K}N_r}^l$ possible user and mode set. As the total number of users \tilde{K} and number of receive antennas per user N_r increase, the search size quickly becomes too large to be tractable.
- **Iterative Precoder/Equalizer Design:** For *every* possible user and mode set, an iterative algorithm is needed to find the optimum precoder and equalizer [64] for the sum throughput. This iterative calculation incurs a non-trivial computational complexity. Moreover, it was shown in [89] that this iterative algorithm does not always converge.

3.3.2 User and Antenna Selection with BD

A joint user/antenna selection algorithm was proposed in [85]. In this algorithm, each MS only selects a subset of receive antennas, and disables the remaining ones. Therefore the problem reduces to finding the optimum user and antenna subset for maximizing the sum throughput.

$$C_{\max} = \max_{L_k, \mathbf{T}_k, \mathbf{R}_k, \mathbf{Q}_k} \sum_{k=1}^{\tilde{K}} \log_2 \left| \mathbf{I} + \frac{1}{\sigma_n^2} \mathbf{R}_k^\dagger \mathbf{H}_k \mathbf{T}_k \mathbf{Q}_k \mathbf{T}_k^\dagger \mathbf{H}_k^\dagger \mathbf{R}_k \right|, \quad (3.7)$$

$$\mathbf{T}_k \in \mathbb{U}(N_t, L_k), \mathbf{R}_k \in \mathcal{R}^{(N_r, L_k)}, \sum_{k=1}^{\tilde{K}} \text{trace}(\mathbf{Q}_k) \leq P,$$

$$\sum_{k=1}^{\tilde{K}} L_k \leq N_t, 0 \leq L_k \leq N_r, \forall k, \quad (3.8)$$

where $\mathcal{R}^{(N_r, L_k)}$ is the set of $N_r \times L_k$ antenna selection matrices formed by taking L_k columns from the $L_k \times L_k$ identity \mathbf{I}_{N_r} . Note that in (3.7), L_k denotes the number of selected antennas

for user k . The number of data streams for user k is determined by water-filling over its effective channel $\mathbf{R}_k^\dagger \mathbf{H}_k \mathbf{T}_k$. Hence, adapting the number of receive antennas L_k implicitly adapts the transmission mode. In the medium to high SNR range, water-filling tends to pour water in every eigenmode. In such a case, the number of streams will be equal to the number of antennas L_k .

Joint user/antenna selection (3.7) is a special case of the multi-mode multiuser scheduling (3.5), by restricting \mathbf{R}_k to be antenna selection matrix. It provides the following advantages, compared to the multi-mode scheduling.

- **Avoidance of iterative computation** - Because \mathbf{R}_k is restricted to be antenna selection matrices, \mathbf{T}_k can be calculated in closed-form at the BS without the iterative process in [64], hence the complexity to calculate the sum throughput for a *given* user and antenna subset is substantially reduced.
- **Reduced Feedback Overhead** - In the joint user/mode selection (3.5), \mathbf{R}_k has to be computed at the BS and forwarded to MS k via a control channel. Therefore a total of $N_r L_k$ complex numbers need be fed back. For antenna selection, because \mathbf{R}_k are a special set of antenna selection matrices, the BS only needs to feedback the *index* of the optimal \mathbf{R}_k to MS k , thus the overhead (in number of bits) is greatly reduced. For example, $\log_2 \sum_{L_k=0}^{N_r} \text{card}(\mathcal{R}^{(N_r, L_k)}) = N_r$ bits are sufficient to send \mathbf{R}_k to MS k .

Numerical results show that joint user and antenna selection can increase the sum throughput by up to 15%, compared to only user selection [85].

Exhaustive search has been used in [85] to find the optimum user and antenna set with the highest sum throughput. However, a total of $\sum_{l=1}^{N_t} C_{\tilde{K}N_r}^l$ possible user/antenna sets need to be searched over, which is still very complicated.

3.4 Low-Complexity Joint User/Antenna Selection Algorithms

To exploit the benefits of multi-mode MU-MIMO while keeping the computational complexity low, two low-complexity joint user and antenna selection algorithms are proposed. The first algorithm uses effective channel energy as the selection metric, while the second proposed algorithm greedily optimizes the receive antenna and user subset. Both algorithms aim to maximize the sum rate capacity achieved under the BD signal structure, which well approximates the actual throughput with instantaneous link adaptation [26][36] under a target error rate.

Consider \tilde{K} users, and let \mathcal{A}_k and \mathcal{S}_k denote the index of the *unselected* and the *selected* antennas for MS k , where \mathcal{A}_k and \mathcal{S}_k are subsets of $\{1, 2, \dots, N_r\}$. Let $L_k = \text{card}(\mathcal{S}_k)$ denote the number of selected receive antennas for user k . For example, if $N_r = 4$ and $\mathcal{S}_k = \{1, 3\}$, it means that antenna 1 and antenna 3 of user k are chosen. Let \mathcal{K} denotes the index of active users, which is a subset of $\{1, 2, \dots, \tilde{K}\}$.

3.4.1 Effective Energy Based User/Antenna Selection Algorithm

In the first proposed algorithm, the selection metric is based on a lower bound of the sum throughput, derived in terms of the *effective channel energy*.

Recall (3.7) and note that \mathbf{Q}_k is the transmit covariance matrix of user k , determined by water-filling over the eigenmodes of the effective channel. In the medium to high SNR regime, water-filling pours approximately the same amount of power to every eigenmodes, hence \mathbf{Q}_k tends to be an identity matrix. Without loss of generality, consider a set of active users $\mathcal{K} = \{1, 2, \dots, K\}$. Assuming $\mathbf{Q}_k = \frac{P}{\sum_{l=1}^K L_l} \mathbf{I}_{L_k \times L_k}$, the capacity expression in (3.7),

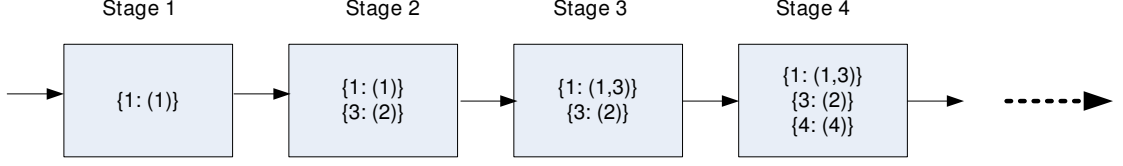


Figure 3.1: Block diagram of the proposed low-complexity user/antenna selection algorithm, with $\{k : \mathcal{S}_k\}$ denotes user k and its selected antenna set \mathcal{S}_k . For example, in stage 1, antenna 1 of user 1 is selected. In stage 2, antenna 2 of user 3 is selected.

is lower bounded by

$$\begin{aligned}
C &\geq \sum_{k=1}^K \log_2 \det \left(\mathbf{I}_{L_k \times L_k} + \frac{P}{\sigma_n^2 \sum_{l=1}^K L_l} \mathbf{H}_{\mathcal{S}_k} \mathbf{T}_k \mathbf{T}_k^\dagger \mathbf{H}_{\mathcal{S}_k}^\dagger \right) \\
&= \log_2 \prod_{k=1}^K \det \left(\mathbf{I}_{L_k \times L_k} + \frac{P}{\sigma_n^2 \sum_{l=1}^K L_l} \mathbf{H}_{\mathcal{S}_k} \mathbf{T}_k \mathbf{T}_k^\dagger \mathbf{H}_{\mathcal{S}_k}^\dagger \right) \\
&> \log_2 \prod_{k=1}^K \det \left(\frac{P}{\sigma_n^2 \sum_{l=1}^K L_l} \mathbf{H}_{\mathcal{S}_k} \mathbf{T}_k \mathbf{T}_k^\dagger \mathbf{H}_{\mathcal{S}_k}^\dagger \right) \tag{3.9}
\end{aligned}$$

where \mathcal{S}_k is the index set of the selected antennas of user k , and $\mathbf{H}_{\mathcal{S}_k} = \mathbf{R}_k^\dagger \mathbf{H}_k$ denotes the channel associated with the selected receive antennas of user k . This bound is tight in the high SNR regime, and is less tight for low SNR region.

Therefore, a lower bound on the sum capacity is derived based on the *effective channel energy*

$$E = \prod_{k=1}^K \det \left(\frac{P}{\sigma_n^2 \sum_{l=1}^K L_l} \mathbf{H}_{\mathcal{S}_k} \mathbf{T}_k \mathbf{T}_k^\dagger \mathbf{H}_{\mathcal{S}_k}^\dagger \right) \tag{3.10}$$

An energy-based selection algorithm is proposed to maximize the effective energy in (3.10), and therefore maximize the sum throughput lower bound.

Algorithm 5. *Energy-based user/antenna selection algorithm:*

1. Stage $i = 0$: Set all antennas of all MSs inactive, by letting $L_1 = \dots = L_{\tilde{K}} = 0$, $\mathcal{K} = \phi$, $\mathcal{S}_1 = \dots = \mathcal{S}_{\tilde{K}} = \phi$, $\mathcal{A}_1 = \dots = \mathcal{A}_{\tilde{K}} = \{1, 2, \dots, N_r\}$,

2. Stage $i = 1$: Find the best antenna \bar{j} of the best user \bar{k} with the largest Frobenius norm

$$(\bar{k}, \bar{j}) = \arg \max_{k=1, \dots, \tilde{K}; j=1, \dots, N_r} \|\mathbf{h}_{k,j}\|_F^2, \quad (3.11)$$

where $\mathbf{h}_{k,j}$ denotes the j th row of \mathbf{H}_k . Activate antenna \bar{j} of user \bar{k} . Let $E_{temp} = \|\mathbf{h}_{\bar{k},\bar{j}}\|_F^2$.

3. Stage $i = i + 1$, $i \leq N_t$.

(a) For every unselected antenna j of every user k , temporarily activate it and calculate the effective channel energy $E_{k,j}$ in (3.10).

(b) Find the best antenna \bar{j} of the best user \bar{k}

$$(\bar{k}, \bar{j}) = \arg \max_{k=1, \dots, \tilde{K}; j=1, \dots, N_r} E_{k,j}. \quad (3.12)$$

(c) If $E_{temp} \leq E_{\bar{k},\bar{j}}$, activate antenna \bar{j} of user \bar{k} , let $E_{temp} = E_{\bar{k},\bar{j}}$. Return to step

(3). Else, quit the algorithm.

A block diagram of the algorithm is given in Fig. 3.1. The key idea is to allocate a maximum of N_t streams to a subset of users, and find the optimum antennas to receive them. At the beginning, all receive antennas of all users are disabled. In the first step, the best receive antenna with the highest channel energy is activated. Then from the remaining inactive antennas of all users, the best receive antenna of the best user that produces the maximum *effective channel energy* (3.10) with the already activated antennas is selected and activated. This newly activated antenna is allowed to cooperate with the active receive antennas associated with the same MS, but not allowed to cooperate with the other users. The BS keeps adding more antennas to the system, until the aggregate number of active receive antennas reaches N_t , or the channel energy begins to decrease. Therefore this algorithm needs to undergo a maximum of N_t iterations, where in each iteration no more than $\tilde{K}N_r$ antennas need to be considered. As a result, the size of search space is upper

bounded by $\tilde{K}N_rN_t$, which is greatly simplified than the exhaustive search method where $\sum_{l=1}^{N_t} C_{\tilde{K}N_r}^l$ possible combinations have to be searched over. After the optimum user and antenna set is obtained, water-filling is performed to find the sum throughput.

3.4.2 Throughput-based User/Antenna Selection Algorithm

The previous algorithm greedily optimizes the effective channel energy. In the second proposed algorithm, sum throughput under the BD structure is used as the metric to select the optimum user and antenna set.

Algorithm 6. *Throughput-based user/antenna selection algorithm:*

1. Stage $i = 0$ and stage $i = 1$: Perform the same operation in the energy-based algorithm.
2. Stage $i = i + 1, i \leq N_t$.

- (a) For every unselected antenna j of every user k , temporarily activate it and calculate the sum throughput

$$C_{k,j} = \sum_{k=1}^{\tilde{K}} \log_2 \det \left(\mathbf{I} + \frac{1}{\sigma_n^2} \mathbf{H}_{S_k} \mathbf{T}_k \mathbf{Q}_k \mathbf{T}_k^\dagger \mathbf{H}_{S_k}^\dagger \right), \quad (3.13)$$

where \mathbf{Q}_k is obtained by water-filling.

- (b) Find the best antenna \bar{j} of the best user \bar{k}

$$(\bar{k}, \bar{j}) = \arg \max_{k=1, \dots, \tilde{K}; j=1, \dots, N_r} C_{k,j}. \quad (3.14)$$

- (c) If $C_{temp} \leq C_{\bar{k}, \bar{j}}$, activate antenna \bar{j} of user \bar{k} , let $C_{temp} = C_{\bar{k}, \bar{j}}$. Return to step (3). Else, quit the algorithm.

This algorithm follows a similar procedure as in the energy-based algorithm. In each iteration, the BS selects the optimal inactive receive antenna that generates the maximum

sum throughput with the already selected antennas, and activates it. The algorithm terminates when the number of total receive antennas reaches N_t , or the sum throughput begins to decrease. As a result, the number of iterations is upper bounded by N_t , where in each iteration no more than $\tilde{K}N_r$ antennas need to be searched over.

3.4.3 Numerical Results

In this section, sum throughput of the following schemes are compared.

- Iterative water-filling for DPC [51]
- Round-Robin algorithm (randomly selecting K users out of totally \tilde{K} users)
- BD with user selection but *without antenna selection* [84] (capacity based, near optimal)
- BD with the proposed throughput-based low-complexity user/antenna selection
- BD with the proposed energy-based low-complexity user/antenna selection
- BD with optimal exhaustive user/antenna selection [85]

Fig. 3.2 depicts the sum throughput in bit/s/Hz versus the total number of users \tilde{K} , for a $N_t = 12$, $N_r = 4$ MU-MIMO system and various SNR values, averaged over 2500 channel realizations.

- DPC has the highest sum throughput, because it is the capacity optimal approach for MIMO broadcast channels.
- Round-robin scheduling has the lowest sum throughput performance among all simulated broadcast transmission techniques. If $\tilde{K} \leq \lfloor M_T/M_R \rfloor$, the BS will support all \tilde{K} users at the same time with BD, and the sum throughput increases as \tilde{K} increases.

If $\tilde{K} > \lfloor M_T/M_R \rfloor$, the BS cannot support all users at the same time, therefore a random set of $\lfloor M_T/M_R \rfloor$ users are selected for each channel realization. Since the random selection does not exploit the multiuser diversity, the sum throughput becomes a constant when $\tilde{K} \geq \lfloor M_T/M_R \rfloor$.

- User selection improves throughput due to multiuser diversity. With BD, each user's channel after precoding is the projection of its original channel into the (active) users' null space. If there are two users and each of them lies in the null space of each other, the projection into each other's null space will result in a small energy loss, and hence yields a higher sum throughput. As \tilde{K} increases, it is more likely to find a subset of users whose channels are in the null space of each other, hence the throughput is improved due to multiuser diversity.
- Joint user and receive antenna selection provides both multiuser diversity and receive antenna selection diversity, thereby outperforming user selection. Compared to BD with only user selection [84], performing additional antenna selection (i.e., optimizing the number of streams) with the proposed algorithms can increase the sum throughput by up to 16%. This throughput gain is even higher compared to the round-robin scheme without any user selection. This can be explained from two aspects. (1) The total number of active receive antennas, summed over all selected users, is upper bounded by the number of BS transmit antennas. Because each user can use a smaller number of receive antennas, more users can be supported at the same time. (2) If a user's channel has a low rank, using all its receive antennas at the same time will generate a lower channel energy and subsequently reduce the channel capacity. Antenna selection avoids this scenario by choosing different antennas distributed over various users, which are less likely to be rank deficient.
- The proposed low-complexity user/antenna selection algorithms achieve approximately

98% of the optimal throughput of the brute-force search, with significantly lower complexity.

It is observed that the throughput-based algorithm slightly outperforms the energy-based algorithm. This is because channel energy is derived as a function of the throughput *lower bound*, assuming no water-filling and medium to high SNR. The throughput-based algorithm directly uses sum throughput as the selection metric, therefore performs more accurate user and antenna selection. The throughput difference, however, is very small with i.i.d. Gaussian channel, particularly at medium to high SNR range. This agrees with well-known results that water-filling only slightly improves the throughput at low SNR range, while the gain is negligible at SNR increases.

In terms of complexity, the throughput-based algorithm performs additional water-filling operation than the energy-based algorithm, and incurs a slightly higher complexity. This complexity increase, however, is very small. Analytical results in the next section will show that both algorithm have a complexity linear of \tilde{K} . Hence, the throughput-based algorithm is likely to be more suitable at low SNR range, while the energy-based algorithm should be used otherwise to reduce the computational complexity.

Fig. 3.3 plots the sum throughput versus the total number of users, for $N_t = 10$ and $N_r = 2$. Again, the proposed low-complexity user/antenna selection algorithms outperform BD with only user selection by 8%-10% in terms of sum throughput, and achieves most of the throughput with the optimal exhaustive search. With fewer receive antennas per MS, the throughput gain with joint user/antenna scheduling is less significant than the scenario of $N_r = 4$. This agrees well with the intuition: a larger receive antenna array creates more degree of freedom, therefore provides higher throughput gain.

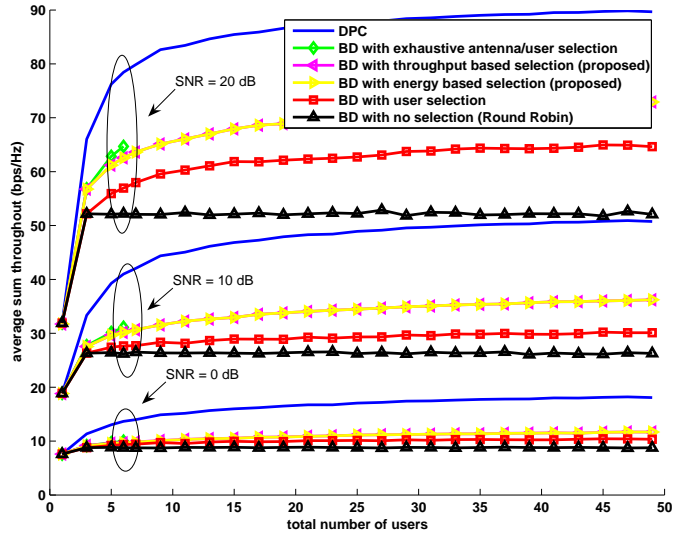


Figure 3.2: Sum throughput for $N_t = 12$, $N_r = 4$, and different number of users \tilde{K} .

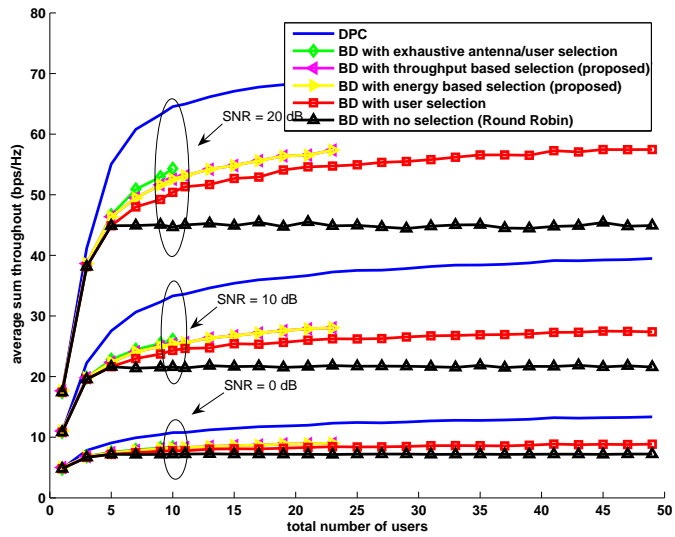


Figure 3.3: Sum throughput for $N_t = 10$, $N_r = 2$, and different number of users \tilde{K} .

3.4.4 Effects of Channel Correlations

The user and antenna selection problem discussed in this dissertation are based on instantaneous channel, where the optimum subset is selected with regard to that particular channel realization. As channel varies, the optimum user/antenna subset varies as well and needs to be selected accordingly. Channel correlation will not directly impact the system model of the proposed algorithms.

The throughput gain due to receive antenna selection will be more significant in the case of channel correlation. In such a case, the system tends to use different antennas of different users which are less correlated, and avoids using a group of highly correlated antennas of the same user. Therefore receive antenna selection is more advantageous in a correlated channel.

3.5 Computational Complexity Analysis

In this section, the computational complexity of the proposed user/antenna selection algorithm is analytically compared to that of the exhaustive search. Complexity is measured in terms of the number of flops φ , defined as a real floating point operation. A complex addition and multiplication have 2 and 6 flops, respectively. The complexity of several matrix operations can be found in [85].

3.5.1 Complexity of Exhaustive User/Antenna Selection

In the exhaustive search, the BS searches over all possible $\sum_{l=1}^{N_t} C_{K N_r}^l$ user/antenna combinations. For each combination, the complexity to compute the sum capacity is different, because the number of active users and the number of active antennas for each user are different. Therefore a *lower bound* on the complexity of the exhaustive search is provided, which is the best case for exhaustive search.

For a particular user/antenna combination, suppose there are totally $i \leq N_t$ active

receive antennas, distributed over K active users. The flop count to calculate \mathbf{T}_k from $\tilde{\mathbf{H}}_k$ is lower bounded by $24N_t + 48N_t^2 + 54N_t^3$. The flop count to perform SVD for $\mathbf{R}_k^\dagger \mathbf{H}_k \mathbf{T}_k$ is lower bounded by 1 ($L_k=1$). Water-filling over i streams requires $2i^2 + 6i$ flops. Therefore, flop count φ is lower bounded by

$$\varphi > \sum_{i=1}^{N_t} C_{\tilde{K}N_r}^i (K (24N_t + 48N_t^2 + 54N_t^3 + 1) + 2i^2 + 6i) \quad (3.15)$$

$$\begin{aligned} &> \sum_{i=1}^{N_t} C_{\tilde{K}N_r}^i \left(\left\lfloor \frac{i}{N_r} \right\rfloor (24N_t + 48N_t^2 + 54N_t^3) + 2i^2 + 6i \right) \\ &\approx \mathcal{O} \left(\frac{N_t^5}{N_r} C_{\tilde{K}N_r}^{N_t} \right). \end{aligned} \quad (3.16)$$

3.5.2 Complexity of Throughput-based Low-Complexity Algorithm

Similarly, an exact flop counts analysis of the algorithm is difficult because the number of active users, and the number of antennas for each active user, vary in each stage of the algorithm. Therefore an *upper bound* of the complexity is provided, which is the worse case.

1. $i = 1$: Compute the Frobenius norm of $\mathbf{h}_{k,j}$ takes $4N_t$ flops, $1 \leq k \leq \tilde{K}$, $1 \leq j \leq N_r$. Therefore the total flop count is $4N_t N_r \tilde{K}$.
2. $i = 2, \dots, N_t$: Suppose there are $i \leq N_t$ active receive antennas, distributed over $K \leq N_t$ selected users. For each selected MS k , computing \mathbf{T}_k from $\tilde{\mathbf{H}}_k$ requires fewer than $126N_t^3$ flops. Computing the eigenvalues of MS k requires fewer than $24N_r N_t^2 + 48N_r^2 N_t + 54N_t^3$ flops. Water-filling operated over the eigenmodes of the K selected MSs requires fewer than $2N_t^2 + 6N_t$ flops.

Therefore, the number of total flops is upper bounded by

$$\begin{aligned}
\varphi &< \sum_{i=2}^{N_t} (\tilde{K}N_r - i) [K (126N_t^3 + 24N_rN_t^2 + 48N_r^2N_t + 54N_t^3) + 2N_t^2 + 6N_t] \\
&\quad + 4N_rN_t\tilde{K} \\
&< \sum_{i=2}^{N_t} (\tilde{K}N_r) [N_t (126N_t^3 + 24N_rN_t^2 + 48N_r^2N_t + 54N_t^3) + 2N_t^2 + 6N_t] \\
&\quad + 4N_rN_t\tilde{K} \\
&\approx \mathcal{O}(\tilde{K}N_rN_t^5). \tag{3.17}
\end{aligned}$$

3.5.3 Complexity of Energy-based Low-Complexity Algorithm

An *upper bound* of the complexity of the proposed algorithm is developed which gives the worse case.

1. $i = 1$: Calculating the Frobenius norm of $\mathbf{h}_{k,j}$ requires $4N_t$ flops, so the total number of flops is $4N_tN_r\tilde{K}$.
2. $i = 2, \dots, N_t$: For each selected MS k , computing \mathbf{T}_k from $\tilde{\mathbf{H}}_k$ requires fewer than $126N_t^3$ flops. Computing the sum energy $E_{k,j}$ requires less than $12N_t^3$ flops. The total flops is upper bounded by

$$\begin{aligned}
\varphi &< \sum_{i=2}^{N_t} (\tilde{K}N_r - i) [K \times (126N_t^3 + 12N_t^3)] + 4N_rN_t\tilde{K} \\
&\approx \mathcal{O}(\tilde{K}N_rN_t^5). \tag{3.18}
\end{aligned}$$

In summary, the proposed low-complexity user/antenna scheduling algorithms have a complexity growing linearly with the total number of users \tilde{K} and the number of receive antennas per user N_r . Intuitively, this can be explained as follows.

- The number of iterations is upper bounded by N_t , because the algorithm terminates if N_t receive antennas are chosen.

- In each iteration, the number of receive antennas to search over is upper bounded by $\tilde{K}N_r$, which is the total number of antennas at mobile terminal side.

Therefore the maximum number of antennas to search over is approximately $\tilde{K}N_rN_t$, which scales linearly with \tilde{K} . The exhaustive user/antenna scheduling, however, has a complexity

$$\begin{aligned} \sum_{l=1}^{N_t} C_{\tilde{K}N_r}^l &> C_{\tilde{K}N_r}^{N_t} \\ &= (\tilde{K}N_r) \times (\tilde{K}N_r - 1) \times \cdots (\tilde{K}N_r - N_t + 1) \\ &\approx (\tilde{K})^{N_t} (N_r)^{N_t}, \end{aligned}$$

as $\tilde{K} \rightarrow \infty$. Because N_r and N_t are fixed numbers, the complexity grows polynomially with \tilde{K} .

The ratio of complexities of the proposed and exhaustive search is upper bounded by

$$\eta \leq \frac{\tilde{K}N_rN_t^5}{\frac{N_t^5}{N_r}C_{\tilde{K}N_r}^{N_t}} = \frac{\tilde{K}N_r^2}{C_{\tilde{K}N_r}^{N_t}}. \quad (3.19)$$

An upper bound of the complexity ratio η is plotted in Fig. 3.4. For example, η is less than 4.7189×10^{-8} for a MU-MIMO system with $\tilde{K} = 20$, $N_t = 10$, $N_r = 2$. Hence the proposed algorithms significantly reduce the search complexity, and make user/antenna selection a practical technique to exploit the multiuser and multi-mode switching gain for MU-MIMO systems.

The throughput-based algorithm performed additional water-filling operation than the energy-based algorithm, and incurs a higher complexity. This complexity increase, however, is very small. Because the two proposed algorithm have similar throughput performance as shown in Fig. 3.2 and Fig. 3.3, we conclude that the throughput-based algorithm should be used at low SNR range, and the energy-based algorithm should be used otherwise to reduce the computational complexity.

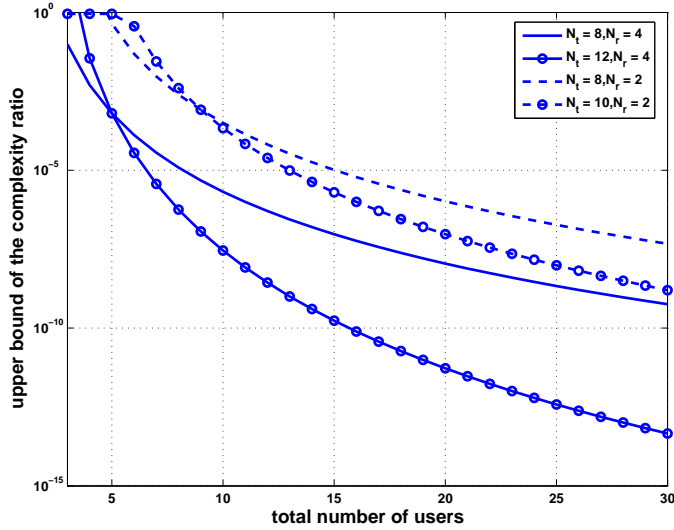


Figure 3.4: Upper bound of the complexity ratio of the proposed low-complexity method and the brute-force search.

3.6 Conclusions

In this chapter, multiuser multi-mode switching for MIMO broadcast systems with BD is studied, in the framework of joint user/antenna selection. The objective is to obtain the optimal user and antenna set to maximize system sum throughput. To avoid the prohibitive computational complexity of the brute-force search, two near-optimal user/antenna selection algorithms are proposed, which have linear complexity in $\tilde{K}N_r$. Simulation results demonstrate that the proposed low-complexity algorithms achieve approximately 98% of the optimal throughput of the exhaustive search, and outperform conventional BD without user scheduling and BD with only user selection. Future work will focus on the generalization of the proposed algorithm to include fairness constraint and delay constraint.

Chapter 4

Uplink Power Control in Multi-Cell MIMO Networks

MIMO systems have been extensively studied in the single-user and single-cell broadcast environments. The application of MIMO in an cellular network, however, is fundamentally different. Transmission of each cell acts as co-channel interference to other cells, and the network is essentially interference-limited.

In this chapter, power control is proposed as an interference management solution for the uplink transmission of cellular MIMO network. Specifically, a spatial multiplexing system where each transmit antenna sends an independent data substream is considered, with an MMSE detector at base stations. The objective is to allow *each* substream of *each* user to meet a certain signal-to-interference and noise ratio (SINR), while minimizing the sum transmit power, mutual interference and prolonging battery life. Because of the multi-antenna receiver at the base station, MIMO power control is fundamentally different from the single-antenna power control counterpart, therefore it requires novel treatment. In this chapter, different cellular MIMO power control solutions will be proposed, with various power allocation schemes, channel knowledge requirement, and performance and complexity tradeoff.

4.1 Introduction

In this section, power control for single-antenna cellular network is first introduced. Various existing single-antenna power control algorithms are presented. Then cellular MIMO power control problem is described.

4.1.1 Single-Antenna Power Control

In an interference-limited multiuser system, the performance of each user depends not only on its own transmission, but also on the transmissions of the other users. As one user increases its power to improve its performance, it generates more interference and degrades the other users' performance. Power control is a well-known technique to coordinate the transmitters such that the users can achieve a balanced QoS.

Prior power control schemes for single-input single-output (SISO) cellular systems were primarily based on a fixed SINR objective [1, 34, 44, 54, 101]. Several other researchers have studied SISO power control with a utility-based game theory approach, where utility is defined as the ratio of throughput to power [58–60, 100]. It was proven that the Nash equilibrium of the power control game corresponds to the SINR-balanced point [59, 100], where the output SINR of each user is equal to a fixed value that maximizes an *efficiency function*. Hence with such an utility definition, utility-based power control is a special case of the fixed-SINR power control. Pricing was introduced in [74, 75] to further improve the sum utility. For more complicated multi-dimensional power control problems, each user needs to determine the power over a higher dimension (e.g., frequency or spatial domain). For example, Yu *et al.* studied power control for a multicarrier interference channel in [105], and proposed an iterative waterfilling algorithm for each user to reach a target rate. This approach for interference-limited channels (like a cellular network) is quite different from the well-known iterative waterfilling for the broadcast and MAC channels (like a single-cell system), where the iteration is performed with individual [106] or sum power constraints [51]. In [58], utility-based power control was extended to the multi-carrier CDMA scenario, which is essentially a set of SISO power control problems.

A large category of SISO power control can be described with the *standard power control* framework by Yates [101]. A fixed SINR objective is typically applied. If the power control problem satisfies the positivity, monotonicity and scalability properties, an iterative

standard power control algorithm can be used to obtain the optimal solution.

4.1.2 Multi-Antenna Power Control

Theoretical and simulation results show that conventional MIMO techniques designed for single-user system perform poorly in a multi-cell environment [13, 25]. Novel techniques for dealing with interference are therefore critical to make MIMO viable in cellular networks. A significant amount of prior work on MIMO cellular systems focused on capacity analysis and receiver design for interference mitigation. [8, 13, 29, 30]. Multi-cell MIMO power control has not been adequately studied. This research will adopt a minimum SINR constraint, because it is a critical QoS metric for circuit-switching and even packet-switching data networks [11, 55]. Many delay-sensitive data applications (e.g., VoIP, video streaming) need a SINR guarantee to maintain these services.

The cellular MIMO power control problem in this dissertation is different from prior power control research in several aspects. First, it is a non-orthogonal problem where each antenna interferes with *all* antennas of *all* users, hence it includes previous orthogonal multi-carrier algorithms [58, 105] as special cases. Secondly, unlike in the SISO system where interference on each receive antenna is solely *a linear scalar function of the power*, the effect of interference in MIMO system relies on the specific MIMO receiver structure. Since MIMO receivers are typically non-linear in terms of transmit power vector, which will be discussed in the following sections, the interference is also non-linear and is correlated via the eigenspaces of the channel matrices. On one hand, interference from one transmit antenna does not scale linearly with its power. On the other hand, if one transmit antenna alters its power, interference from other co-cell transmit antennas to the remaining cells will also change even if their power remains constant. Given these fundamental differences, the existing SISO schemes cannot be directly applied even by considering each transmit antenna as an independent user.

To address these issues, two power control techniques are proposed in this dissertation. In the first method, a user's power is equally distributed on its transmit antennas. A lower bound on the post-processing SINR with a linear MMSE receiver is derived, expressed in terms of an eigenvalue approximation of both the desired and interfering users' channel. Using this bound, the MIMO power control problem is formulated in a similar framework in the SISO scenario, and derive closed-form optimal (in terms of the SINR bound) and low-complexity sub-optimal solutions with either full or partial channel knowledge. Intuitively, this approach enforces the worse stream of every user to meet the SINR requirement, causing excess power on antennas which better channels. To reduce the infeasibility probability, a second algorithm based on game theory is proposed that adaptively distributes transmit power on the transmit antennas. The adaptive allocation solution can more effectively exploit the variation of antenna array response, thereby resulting in a higher power efficiency. Numerical results show that adaptive power allocation reduces the sum power by approximately 80%, and leads to 10-12 dB target SINR improvement under the same infeasibility probability.

4.2 System Model

In this section, the system and signal model of the cellular MIMO problem is presented.

4.2.1 Signal Model

Consider the uplink transmission of a multi-cell system with K cells. For now it is assumed each cell consists of one base station with N_r receive antennas, and one active mobile station with N_t transmit antennas and spatial multiplexing. A narrow-band quasi-static flat-fading channel is assumed, where channel remains constant within several frames.

The received signal at the k th BS is represented as

$$\mathbf{y}_k = \sqrt{\frac{P_k d_{k,k}^{-\rho} \chi_{k,k}}{N_t}} \mathbf{H}_{k,k} \mathbf{T}_k \mathbf{x}_k + \sum_{j \neq k} \sqrt{\frac{P_j d_{k,j}^{-\rho} \chi_{k,j}}{N_t}} \mathbf{H}_{k,j} \mathbf{T}_j \mathbf{x}_j + \mathbf{n}_k, \quad (4.1)$$

where $\mathbf{x}_k \in \mathbb{C}^{N_t \times 1}$ is the transmit symbol vector from user k , satisfying $E_x(\mathbf{x}_k \mathbf{x}_k^\dagger) = \mathbf{I}_{N_t}$.

$\chi_{k,j}$, $d_{k,j}$, and $\mathbf{H}_{k,j}$ denote the log-normal shadow fading, the distance, and the channel transfer matrix from the j th MS to the k th BS, respectively. Pathloss exponent is represented by ρ and assumed the same for $\forall k$. There is no specific assumption on the small scale fading captured in $\mathbf{H}_{k,j}$, and this work applies to a variety of MIMO channels (e.g., Rayleigh, Rician, independent or correlated). Matrix $\mathbf{T}_k = \text{diag}\{\mathbf{T}_k^{(1,1)}, \dots, \mathbf{T}_k^{(N_t, N_t)}\}$ is the $N_t \times N_t$ diagonal power loading matrix of user k , P_k is the transmit power of user k , \mathbf{n}_k denotes the additive white Gaussian noise (AWGN) with zero mean and variance $E(\mathbf{n}_k \mathbf{n}_k^\dagger) = \sigma_n^2 \mathbf{I}_{N_t}$. To keep the transmit power of user k at constant, \mathbf{T}_k must satisfy

$$\text{trace}(\mathbf{T}_k \mathbf{T}_k^\dagger) = \sum_{j=1}^{N_t} |\mathbf{T}_k^{(j,j)}|^2 = N_t, \quad k = 1, 2, \dots, K. \quad (4.2)$$

The signal model in (4.1) applies to a set of multi-dimensional power control problems. For example, it incorporates the multi-carrier (OFDM) power control as a special case by modeling $\mathbf{H}_{k,j}$ as a diagonal matrix containing the subcarrier gain. Introducing off-diagonal elements in $\mathbf{H}_{k,j}$ can represent an OFDM system with inter-carrier interference, which is more general.

Spatial multiplexing is used throughout this chapter where each transmit antenna sends an independent stream. Dynamically adjusting the number of substreams has been considered in the *single-user* scenario [56, 68], but the extension to the multi-cell context is not straightforward. Power control with other signaling schemes such as beamforming or linear dispersion codes [69] is an interesting topic for future work.

To avoid the complexity associated with either multiuser receiver [29] or non-linear single-user receivers (e.g., maximum likelihood, BLAST [33]), this study is focused on linear

MMSE receiver, and defer the study on other receivers for future research. The MMSE receiver maximizes the SINR for each user, while mitigating the noise enhancement problem. The power control objective is to enforce the receive SINR γ to meet the fixed target Γ , which can be adjusted according to the propagation environment.

Two levels of channel awareness are studied in this chapter. In the first case, each BS knows the channel of both its in-cell user $\mathbf{H}_{k,k}$ and the out-of-cell users $\mathbf{H}_{k,j}, \forall j$. This case is referred to as the *full-CSI* situation. The channel information is sent back to a central controller to perform power control, or power distribution is calculated at each BS in a distributed way. In the second case, each BS knows only the channel information of its in-cell user, and This case is referred as the *self-CSI* situation.

4.2.2 Multiple Mobiles per Cell

In most practical deployments of MIMO, multiple MSs in each cell will likely be orthogonalized by TDMA, OFDMA or orthogonal CDMA to maintain the highest possible SINR [29, 30]. Although the above model implicitly assumes TDMA, other multi-access options such as SDMA, non-orthogonal CDMA can also apply the proposed approaches.

- With SDMA, multiple mobiles in the same cell occupy the same spectrum and are detected at the base station simultaneously. Suppose there are L users in the k th cell. If $N_r \geq LN_t$, the base station antenna array provides sufficient spatial diversity to decode L users with a linear receiver, therefore it is possible to stack $\mathbf{x}_k = [\mathbf{x}_{k,1}^T, \dots, \mathbf{x}_{k,L}^T]^T$, where $\mathbf{x}_{k,l}$ is the l th user's signal vector. If $N_r < LN_t$, the receive antenna array has insufficient spatial diversity to separate multiple users with a linear receiver. In such a case, SIC can be used to detect the users sequentially, and the proposed work can be applied by treating users decoded afterwards as interference. The MIMO power control techniques proposed in the rest of this chapter can be applied to both these scenarios.

- With non-orthogonal CDMA, each user also receives interference from intra-cell users which is attenuated by a spreading factor. The proposed approaches can be applied by treating the system as a KL *pseudo-cell* system, where K is the actual cell number, L is the number of mobiles per cell.

4.3 Overview of Power Control

Conventional power control objective functions include a fixed SINR target, a fixed capacity target or the maximization of utility, defined as the throughput per unit of power.

4.3.1 SISO Power Control with Fixed SINR Target

Many SISO cellular power control algorithms aim to achieve a pre-defined SINR requirement [34, 44]. Define $\mathbf{P} = (P_1, P_2, \dots, P_K)$ as the power vector. Let $I(\mathbf{P}) = (I_1(\mathbf{P}), I_2(\mathbf{P}), \dots, I_K(\mathbf{P}))$ represent the interference vector, where $I_k(\mathbf{P})$ denotes the *effective* interference that user k must overcome. The users' SINR requirement can be described by a vector inequality of the form

$$\mathbf{P} \geq I(\mathbf{P}). \quad (4.3)$$

A solution is *feasible* if there exists $\mathbf{P} \geq 0$ such that $I(\mathbf{P})$ that satisfies (4.3).

Power control for SISO systems is typically a non-convex optimization problem and difficult to solve. Prior work showed that if the interference function satisfies the *standard* property, then a unique optimal solution can be found by resorting to the following iterative algorithm

$$\mathbf{P}(t+1) = I(\mathbf{P}(t)), \quad (4.4)$$

where t denotes the time instant. An interference function $I(\mathbf{P})$ is *standard* if it satisfies [101]:

1. *Positivity*: $I(\mathbf{P}) > 0$

2. *Monotonicity: If $\mathbf{P} > \mathbf{P}'$, then $I(\mathbf{P}) > I(\mathbf{P}')$*

3. *Scalability: For all $\alpha > 1$, $\alpha I(\mathbf{P}) > I(\alpha\mathbf{P})$*

If $I(\mathbf{P})$ is a standard interference function, the iteration (4.4) is called *standard power control algorithm* and the following theorems follows. [101].

Theorem 4.3.1. *If the standard power control algorithm has a fixed point, then it is unique.*

Theorem 4.3.2. *If $I(\mathbf{P})$ is feasible, then for any initial power vector \mathbf{P} , the standard power control algorithm converges to a unique fixed point \mathbf{P}^* .*

4.3.2 Power Control with Fixed Capacity Target

In [105], Yu et al. studied the power control for a multi-carrier DSL system. The interference channel was modeled as a noncooperative game where self-interested users compete with each other to reach their target capacity. A distributed iterative algorithm was proposed, where each user applied waterfilling to maximize its own capacity, and then adjusted the power iteratively until the capacity target was obtained. This algorithm can also be applied to the cellular MIMO systems, by applying the power allocation in the frequency domain to the spatial domain.

4.3.3 Power Control for Utility Maximization

Utility can be defined in different ways. In most utility-based power control research, the fundamental definition is the throughput per unit of energy, expressed as $u = \frac{LRf(\gamma)}{MP}$, where L and M are the number of information bits and total number of bits in a packet, R is the transmission rate, P is the transmit power, and $f(\gamma)$ is the *efficiency function* representing the packet success rate. It was shown in [60, 75] that in a utility maximizing power control game, there exists a unique Nash equilibrium where no user can improve its utility given the power level of other users. This equilibrium corresponds to a point where all

users are SINR-balanced with the output SINR equal to γ^* , which satisfies $f(\gamma^*) = \gamma^* f'(\gamma^*)$. Hence, when utility is defined as above, the utility-based power control corresponds to a special case of the fixed SINR target power control problem.

4.4 MIMO Power Control with Equal Power Allocation and Full-CSI

This section presents a simple case where each user's transmit power is equally distributed to its antenna array, i.e. $\mathbf{T}_k = \mathbf{I}_{N_t}$, for $k = 1, \dots, K$.

The basic idea in this section is to enforce a group of antennas associated with the same user to transmit at the same power, and enforces the worse channel to reach the SINR target. Although this is a suboptimal approach where user with better channel is allocated with excess power, it significantly simplifies the problem formulation and enables to approximate the interference as a linear function of the power vector, therefore a similar framework as in the SISO case can be applied. A necessary and sufficient condition on the existence of a feasible solution is presented, and the closed-form solution optimal in terms of a SINR lower bound is derived. This problem is proven to fall into the *standard* power control category, and then propose a low-complexity 1-bit power control algorithm. Full CSI is assumed through this section.

4.4.1 Signal Model

With a linear MMSE receiver, an MMSE weighting matrix \mathbf{G}_k is applied to the received signal \mathbf{y}_k to obtain the estimate

$$\hat{\mathbf{x}}_k = \mathbf{G}_k \mathbf{y}_k. \quad (4.5)$$

According to [10, 29, 65], the linear MMSE receiver is given as

$$\mathbf{G}_k = \sqrt{\frac{N_t}{P_k d_{k,k}^{-\rho} \chi_{k,k}}} \mathbf{H}_{k,k}^\dagger \left(\mathbf{H}_{k,k} \mathbf{H}_{k,k}^\dagger + \sum_{j \neq k} \frac{P_j d_{k,j}^{-\rho} \chi_{k,j}}{P_k d_{k,k}^{-\rho} \chi_{k,k}} \mathbf{H}_{k,j} \mathbf{H}_{k,j}^\dagger + \frac{N_t \sigma_n^2}{P_k d_{k,k}^{-\rho} \chi_{k,k}} \mathbf{I} \right)^{-1}. \quad (4.6)$$

Denoting the post-processing SINR of the k th user's s th stream as $\gamma_{k,s}$, a lower bound on the minimum SINR of the k th user is provided as follows.

Lemma 2. Consider a cellular MIMO system with K cells. With the linear MMSE receiver, the minimum post-processing SINR of the k th user is bounded as

$$\gamma_{k,\min} = \min_{s \in [1, N_t]} \gamma_{k,s} \geq \frac{P_k d_{k,k}^{-\rho} \chi_{k,k}}{\mu_{\max} \left(\sum_{j \neq k} P_j d_{k,j}^{-\rho} \chi_{k,j} \mathbf{\Omega}_{k,j,1} + N_t \sigma_n^2 \mathbf{\Omega}_{k,j,2} \right)}, \quad (4.7)$$

where

$$\mathbf{\Omega}_{k,j,1} = \left(\mathbf{H}_{k,k}^\dagger \mathbf{H}_{k,k} \right)^{-1} \mathbf{H}_{k,k}^\dagger \mathbf{H}_{k,j} \mathbf{H}_{k,j}^\dagger \mathbf{H}_{k,k} \left(\mathbf{H}_{k,k}^\dagger \mathbf{H}_{k,k} \right)^{-1}, \quad (4.8)$$

$$\mathbf{\Omega}_{k,j,2} = \left(\mathbf{H}_{k,k}^\dagger \mathbf{H}_{k,k} \right)^{-1}, \quad (4.9)$$

and $\mu_{\max}(\cdot)$ is the maximum eigenvalue of a Hermitian matrix.

Proof: see the Appendix. □

It is easy to see that the MIMO receiver \mathbf{G}_k relies on the matrix channel and is non-linear in \mathbf{P} , hence the interference after MMSE detection is also non-linear in \mathbf{P} . As a result of the non-linearity, it is very difficult to obtain a closed-form optimal solution by solving $\mathbf{P} = I(\mathbf{P})$, thus the conventional SISO power control framework cannot be directly applied.

4.4.2 Problem Formulation

The multi-cellular MIMO power control aims to minimize the sum transmit power $P_\Sigma = \sum_{k=1}^K P_k$ subject to

$$\gamma_{k,\min} \geq \Gamma_k. \quad (4.10)$$

The constraint functions (4.10) of the optimization problems are in terms of the maximum eigenvalue $\mu_{\max} \left(\sum_{j \neq k} P_j d_{k,j}^{-\rho} \chi_{k,j} \mathbf{\Omega}_{k,j,1} + N_t \sigma_n^2 \mathbf{\Omega}_{k,j,2} \right)$ in (4.7), which cannot be expressed as a linear function of \mathbf{P} to obtain a closed-form solution as in the SISO case. To

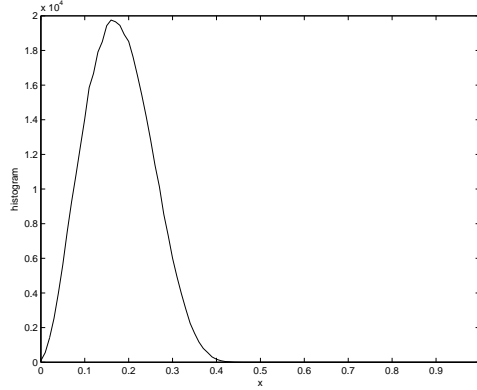


Figure 4.1: Histogram of the normalized approximation error x

ease the problem, constraint function is relaxed to be a linear function of the power. The following theorem regarding the eigenvalues of a composite matrix proves to be useful.

Theorem 4.4.1. (Weyl [47]) *Let $\mathbf{A}, \mathbf{B} \in \mathbb{C}^{n \times n}$ be Hermitian and let the eigenvalues $\mu_k(\mathbf{A}), \mu_k(\mathbf{B})$, and $\mu_k(\mathbf{A} + \mathbf{B})$ be arranged in increasing order. For each $k = 1, 2, \dots, n$, it follows that*

$$\mu_k(\mathbf{A}) + \mu_1(\mathbf{B}) \leq \mu_k(\mathbf{A} + \mathbf{B}) \leq \mu_k(\mathbf{A}) + \mu_n(\mathbf{B}). \quad (4.11)$$

Choosing $k = n$, the above theorem states that the maximum eigenvalue of a composite matrix is upper bounded by the sum of the maximum eigenvalue of each matrix. The tightness of this bound can be evaluated by the relative error

$$x = \frac{\mu_{\max}(\mathbf{H}_1 \mathbf{H}_1^\dagger) + \mu_{\max}(\mathbf{H}_2 \mathbf{H}_2^\dagger) - \mu_{\max}(\mathbf{H}_1 \mathbf{H}_1^\dagger + \mathbf{H}_2 \mathbf{H}_2^\dagger)}{\mu_{\max}(\mathbf{H}_1 \mathbf{H}_1^\dagger + \mathbf{H}_2 \mathbf{H}_2^\dagger)} \quad (4.12)$$

where elements of $\mathbf{H}_1, \mathbf{H}_2$ are i.i.d. complex Gaussian random variables with zero mean and variance 1. Fig. 4.1 plots the histogram of x obtained with 4×10^6 independent channel realizations. It is shown that for 95% of the channel realizations, the approximation error is less than 30%, and almost never exceeds 40%. Therefore this upper bound is reasonably tight.

Extending the above theorem to K matrices, the following corollary is obtained.

Corollary 4.4.2. Let $\mathbf{A}_1, \mathbf{A}_2, \dots, \mathbf{A}_K \in \mathbb{C}^{n \times n}$ be Hermitian, then

$$\sum_k \mu_{\min}(\mathbf{A}_k) \leq \mu_j \left(\sum_k \mathbf{A}_k \right) \leq \sum_k \mu_{\max}(\mathbf{A}_k), \text{ for } 1 \leq k \leq K, 1 \leq j \leq n. \quad (4.13)$$

Hence the constraint in (4.10) is relaxed to

$$\begin{aligned} \gamma_{k,\min} &\geq \frac{P_k d_{k,k}^{-\rho} \chi_{k,k}}{\mu_{\max} \left(\sum_{j \neq k} P_j d_{k,j}^{-\rho} \chi_{k,j} \boldsymbol{\Omega}_{k,j,1} + N_t \sigma_n^2 \boldsymbol{\Omega}_{k,j,2} \right)} \\ &\geq \frac{P_k d_{k,k}^{-\rho} \chi_{k,k}}{\sum_{j \neq k} P_j d_{k,j}^{-\rho} \chi_{k,j} \cdot \mu_{\max}(\boldsymbol{\Omega}_{k,j,1}) + \sigma_n^2 N_t \mu_{\max}(\boldsymbol{\Omega}_{k,j,2})}. \end{aligned} \quad (4.14)$$

Problem Formulation: The objective of the multi-cellular power optimization problem is to minimize the sum transmit power $P_{\Sigma} = \sum_{k=1}^K P_k$ subject to

$$P_k \geq \frac{d_{k,k}^{\rho}}{\chi_{k,k}} \left(\sum_{j \neq k} P_j d_{k,j}^{-\rho} \chi_{k,j} \mu_{\max}(\boldsymbol{\Omega}_{k,j,1}) + \sigma_n^2 N_t \mu_{\max}(\boldsymbol{\Omega}_{k,j,2}) \right) \Gamma_k, \quad (4.15)$$

$$P_1, P_2, \dots, P_K > 0, \quad \text{for } k = 1, 2, \dots, K. \quad (4.16)$$

Note that this formulation is based on the proposed SINR bound under the *equal allocation* assumption, and the remaining discussion in this section is based on this bound.

4.4.3 Optimal Solution

With the derivation in the previous section, the interference function $I(\mathbf{P})$ is expressed as

$$I(\mathbf{P}) = \mathbf{\Lambda}(\mathbf{F}\mathbf{P} + \mathbf{N}), \quad (4.17)$$

where $\mathbf{\Lambda} = \text{diag}\{\Gamma_1, \Gamma_2, \dots, \Gamma_K\}$ is a diagonal target SINR matrix for the K users. Referring to (4.15), \mathbf{F} is given as

$$\mathbf{F}_{k,j} = \begin{cases} 0 & k = j \\ \frac{d_{k,j}^{-\rho} \chi_{k,j}}{d_{k,k}^{-\rho} \chi_{k,k}} \mu_{\max}(\boldsymbol{\Omega}_{k,j,1}) & k \neq j \end{cases} \quad (4.18)$$

\mathbf{N} is a $N_t \times 1$ noise vector where the k th element is $\frac{N_t \sigma_n^2}{d_{k,k}^{-\rho} \chi_{k,k}} \mu_{\max}(\boldsymbol{\Omega}_{k,j,2})$. Recall that $\boldsymbol{\Omega}_{k,j,2}$ is Hermitian and positive semi-definite, thus $\mu_{\max}(\boldsymbol{\Omega}_{k,j,2}) > 0$, $\mathbf{N} > \mathbf{0}$.

To find a feasible power vector \mathbf{P} that achieves the target SINR, the parameters of the system must allow for a *feasible* solution. The following lemma describes the necessary and sufficient conditions for the existence of a feasible solution.

Lemma 3. The multi-cell MIMO power control problem has a feasible power vector \mathbf{P} satisfying the SINR constraint, if $\rho_{\mathbf{G}} < 1$ where $\mathbf{G} = \mathbf{\Lambda F}$, $\rho_{\mathbf{G}}$ is the spectral radius (magnitude of maximum singular value) of \mathbf{G} .

Proof: Proof for this lemma can be found in [1]. □

If the MIMO power control is feasible, the closed-form feasible power vector is derived as

$$\mathbf{P}^* = (\mathbf{I} - \mathbf{\Lambda F})^{-1} \mathbf{\Lambda N}. \quad (4.19)$$

It is a fixed point because it satisfies $\mathbf{P} = I(\mathbf{P})$. In the next section it will be proven that it is optimal in terms of minimum sum power. After the optimal solution is achieved, each BS only needs to send P_k^* to its MS, therefore the feedback overhead is small.

4.4.4 Standard Power Control Algorithm

The main complexity of the closed-form solution (4.19) comes from the matrix inversion and computing the maximum eigenvalues. An alternative method is to apply the iterative algorithm (4.4) that avoids matrix inversion. As discussed above, if the interference function $I(\mathbf{P})$ is standard, the iterative algorithm (4.4) converges to a unique fixed point whenever a feasible solution exists. In view of this fact, it will be proven that $I(\mathbf{P})$ in (4.15) is standard.

Lemma 4. The cellular MIMO power control problem in (4.15) satisfies the positivity, monotonicity and scalability properties and is therefore standard. Given it is feasible, for any initial power vector \mathbf{P} , the standard power control algorithm converges to a unique fixed point \mathbf{P}^* .

Proof: The positivity, monotonicity and scalability can be proven by noting that $\mathbf{\Omega}_{k,j,1}$, $\mathbf{\Omega}_{k,j,2}$ are positive semi-definite, and hence $\mu_{\max}(\mathbf{\Omega}_{k,j,1}) > 0$, $\mu_{\max}(\mathbf{\Omega}_{k,j,2}) > 0$.

Now it has been proven that the iterative algorithm converges to a fixed point, whenever the problem is feasible. Because the fixed point for any standard power control problem is unique (see Theorem 1), the solution obtained with the iterative approach should be exactly the same as the closed form solution (4.19). Finally according to Lemma 1 in [101], this unique fixed point achieves the minimum sum power among all feasible power \mathbf{P} , hence this fixed point is the optimal solution.

4.4.5 Low Complexity Iterative Power Control

The closed-form and the iterative solutions are based on the assumption that a centralized controller has perfect instantaneous channel information (e.g. $\mathbf{H}_{k,j}$ and $d_{k,j}$, $\forall k, j$). In wireless communication, the radio propagation channel varies constantly due to the changing in the environment, hence updating channel information instantaneously requires a lot of feedback overhead to the centralized controller. These facts motivate a distributed power control scheme, which allows each BS to determine the power of its MS independently.

A fixed-step, 1-bit binary control algorithm was proposed in [44]. In this algorithm, each BS measures the SINR value and commands its associated mobile to increase/decrease its power if the SINR is below/above Γ_k , expressed as

$$P_k(n+1) = \begin{cases} \delta P_k(n) & \text{if } P_k(n) \leq I_k(\mathbf{P}(n)) \\ \delta^{-1} P_k(n) & \text{if } P_k(n) > I_k(\mathbf{P}(n)) \end{cases} . \quad (4.20)$$

where $\delta > 1$ is the power control step size. This scheme requires only 1-bit UP/DOWN command every power control cycle. In addition, it is simple to implement because each receiver independently determines the power control command based on a single comparison [1].

The convergence of this 1-bit algorithm for the standard power control problem was proven in [44] for different step sizes. Since it has been proven that multi-cell MIMO power control is standard, the proof of convergence follows implicitly.

4.5 MIMO Power Control with Equal Power Allocation and Self-CSI

The perfect CSI requirement is usually not satisfied in a practical cellular system. In this section, an enhanced multi-cell MIMO power control scheme is proposed that requires only self-CSI information. The fundamental idea is to estimate the covariance matrix of the *composite noise and interference* at each BS, and then perform power control with the estimated covariance matrix. Only the sum interference covariance is required, instead of each interfering users' true channels (e.g. $\mathbf{H}_{k,j}$ and $d_{k,j}$, $\forall k, j$).

4.5.1 Problem Formulation

The received signal model is the same as in (4.1). In contrast to the full-CSI aware system, the k th BS has only knowledge of its in-cell user's channel $\mathbf{H}_{k,k}$, while $\mathbf{H}_{k,j}$, $j \neq k$ are not known.

The k th BS detects the k th user's symbol \mathbf{x}_k and obtains the estimate $\hat{\mathbf{x}}_k$. The k th user's contribution to the k th BS is subtracted from \mathbf{y}_k to obtain the composite noise estimate

$$\tilde{\mathbf{y}}_k = \mathbf{y}_k - \sqrt{\frac{P_k d_{k,k}^{-\rho} \chi_{k,k}}{N_t}} \mathbf{H}_{k,k} \hat{\mathbf{x}}_k = \sqrt{\frac{P_k d_{k,k}^{-\rho} \chi_{k,k}}{N_t}} \mathbf{H}_{k,k} (\mathbf{x}_k - \hat{\mathbf{x}}_k) + \sum_{j \neq k} \sqrt{\frac{P_j d_{k,j}^{-\rho} \chi_{k,j}}{N_t}} \mathbf{H}_{k,j} \mathbf{x}_j + \mathbf{n}_k, \quad (4.21)$$

where the first item on the right hand side is the cancellation error. With a properly chosen Γ_k and channel coding, it is reasonable to assume an acceptably low SER and accurate composite noise estimate. In addition, the noise variance σ_n^2 is normally estimated with a separate subroutine, therefore subtracting it will yield the estimate of the interference

covariance matrix as

$$\begin{aligned}
\bar{\Sigma}_k &= E \left(\left(\sum_j \sqrt{\frac{P_j d_{k,j}^{-\rho} \chi_{k,j}}{N_t}} \mathbf{H}_{k,j} \mathbf{x}_j \right) \left(\sum_j \sqrt{\frac{P_j d_{k,j}^{-\rho} \chi_{k,j}}{N_t}} \mathbf{H}_{k,j} \mathbf{x}_j \right)^\dagger \right) \\
&= \sum_{j \neq k} \frac{P_j d_{k,j}^{-\rho} \chi_{k,j}}{N_t} \mathbf{H}_{k,j} \mathbf{H}_{k,j}^\dagger.
\end{aligned} \tag{4.22}$$

Using the estimated covariance matrix, the post-processing SINR lower bound for $\gamma_{k,\min}$ is derived as

$$\begin{aligned}
\gamma_{k,\min} &\geq \frac{P_k d_{k,k}^{-\rho} \chi_{k,k}}{N_t \max_i \left\{ \left(\mathbf{H}_{k,k}^\dagger \mathbf{H}_{k,k} \right)^{-1} \mathbf{H}_{k,k}^\dagger \bar{\Sigma}_k \mathbf{H}_{k,k} \left(\mathbf{H}_{k,k}^\dagger \mathbf{H}_{k,k} \right)^{-1} + \sigma_n^2 \left(\mathbf{H}_{k,k}^\dagger \mathbf{H}_{k,k} \right)^{-1} \right\}^{(i,i)}} \\
&\geq \frac{P_k d_{k,k}^{-\rho} \chi_{k,k}}{N_t \mu_{\max} \left(\left(\mathbf{H}_{k,k}^\dagger \mathbf{H}_{k,k} \right)^{-1} \mathbf{H}_{k,k}^\dagger \bar{\Sigma}_k \mathbf{H}_{k,k} \left(\mathbf{H}_{k,k}^\dagger \mathbf{H}_{k,k} \right)^{-1} \right) + \sigma_n^2 \mu_{\max} \left(\left(\mathbf{H}_{k,k}^\dagger \mathbf{H}_{k,k} \right)^{-1} \right)} \\
&= \frac{P_k d_{k,k}^{-\rho} \chi_{k,k}}{\mu_{\max} \left(\sum_{j \neq k} P_j d_{k,j}^{-\rho} \chi_{k,j} \boldsymbol{\Omega}_{k,j,1} \right) + \sigma_n^2 N_t \mu_{\max} \left(\boldsymbol{\Omega}_{k,j,2} \right)},
\end{aligned} \tag{4.23}$$

where $\boldsymbol{\Omega}_{k,j,1}, \boldsymbol{\Omega}_{k,j,2}$ can be found in (4.8)(4.9).

As a result, the multi-cell MIMO power control problem with self-CSI is formulated as

$$P_k \geq \frac{d_{k,k}^\rho}{\chi_{k,k}} \left(\mu_{\max} \left(\sum_{j \neq k} P_j d_{k,j}^{-\rho} \chi_{k,j} \boldsymbol{\Omega}_{k,j,1} \right) + \sigma_n^2 N_t \mu_{\max} \left(\boldsymbol{\Omega}_{k,j,2} \right) \right) \Gamma_k, \tag{4.24}$$

$$P_1, P_2, \dots, P_K > 0, \quad \text{for } k = 1, 2, \dots, K. \tag{4.25}$$

Note that this formulation is similar to the case with perfect channel knowledge as in (4.15). The key observation is that it involves the maximum eigenvalue of the composite noise covariance matrix which can be estimated, rather than the covariance matrix of *each* user.

4.5.2 Standard Power Control Algorithm

Similar to the full-CSI scenario, it can be proven that $I(\mathbf{P})$ in (4.24) is a standard function, therefore the self-CSI problem is a standard power control problem.

Lemma 5. The interference function in (4.24) satisfies the positivity, monotonicity and the scalability properties, therefore the self-CSI power control problem is *standard*.

Proof: The positivity, monotonicity and scalability can be proven by noting $\mathbf{\Omega}_{k,j,1}$, $\mathbf{\Omega}_{k,j,2}$ are positive semi-definite and $\mu_{\max}(\mathbf{\Omega}_{k,j,1}) > 0$, $\mu_{\max}(\mathbf{\Omega}_{k,j,2}) > 0$. For brevity, the full proof is not included in the paper. \square

Because the self-CSI power control problem is standard, the iterative algorithm in (4.4) can be used to obtain the fixed point. Following Theorem 1 and 2, if the problem is feasible, then there exists a unique fixed point and the iterative algorithm converges to this unique point regardless of the initial power \mathbf{P} .

4.5.3 Discussion on Synchronization

For easier analysis, perfect synchronization is assumed among the multiple cells and users. Although this is clearly unrealizable in current systems, this assumption does not jeopardize the integrity of the results. In [101], it was proven that if $I(\mathbf{P})$ is feasible, the standard power control algorithm converges asynchronously, where some users adjust their power more frequently than other users and perform power updates with the outdated information of the other users' interference. Because it has been proven that both the full-CSI and self-CSI scenarios are standard, it follows that the proposed schemes are valid for asynchronous systems.

4.5.4 Numerical Results

Consider a cellular system where all cells are hexagonal of radius $R = 1000$ meters. A universal frequency reuse pattern is applied. Mobiles are uniformly distributed within the cells. The pathloss exponent is $\rho = 3$ for $\forall k$, and the variance of log-normal shadow-fading is 8 dB.

Fig. 4.2 demonstrates the convergence of the 1-bit algorithm in a $K = 7$ cellular

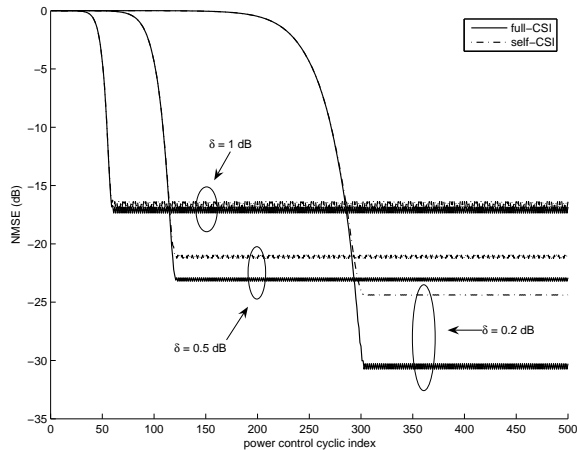


Figure 4.2: Convergence of the 1-bit power control algorithm with equal power allocation and different step size δ : $K = 7$, $\sigma_n^2 = 0.01$, $N_t = 4$, $N_r = 6$, $\Gamma = 6$ dB.

system. The target SINR is 6 dB, and the AWGN noise variance is $\sigma_n^2 = 0.01$. The vertical axis shows the normalized mean square error (NMSE) for each iteration $NMSE = \|\mathbf{P} - \mathbf{P}^*\|^2 / \|\mathbf{P}^*\|^2$, averaged over 1000 independent channel realizations. Fig. 4.2 confirms the convergence with step size δ ranging from 0.2 dB to 1 dB, with either self-CSI and full-CSI. As expected, larger δ allows faster convergence, but smaller δ allows finer resolution and lower steady-state NMSE. Because a finer resolution can help more if the available channel information is more abundant, the full-CSI case enables more NMSE reduction and provides a higher advantage than the self-CSI case, as δ decreases.

4.6 MIMO Power Control with Adaptive Power Allocation

A common issue for any power control problem is the infeasibility. Typically, users with poor channels (e.g., located near cell edge) are commanded to use more power, and generate significant interference to the adjacent cells. Other cells then need to increase their power to meet their own SINR target, which consequently force the original cell to increase its power in response. In certain channel settings, the target SINR cannot be achieved by all users simultaneously, thus infeasibility occurs.

In the previous sections, antennas of the same user are allocated with the same power, which is chosen such that the worst antenna can reach the SINR target. Because antennas with better channels are allocated with more than necessary power, this approach results in excess interference and leads to a higher infeasibility rate. An intuitively better approach is to adaptively distribute a user's power to its antenna array, such that its power is minimized subject to the SINR constraint. In contrast to the equal allocation scheme whose feasible region is a set of scalars, the feasible region of the adaptive schemes is a set of both scalars and matrices (i.e., P_k and \mathbf{T}_k), therefore it has an exponentially increasing number of possible solutions. More importantly, due to the non-linearity of the composite interference in terms of \mathbf{P} , obtaining a closed-form solution is very difficult. In this section an algorithm will be proposed where users sequentially update their own power until converging at a fixed point.

4.6.1 Signal Model

The signal model follows (4.1), where $\mathbf{T}_k \in \mathbb{C}^{N_t \times N_t}$ is the diagonal power loading matrix of user k satisfying sum power constraint $\sum_{j=1}^{N_t} \left(\mathbf{T}_k^{(j,j)} \right)^2 = N_t$, $k = 1, 2, \dots, K$. Following similar derivation in the Appendix, the post-processing SINR of stream s for cell k is given as

$$\gamma_{k,s} = \frac{P_k \left(\mathbf{T}_k^{(s,s)} \right)^2}{\zeta_{k,s}} - 1, \quad (4.26)$$

where

$$\zeta_{k,s} = \left(\left(d_{k,k}^{-\rho} \chi_{k,k} \mathbf{H}_{k,k}^\dagger \left(\sum_{j \neq k} P_j d_{k,j}^{-\rho} \chi_{k,j} \mathbf{H}_{k,j} \mathbf{T}_j \mathbf{T}_j^\dagger \mathbf{H}_{k,j}^\dagger + N_t \sigma_n^2 \mathbf{I} \right)^{-1} \mathbf{H}_{k,k} + \frac{1}{P_k} \mathbf{I} \right)^{-1} \right)^{(s,s)} \quad (4.27)$$

denotes the effective interference after MMSE processing. An estimate of $\zeta_{k,i}$ can be obtained at the k th BS by the method in Section V, therefore a partial-CSI is assumed in this

section. Denote $\mathbf{T} = [\mathbf{T}_1^T, \dots, \mathbf{T}_K^T]^T$, the objective is to find

$$\{\mathbf{P}_{\text{opt}}, \mathbf{T}_{\text{opt}}\} = \arg \min_{\mathbf{P} \geq \mathbf{0}, \text{trace}\{\mathbf{T}_k \mathbf{T}_k^\dagger\} = N_t, k \in [1, K]} \sum_{k=1}^K P_k, \quad (4.28)$$

such that $\gamma_{k,s} \geq \Gamma_k, \forall s \in [1, N_t], k \in [1, K]$.

4.6.2 Iterative Algorithm for Adaptive Power Allocation

Obtaining a closed-form optimal solution $\{\mathbf{P}_{\text{opt}}, \mathbf{T}_{\text{opt}}\}$ for the adaptive scheme is very difficult. In this section, a low-complexity suboptimal approach based on game theory is proposed. The basic idea is to sequentially update each user's transmission, by treating other users as fixed interference, until all users converge to a fixed point. First, a necessary condition of the fixed point to minimize sum power is specified, provided in the following Lemma. Each user will be enforced to satisfy this necessary condition at each iteration of the proposed algorithm, thus if the algorithm converges at a fixed point, the necessary condition will be satisfied and the sum power is minimized.

Lemma 6. Consider a K -user system. At the fixed point $\{\mathbf{P}_{\text{opt}}, \mathbf{T}_{\text{opt}}\}$, each user performs channel inversion with respect to the interference from other users, such that the effective SINR of the k th user's N_t substreams is equal to Γ_k , for $k = 1, \dots, K$.

Proof: Without loss of generality, consider user k . The remaining $K - 1$ users are treated as fixed interference, and the problem reduces to deciding $\{P_k, \mathbf{T}_k\}$ such that the N_t streams of user k meet Γ_k . It is well known in the power control literature that for a set of parallel N_t eigenchannels and fixed power P , the optimal approach for maximizing the minimum SINR is *channel inversion*, i.e., allocate power inverse proportionally to the effective channel gain $\frac{1}{\zeta_{k,s}}$. In other words, under a given Γ_k , P_k is minimized by enforcing $\gamma_{k,s} = \Gamma_k$, for $s \in [1, N_t]$, otherwise P_k can always be decreased while meeting Γ_k . \square

Lemma 5 suggests that the optimum power loading follows the *channel inversion* principle. Consider $\frac{1}{\zeta_{k,s}}$ as the *effective* channel gain, antennas with good channels are

allocated less power, while antennas in deep fades are given more power to meet the SINR target. This is different from the waterfilling approach where more power is given to better channels.

The merit of Lemma 5 is that it specifies a criterion to perform power adaptation for each user. An iterative algorithm is proposed as follows. At each iteration, $\{P_k, \mathbf{T}_k\}$ is optimized from user 1 to user K in numerical order. For each user k , treat the other users as interference and assume they maintain the power in the previous iteration, and optimize $\{P_k, \mathbf{T}_k\}$. Power optimization is conducted according to channel inversion (e.g., Lemma 5) to minimize the power of *each* single user. This process repeats until a fixed point is reached.

Algorithm 7. Iterative Channel Inversion Power Control

1. Let $i = 0$, set the initial power vector $\mathbf{P}^0 = (0, 0, \dots, 0)$, where $P_k^0 = 0$ is the initial power level for user k . Let $\mathbf{T}^0 = [\mathbf{T}_1^0; \dots; \mathbf{T}_K^0] = [\mathbf{I}_{N_t}; \dots; \mathbf{I}_{N_t}]$ be the initial power loading matrix.

2. Let $i = i + 1$.

For $k = 1$ to K ,

(a) Given $\{\mathbf{P}^{i-1}, \mathbf{T}^{i-1}\}$, compute the effective interference $\zeta_{k,s}$ with

$[\mathbf{T}_1^n, \dots, \mathbf{T}_{k-1}^n, \mathbf{T}_{k+1}^{n-1}, \dots, \mathbf{T}_K^{n-1}]$ and $[p_1^n, \dots, p_{k-1}^n, p_{k+1}^{n-1}, \dots, p_K^{n-1}]$ as in (4.27), for $s \in [1, N_t]$.

(b) Calculate the optimum loading matrix \mathbf{T}_k^i as

$$(\mathbf{T}_k^i)^{(s,s)} = \sqrt{\frac{\zeta_{k,s} N_t}{\sum_{j=1}^{N_t} \zeta_{k,j}}}, \forall s \in [1, N_t]. \quad (4.29)$$

(c) Calculate the optimum transmit power P_k^i , according to

$$P_k^i = \frac{\zeta_{k,s}}{\left((\mathbf{T}_k^i)^{(s,s)}\right)^2} (\Gamma_k + 1), \forall s \in [1, N_t]. \quad (4.30)$$

end.

end.

3. If $\max_k \|P_k^i - P_k^{i-1}\|/P_k^{i-1} \geq \eta$, go to step 2), otherwise stop. η is a small value scalar to determine whether convergence is reached.

The key idea follows the block coordinate descent algorithm, where each user iteratively updates its power with regard to the other user's power in the previous state, until the iteration converges. After the optimum strategy of user k is obtained, the k th BS send $N_t + 1$ numbers (i.e. $P_{k,\text{opt}}, \mathbf{T}_{k,\text{opt}}$) to the k th mobile, where $\mathbf{T}_{k,\text{opt}}$ is diagonal. The feedback can be implemented on the specific feedback channel, such as in WiMAX/IEEE802.16 [35].

In terms of complexity, waterfilling performs SVD and calculates the optimum water-level in each iteration, so is highly computationally demanding. In contrast, equal power allocation power control is much less complicated because it only requires the *largest eigenvalue*, and adaptive power allocation requires no eigenvalue computation at all. The feedback overhead of power control and waterfilling are approximately the same, as the power on each antenna is the information to be fed back.

4.6.3 Convergence of Adaptive Power Allocation

Let P_k denotes the scalar sum power, and $\mathbf{T}_k = \text{diag} \left\{ \mathbf{T}_k^{(1,1)}, \dots, \mathbf{T}_k^{(N_t, N_t)} \right\}$ denotes the positive semi-definite power loading matrix of user k , satisfying $\text{trace}(\mathbf{T}_k \mathbf{T}_k') = N_t$. Let the power vector of user k be $\mathbf{p}_k = P_k \times \left[\left(\mathbf{T}_k^{(1,1)} \right)^2; \dots; \left(\mathbf{T}_k^{(1,1)} \right)^2 \right]$. The objective is to show that if there exists a fixed point $[\mathbf{p}_1^F, \dots, \mathbf{p}_K^F]$ where the SINR target is reached universally for all users, the proposed algorithm will converge to this fixed point. To prove this, it will be shown that for the proposed iterative algorithm, the transmit power vector is monotonically increasing, while upper bounded by the power at the fixed point. Therefore, if a bounded fixed point exists, the proposed algorithm will converge.

To prove the convergence, we first derive the following lemma.

Corollary 1. The interference function $I_k(\cdot)$ satisfies monotonicity property. In other words,

$$I_k(\mathbf{p}_1, \dots, \mathbf{p}_{k-1}, \mathbf{p}_{k+1}, \dots, \mathbf{p}_K) \geq I_k(\mathbf{p}'_1, \dots, \mathbf{p}'_{k-1}, \mathbf{p}'_{k+1}, \dots, \mathbf{p}'_K) \quad (4.31)$$

if $\mathbf{p}_j \geq \mathbf{p}'_j$, $j \neq k$.

Proof: The received signal of each user is given by (4.1). With MMSE receiver, the post-processing data vector \hat{x} is derived as $\hat{\mathbf{x}}_k = \mathbf{G}_k \mathbf{y}_k$, where the MMSE equalizer \mathbf{G}_k is given in (4.6). Hence, the effective inter-user interference plus noise on the s th stream of user k , which is the s th element of $I_k(\cdot)$, is given as

$$\epsilon_{k,s} = \sigma_n^2 (\mathbf{G}_k \mathbf{G}'_k)^{(s,s)} + \sum_{j \neq k} \frac{d_{k,j}^{-\rho} \chi_{k,j}}{N_t} \sum_{l=1}^{N_t} p_{j,l} \left((\mathbf{G}_k \mathbf{H}_{k,j})_{(:,l)} (\mathbf{G}_k \mathbf{H}_{k,j})'_{(:,l)} \right)^{(s,s)}, \quad (4.32)$$

where $(\cdot)_{(:,l)}$ denotes the l th column of a matrix. Because the coefficients of $p_{j,l}$ ($j \neq k$, $l = 1, \dots, N_t$) are positive, the monotonicity property is established.

Proof of Convergence: The convergence is proven as follows. In the first iteration, user 1 increases its power \mathbf{p}_k^1 with regard to $\mathbf{p}_2^0, \dots, \mathbf{p}_K^0$, such that SINR of user 1 is equal to Γ_1 . The SINR of other users are equal to 0 because their power vectors are all 0. Then user 2 increases its power \mathbf{p}_2^1 with regard to $\mathbf{p}_1^1, \mathbf{p}_3^0, \dots, \mathbf{p}_K^0$, such that its SINR reaches the target Γ_2 . The SINR of user 1 will be lower than Γ_1 because user 2 transmits at a higher power now. This procedure is repeated until user K updates its power \mathbf{p}_K^1 , after which user K will have an SINR of Γ_K , and all other users' SINR are lower than their respective targets.

In the second iteration, because power for user 2 to user K are all increased, the interference received by user 1 is also increased, i.e. $I_1(\mathbf{p}_2^1, \dots, \mathbf{p}_K^1) > I_1(\mathbf{p}_2^0, \dots, \mathbf{p}_K^0)$. Therefore user 1 increases its power

$$\mathbf{p}_1^2 = (\mathbf{\Lambda}_1 + \mathbf{I}_{N_t}) \times I_1(\mathbf{p}_2^1, \dots, \mathbf{p}_K^1), \quad (4.33)$$

to meet the SINR target, i.e. $\mathbf{p}_1^2 > \mathbf{p}_1^1$. Meanwhile as user 1 increases its power to reach Γ_1 , it generates more interference to the other users and causes all other users' SINR below their targets. Next for user 2, it increases its power \mathbf{p}_2^2 to satisfy Γ_2 , as it observes higher interference $I_2(\mathbf{p}_1^2, \mathbf{p}_3^1, \dots, \mathbf{p}_K^1) > I_2(\mathbf{p}_1^1, \mathbf{p}_1^1, \dots, \mathbf{p}_K^0)$. Now user 2 meets its SINR, and causes other users' SINR below their target. This procedure is repeated until user K is updated, and then move to the next iteration. Note that throughout the iteration, *the SINR of each user is upper bounded by its SINR target.*

In summary, the power sequence \mathbf{p}_k^i is monotonically increasing, as $i \rightarrow \infty$, for $k = 1, \dots, K$. In addition, sequence \mathbf{p}_k^i is upper bounded by fixed point \mathbf{p}_k^F , if a fixed point exists. To see this, recall that the \mathbf{p}_k^i is updated as

$$\mathbf{p}_k^i = (\mathbf{\Lambda}_k + \mathbf{I}_{N_t}) \times I_k(\mathbf{p}_1^i, \dots, \mathbf{p}_{k-1}^i, \mathbf{p}_{k+1}^{i-1}, \dots, \mathbf{p}_K^{i-1}). \quad (4.34)$$

Assume user k is the first user that exceeds its fixed point \mathbf{p}_k^F and it happens in iteration i , i.e. $\mathbf{p}_k^i > \mathbf{p}_k^F$. However, this is impossible because $I_k(\mathbf{p}_1^i, \dots, \mathbf{p}_{k-1}^i, \mathbf{p}_{k+1}^{i-1}, \dots, \mathbf{p}_K^{i-1}) \leq I_k(\mathbf{p}_1^F, \dots, \mathbf{p}_{k-1}^F, \mathbf{p}_{k+1}^F, \dots, \mathbf{p}_K^F)$, as $\mathbf{p}_j^i \leq \mathbf{p}_j^F$ ($j < k$) and $\mathbf{p}_j^{i-1} \leq \mathbf{p}_j^F$ ($j > k$).

Now we have shown that \mathbf{p}_k^i is monotonically increasing and upper bounded by the fixed point \mathbf{p}_k^F . The iteration will not terminate unless all users reach their SINR target. Therefore, if there exists a fixed point where the SINR target is satisfied for all users, the proposed algorithm will converge to it.

A numerical evaluation of the convergence is demonstrated in Fig. 4.3 by plotting the NMSE vs. iteration number, where $\Gamma = 6$ dB and $\sigma_n^2 = 0.01$, averaged over 1000 channel realizations. It is shown that if there exists a feasible solution, the algorithm typically requires less than 20 iterations to converge. Convergence is slightly faster with a larger receive antenna array or a smaller transmit antenna array, due to the higher receive diversity $N_r - N_t + 1$. Similarly, a smaller number of cells lead to a faster convergence.

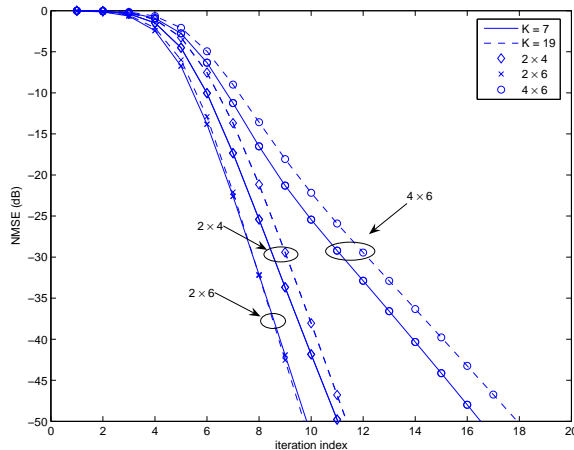


Figure 4.3: Convergence of the iterative algorithm given that the channel provides a feasible solution: $\Gamma = 6$ dB, $\sigma_n^2 = 0.01$.

4.7 Numerical Results

Consider a cellular system where all cells are hexagonal of radius $R = 1000$ meters. Mobiles are uniformly distributed within the cells. The pathloss exponent is $\rho = 3$ for $\forall k$, and the variance of log-normal shadow-fading is 8 dB. For brevity, a system with N_t transmit and N_r receive antennas is denoted as a $N_t \times N_r$ system.

4.7.1 Adaptive vs Equal Allocation Power Control

Fig. 4.4 compares the infeasibility probability of equal and adaptive power allocation, where 19 cells are considered. For each target SINR, 1000 independent channel realizations are simulated. For each channel realization, infeasibility occurs if the iterative algorithm does not converge after 1000 loops. Simulation results suggest that the adaptive algorithm substantially reduces the infeasibility probability, and consequently increases the achievable target SINR under a certain infeasibility rate. For example, for a 2×4 system, if the infeasibility is required to be less than 10%, the maximum achievable target SINR with equal power allocation is 7 dB, while adaptive power allocation can achieve a target SINR up to 17 dB.

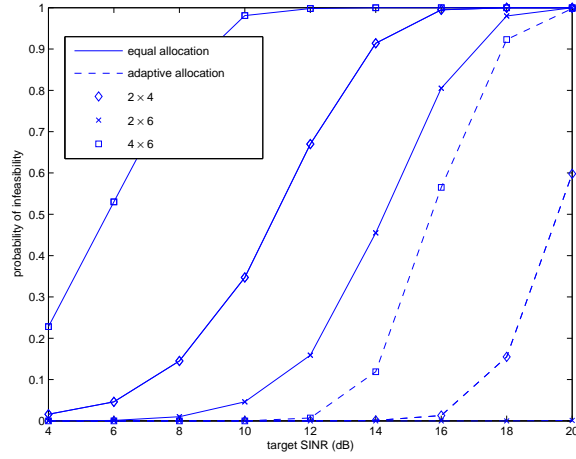


Figure 4.4: Probability of infeasibility with equal power allocation and adaptive power allocation: $K = 19$, $\sigma_n^2 = 0.01$.

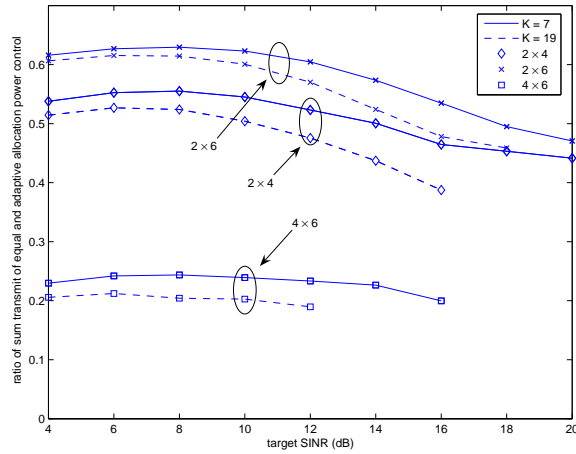


Figure 4.5: Average ratio of sum transmit power between adaptive power allocation and equal power allocation power control: $\sigma_n^2 = 0.01$.

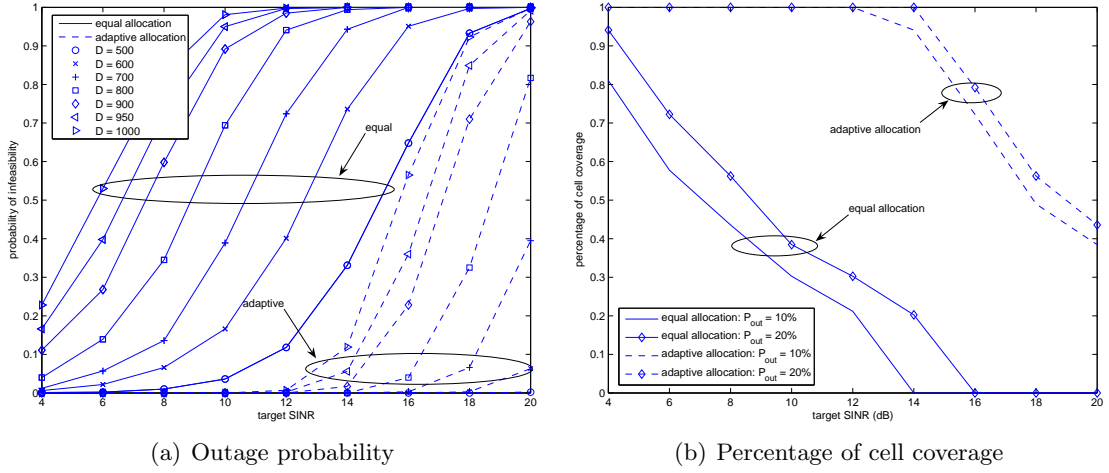


Figure 4.6: Cell coverage comparison of equal and adaptive PC with $K = 19$, $N_t = 4$, $N_r = 6$, $\sigma_n^2 = 0.01$.

Fig. 4.5 plots the ratio of average sum transmit power obtained with these two approaches, when both algorithms obtain a feasible solution. It is shown that the adaptive allocation scheme substantially reduces the sum power, by up to 80%. Additionally, power reduction is more effective when the number of users K , the number of transmit antennas N_t , and the target SINR Γ are large. This is because adaptive power allocation efficiently exploits the multiuser MIMO channels (e.g., multiuser diversity), hence power reduction is more significant with larger K . A larger receive antenna number N_r , however, reduces the channel variation by providing more receive diversity, and diminishes the improvement of the adaptive scheme.

4.7.2 Cell Coverage Evaluation

In this section the cell coverage capability is investigated by evaluating the coverage radius $D(P_{\text{out}}, \Gamma)$, defined such that if all MSs are within D meters from their associated BSs, the infeasibility probability is less than $P_{\text{out}}(D, \Gamma)$, under a target SINR of Γ . Likewise, $P_{\text{out}}(D, \Gamma)$ is defined as the outage probability.

Fig. 4.6(a) shows the outage probability P_{out} with different coverage radius D and

target Γ , for both equal and adaptive allocation schemes. The adaptive power allocation can dramatically reduce the outage probability under the same coverage and SINR constraint. Fig. 4.6(b) depicts the cell coverage rate $D^2(P_{\text{out}}, \Gamma) / R^2$ for both schemes. The adaptive power allocation can significantly increase the cell coverage rate. For example at $P_{\text{out}} = 10\%$ and $\Gamma = 8$ dB, the equal power allocation covers only 50% of the cell, while adaptive power allocation can serve the entire cell.

4.7.3 Power Control vs Iterative Waterfilling

Fig. 4.7 compares the throughput per user for both iterative waterfilling and the proposed power control schemes in a 7-cell system. The target SINR Γ translates into the target throughput for iterative waterfilling as $T = N_t \log_2(1 + \Gamma)$. The simulation setting is given as follows:

- The throughput is calculated at the *fixed point* obtained by each algorithm.
- For iterative waterfilling, the mobile's maximum power P_{max} is chosen to be significantly higher than \bar{P} , which is the average power at the fixed points of power control. Note that waterfilling can transmit at any power level from 0 to P_{max} .
- Waterfilling is infeasible if one or more users do not achieve the target throughput.
- The throughput of power control is defined to be zero in the case of infeasibility, while iterative waterfilling has a non-zero throughput even when infeasible. To make a fair comparison, the throughput is averaged over channels that are feasible for both power control and iterative waterfilling.

Fig. 4.7(a) shows that the power control schemes obtain higher average throughput than waterfilling at low-to-moderate SINRs. For 2×4 or 2×6 cases, the average throughput of power control is approximately 2 bps/Hz higher than iterative water-filing, when $\Gamma \leq 18$

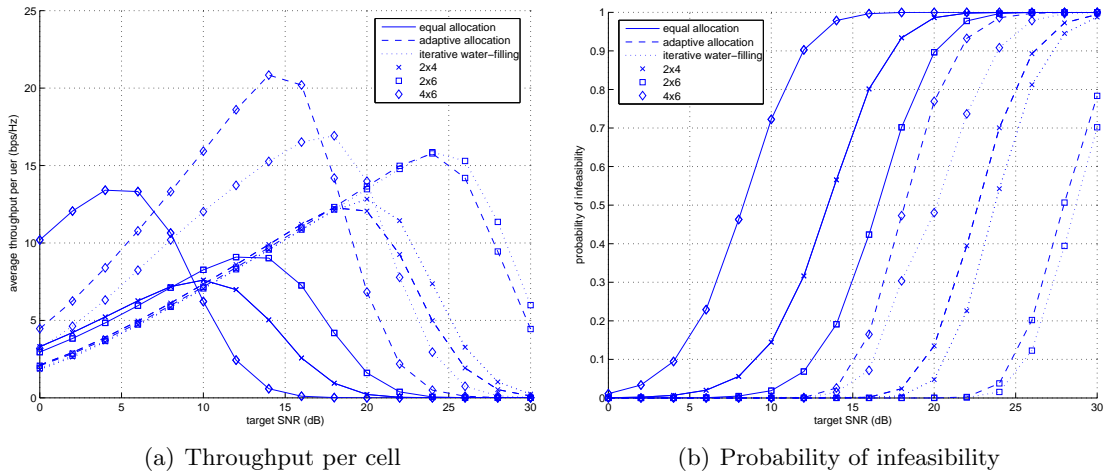


Figure 4.7: Throughput and outage probability comparison of proposed power control and the iterative waterfilling algorithm: $K = 7$, $\sigma_n^2 = 0.01$.

dB. For 4×6 case, power control has 3-5 bps/Hz higher throughput when $\Gamma \leq 14$ dB. The throughput of power control drops quickly to zero at high SINRs due to infeasibility, while waterfilling can still maintain a link. Note that power control and waterfilling are performed with completely different objectives (e.g., target SINR vs target rate). The throughput in Fig. 4.7(a) is obtained at the *fixed point* of different algorithms, which is different from the conventional problem of *throughput maximization* with a fixed sum power. Additionally, the complexity of iterative waterfilling is significantly higher, due to the iterative SVD operations. Hence power control is more effective at low-to-moderate SINRs, which is the more common case in cellular networks. Waterfilling is well suited to high SINRs, so is probably more appropriate for wireless LANs.

The performance gain of power control over waterfilling is possibly the result from the non-convexity of the sum capacity in terms of the power vector \mathbf{P} . In a single-user MIMO link, it is well-known that waterfilling is optimal due to the convexity of the capacity with regards to the power. In cellular systems, however, the sum capacity is no longer convex because each user's power appears in the denominator of the other users' SINR.

Fig. 4.7(b) compares the infeasibility probability of power control and waterfilling. The adaptive power allocation power control significantly outperforms the equal allocation scheme, approximately achieving a SINR improvement of 10-12 dB in most channel settings. Waterfilling outperforms power control in terms of infeasibility probability by 1-2 dB SINR improvement, at the cost of higher computational cost and reduced throughput at lower SINR. In summary, power control - suitably modified for MIMO systems - is a promising means for alleviating the interference problem in cellular MIMO systems.

4.8 Conclusions

Multi-dimensional power control problem for an uplink cellular MIMO spatial multiplexing system is studied. This work includes several previous OFDM power control algorithms as special cases by taking inter-carrier interference into account, and includes some utility maximizing power control as special cases if the utility maximizing SINR is used as the target. Solutions were provided where each user's power is equally or adaptively allocated to its antenna array. Simulation results show that the average throughput of adaptive power control outperforms iterative waterfilling by 2-5 bps/Hz at low-to-moderate SINRs (e.g., below 10 dB), while iterative waterfilling is more effective at high SINR. In terms of the probability of infeasibility, adaptive power allocation provides 10-12 dB target SINR improvement at the same infeasibility probability, compared to equal power allocation, which effectively increases the cell coverage and reduces power consumption at mobile terminals. Waterfilling outperforms the adaptive power allocation power control by 1-2 dB target SINR gain at the same infeasibility probability, at the cost of much higher computational complexity.

Chapter 5

Coordinated Multi-cell MIMO with Cellular Block Diagonalization (CBD)

In the previous chapters, block diagonalization has been proposed as a MIMO broadcast transmission scheme. In this chapter, BD techniques are studied in the cellular network as a cooperative MIMO transmission scheme. The idea in the context of coordinated MIMO is to apply the concept of BD across multiple cells, such that the transmission to multiple cells are collaboratively optimized. Although the concept of BD based multi-user MIMO is well understood in the context of single cell operation, for a multi-cellular network MIMO there are a few differences which mandate that the problem be solved differently. In this chapter, the design of BD precoder will be re-evaluated in the multi-cell environment. Novel designs are proposed to address the individual power constraint per base station.

5.1 Background of Coordinated Multi-cell MIMO

Despite the performance potential promised by MIMO in a single-cell channel, deploying MIMO in a commercial wireless cellular system is fundamentally different. A cellular network is essentially interference-limited. Although the problem of CCI has existed in cellular systems for many years, its effect on MIMO systems is more severe because each neighboring base station antenna element acts as a unique interfering source. Interference is a more severe problem for the downlink because complicated interference suppression is not practical for mobile terminals, which need to be power-efficient and compact. The capacity and link robustness promised by MIMO techniques have been shown to degrade severely in a multi-cell environment. As a result, interference must be properly handled to make

MIMO technique successful in a commercial cellular network.

Coordinated transmission for multi-cell MIMO systems have received a lot of attention in recent years. In coordinated MIMO systems, BTSs coordinate with each other to serve the MSs. By sharing information across BTSs and designing the downlink signal coordinately, signals from other cells may be used to assist the transmission of the desired cell instead of acting as interference. Certain BTS coordination techniques have been applied in the commercial cellular networks, such as soft-handoff, power control, etc.

In this dissertation, the application of BD techniques in the cellular network as a cooperative MIMO transmission scheme is studied. The idea in the context of coordinated MIMO is to apply the concept of BD across multiple cells.

5.2 Multi-Cell BD

In this section, the signal model of multi-cell BD is presented.

5.2.1 Problem Formulation

A clustered multi-cell BD infrastructure is proposed as the baseline. The cellular network is divided into a number of disjoint clusters, where each cluster contains a group of B adjacent cells. Typical cluster size B can be 3,4 and 7, etc. BTSs in the same cluster work together as a super BTS to cooperatively transmit to all users in that cluster.

The cluster infrastructure is adopted due to several reasons:

- **Interference mitigation with BD** - BTSs in the same cluster work together as a “super BTS”, to serve all MSs in the cluster. Intra-cluster interference is therefore perfectly eliminated. Inter-cluster interference is much weaker due to path loss.
- **Dynamically configurable cooperation strategy**: Cells in the same cluster are allowed to have a high-level of cooperation, because they are close to each other and

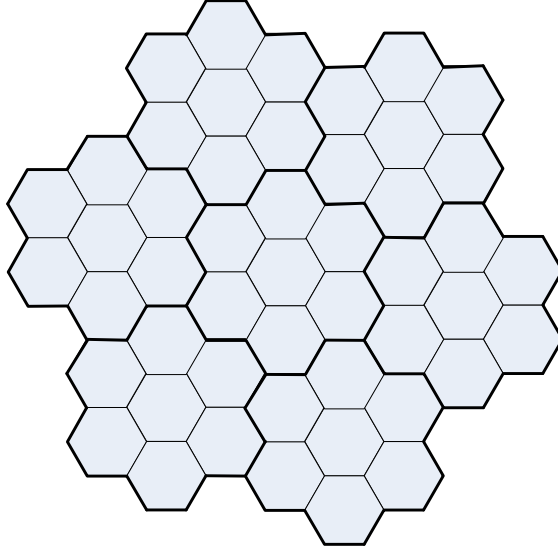


Figure 5.1: Example of the clustered cellular network: cluster size $B = 7$.

easy to share the channel/data information. Cells in different clusters are allowed to have a low-level of cooperation, sharing limited controlling information such as hand-off, user scheduling, etc.

5.2.2 Signal Model

In this section, the signal model of the multi-cell BD is introduced, under the clustered infrastructure.

Consider a cellular network with C clusters, where each cluster consists of B cells. Denote the number of transmit antennas at each BTS by N_t and the number of receive antennas at each MS by N_r . The scenario with different number of receive antennas per MS can be easily incorporated in the introduced framework, but is omitted here for brevity. The B BTSs in the same cluster to work as a super BTS with BN_t antennas, which applies BD to serve all MSs within the cluster. The downlink signal model is given as

$$\mathbf{y}_k^{(c)} = \sum_{b=1}^B \mathbf{H}_k^{(c,b)} \sum_{k=1}^K \mathbf{T}_k^{(c,b)} \mathbf{x}_k^{(c)} + \mathbf{n}_k^{(c)} + \sum_{\bar{c}=1, \bar{c} \neq c}^C \sum_{\bar{b}=1}^B \mathbf{H}_k^{(\bar{c}, \bar{b})} \sum_{k=1}^K \mathbf{T}_k^{(\bar{c}, \bar{b})} \mathbf{x}_k^{(\bar{c})} \quad (5.1)$$

where

- $\mathbf{y}_k^{(c)}$ is the $N_r \times 1$ received signal vector at MS k in cluster c .
- $\mathbf{x}_k^{(c)}$ is the $N_r \times 1$ data symbol vector for user k in cluster c . It is assumed that the number of data streams for each MS is equal to its number of receive antennas, for simplicity. The transmit covariance matrix is $\mathbf{Q}_k = E(\mathbf{x}_k \mathbf{x}_k^\dagger) = \frac{P_{\max}}{KN_r} \mathbf{I}_{N_r \times N_r}$, with power constraint $\text{trace}(\mathbf{Q}_k) = P_{\max}/K$. For simplicity, equal amount of power is allocated to each MS, and each data streams has the same amount of power. Power control can be applied to assign different power to different MSs and streams, e.g., less transmit power to a MS closer to its associated BTS. This will be considered in the future.
- P_{\max} is the sum transmit power constraint of each BTS antenna array. This constraint is constant for all BTSs.
- $\mathbf{T}_k^{(c,b)}$ is the $N_t \times N_r$ precoder for user k on the b th BTS in cluster c .
- $\mathbf{H}_k^{(c,b)}$ is the $N_r \times N_t$ channel transfer matrix from BTS b in cluster c to MS k .
- $\mathbf{n}_k^{(c)}$ is the additive white Gaussian noise at MS k in cluster c , with zero mean and variance $E(\mathbf{n}_k^{(c)} \mathbf{n}_k^{(c)\dagger}) = \sigma_n^2 \mathbf{I}_{N_r \times N_r}$.

Without loss of generality, consider cluster c . Because the B BTSs within this cluster coordinate to work as a super BTS, the signal model is rewritten as

$$\mathbf{y}_k^{(c)} = \mathbf{H}_k^{(c)} \sum_{k=1}^K \mathbf{T}_k^{(c)} \mathbf{x}_k^{(c)} + \mathbf{n}_k^{(c)} + \sum_{\bar{c}=1, \bar{c} \neq c}^C \mathbf{H}_k^{(\bar{c})} \sum_{k=1}^K \mathbf{T}_k^{(\bar{c})} \mathbf{x}_k^{(\bar{c})} \quad (5.2)$$

where

$$\mathbf{H}_k^{(c)} = \left[\mathbf{H}_k^{(c,1)} \quad \mathbf{H}_k^{(c,2)} \quad \dots \quad \mathbf{H}_k^{(c,B)} \right] \quad (5.3)$$

is the aggregate channel transfer matrix from the super BTS to user k , and

$$\mathbf{T}_k^{(c)} = \begin{bmatrix} \mathbf{T}_k^{(c,1)} \\ \mathbf{T}_k^{(c,2)} \\ \vdots \\ \mathbf{T}_k^{(c,B)} \end{bmatrix} \quad (5.4)$$

is the aggregate transmit precoder for user k over all B BTSs. The third term in (5.2) is the inter-cluster interference (ICI). Omitting the ICI, the signal model in (5.2) is exactly the same as in conventional single-cell BD, where a single super BTS transmits to multiple MSs at the same time over the same frequency band. Therefore by applying conventional BD, intra-cluster interference can be perfectly eliminated, given that all BTSs in cluster c have the information of $\mathbf{H}_k^{(c)}$ and $\mathbf{x}_k^{(c)}$, $k = 1, \dots, K$.

Lemma 5.2.1. *Denote a clustered cellular MIMO system with B BTSs per cluster, N_t transmit antennas per BTS and N_r receive antennas per MS. The maximum number of MSs in each cluster, K_{max} , is bounded by*

$$K_{max} \leq \frac{BN_t}{N_r}. \quad (5.5)$$

5.3 Precoder Design for Multi-cell BD

In this section, the precoder design for multi-cell BD is presented, to address the per-BS power constraint problem.

One of the key differences between single cell and multi-cell BD is the power constraint. In the case of single cell multi-user BD, the power constrained is applied only on the total power across all the BTS antenna elements. In the case of a multi-cellular operation, each BTS antenna array in the super BTS has an individual power constraint P_{max} . Recall that $\text{trace}(\mathbf{Q}_k) = \text{trace}(E(\mathbf{x}_k^c \mathbf{x}_k^{c\dagger})) = P_{max}/K$. The sum transmit power at BTS b is given as

$$\text{trace} \left(\sum_{k=1}^K E \left(\mathbf{T}_k^{(c,b)} \mathbf{x}_k^{(c)} \mathbf{x}_k^{(c)\dagger} \mathbf{T}_k^{(c,b)\dagger} \right) \right) \leq P_{max}$$

Substitute $E(\mathbf{x}_k^{(c)}\mathbf{x}_k^{(c)}) = \frac{P_{\max}}{K}\mathbf{I}$, the per-BTS power constraint is

$$\text{trace}\left(\sum_{k=1}^K\left(\mathbf{T}_k^{(c,b)}\mathbf{T}_k^{(c,b)\dagger}\right)\right)\leq K. \quad (5.6)$$

The conventional single-cell BD design, where the unitary $\mathbf{T}_k^{(c)}\in\mathbb{U}(BN_t, N_r)$ obtained from SVD of $\tilde{\mathbf{H}}_k^{(c)}$, does not necessarily satisfy this constraint. The precoder design has to be reconsidered in the multi-cell environment to incorporate the per-BTS constraint (5.6).

In this dissertation, the single-cell BD precoder is extended to the multi-cell BD scenario, to satisfy the per-BTS power constraint. The basic idea is very straightforward: *apply single-cell BD to obtain the initial unitary precoders, then apply a linear scaling to the unitary precoders such that transmit power on each BTS is lower than the maximum power constraint.* The resultant precoders is still unitary. First, construct the aggregate interference matrix for user k in cluster c as

$$\tilde{\mathbf{H}}_k^{(c)}=\left[\mathbf{H}_1^{(c)\dagger}\quad\cdots\quad\mathbf{H}_{k-1}^{(c)\dagger}\quad\mathbf{H}_{k+1}^{(c)\dagger}\quad\cdots\quad\mathbf{H}_K^{(c)\dagger}\right]^\dagger \quad (5.7)$$

where $\mathbf{H}_k^{(c)}$ is given in (5.3). Then, single-cell BD is conducted to calculate $\mathbf{T}_k^{(c)}$, which is unitary and satisfies

$$\tilde{\mathbf{H}}_k^{(c)}\mathbf{T}_k^{(c)}=\mathbf{0}. \quad (5.8)$$

Recall that $\mathbf{T}_k^{(c)}$ is the aggregate precoder for user k , generated by stacking the B precoders on B BTSs (5.4). As a result, the sum transmit power of BTS b is

$$\eta_b=\frac{P_{\max}}{K}\text{trace}\left(\sum_{k=1}^K\mathbf{T}_k^{c,b}\mathbf{T}_k^{c,b\dagger}\right), b=1,\dots,B. \quad (5.9)$$

In the following, the BTS with the highest sum transmit power is found.

$$b_{\text{opt}}=\arg\min_{b=1,\dots,B}\eta_b \quad (5.10)$$

Then a linear scalar ϵ is obtained to scale the transmit power of BTS b_{opt} to P_{max}

$$\epsilon = \frac{K}{\eta b_{\text{opt}}}. \quad (5.11)$$

Then this linear scalar is applied to all the precoders $\mathbf{T}_k^{(c)}, k = 1, \dots, K$, hence the final precoding matrices are

$$\mathbf{T}_k^{(c)} = \eta \times \mathbf{T}_k^{(c)}, k = 1, \dots, K. \quad (5.12)$$

Observation- After this linear scaling, BTSs b_{max} is transmitting at the maximum power P_{max} , and the power of the remaining $B-1$ BTSs is lower than P_{max} . For a particular BTS $b \in [1, B]$, its transmit power is

$$P_b = P_{\text{max}} \frac{\text{trace} \left(\sum_{k=1}^K \left(\mathbf{T}_k^{(c,b)} \mathbf{T}_k^{(c,b)\dagger} \right) \right)}{\text{trace} \left(\sum_{k=1}^K \left(\mathbf{T}_k^{(c,b_{\text{opt}})} \mathbf{T}_k^{(c,b_{\text{opt}})\dagger} \right) \right)} \quad (5.13)$$

Because $\mathbf{T}_k^{(c,b)}, k = 1, \dots, K$ are highly uncorrelated, it is conjectured that P_1, P_2, \dots, P_B are not significantly different from each other.

The per base station power constraint problem has also been considered in other work, e.g., [52]. The approach is to adjust the power of *information data* to users such that the effective transmit power of each base station meets the highest power constraint. This can be solved by various convex optimization tools.

5.4 Future Work with Multi-Cell BD

The above discussed cellular BD precoding requires that channel information and data of users are completely shared among a cluster of base stations to construct the down-link signals. This assumption, however, is not always satisfied in a commercial cellular network. It is easier to exchange channel information among base stations with a high speed backbone network, given that channel state information varies slowly in a low-mobility environment. Information data to users, however, changes much more rapidly with respect

to the wireless channel, especially for real time wireless services. Therefore it is much more difficult to completely share the information data of users across different cells. In this section, the implication of cooperative cellular MIMO system design with different channel requirements are discussed, along with the future research topics.

5.4.1 Joint and Disjoint Processing at Transmitter

For single-cell multi-user BD, a centralized base station knows the channel and information data to all users. Therefore it is possible to construct the BD precoder at the transmitter.

In the case of multi-cellular multi-user BD, cooperative cellular MIMO systems assume that base stations across different cells can collaborate with each other to transmit to users in different cells. The framework of cooperative MIMO assumes that there is a high speed backbone network connecting all base stations as a “super base station” to enable the cooperative downlink. It is interesting to investigate different degrees of constraint on the spatial processing at the transmitter to see the information sharing among base stations impact the downlink signaling design. In this section, it is assumed that channel information is shared across base stations.

- **Data is completely shared.** In such a case it is possible to perfectly orthogonalize the downlink multiuser channel and completely eliminate interference with the proposed cellular BD structure in the previous chapter. The advantage of this method is that different users will operate in non-interfering single-user MIMO channels after precoding, hence transmission optimization for each of them can be independently conducted.
- **Data is completely unshared.** Compared to the data of users, channel state information is easier to be shared among base stations with a high speed backbone

network, assuming that the channel state information varies slowly in a low-mobility environment. Complete sharing of information data of users, however, could be quite difficult because user data changes more rapidly compared to the wireless channel. In this case, it is not possible to completely block diagonalize the channel. Power control is a candidate solution in this case to optimize the power and reduce interference, because it simply relies on the channel state information to optimize the transmit power under a given QoS constraint, without requirement of users' data.

- **Data is partially shared.** Wyner infinite linear or circular cellular model [99] has been considered in many cooperative cellular literature as a simplified system model. Although it is hardly realistic in real practice, this model provides some insights in the multi-cell MIMO environments and allow to develop some closed-for analytical results. Wyner model assumes that each cell only receives interference from its (one or two) adjacent cells, where interference is modeled by a constant scaling factor ($\alpha > 1$). Analytical capacity results with this model has been derived for the uplink MAC channel [41, 80, 81, 86, 88], and for the downlink BC channel in [82] with a *sum power constraint* over all BTSs, and in [88] with *per base station power constraint*.

Wyner model makes it much more easier to deploy the cellular BD signaling model, because each cell only receives interference from its adjacent cells. In this case, information data needs to be shared in only *adjacent cells* and much more realistic than sharing across the entire cellular network. An information theoretical analysis on the capacity is possible by assuming a “dirty-paper” coding based interference pre-cancellation across adjacent cells, following the results in [79, 87, 88]

5.4.2 Multiuser Scheduling

How to schedule different users across different BTSs of a super BTS is another important research topic in the cellular MIMO context.

- TDMA: All resources across all BTS is given to a single user. This scheduling option has been considered in [24] and compared to the cellular DPC approach [23]. It is assumed that only one user in a cluster [24] or in a cell [87] is selected at any time instant, which provides the highest throughput. Users close to the cluster center or base stations are more likely to be served because of their small pathloss and less inference from other cells. The multiuser scheduling diversity is analyzed in [24].
- SDMA: Single user per BTS (or N users per BTS). Compared to TDMA where only one user is served in a cluster at a time, the spectral efficiency may be improved by more advanced scheduling solutions where a collection of users are adaptively served with SDMA, whose sum throughput is maximized. A Greedy scheduling algorithm is proposed as follows. At the initialization, each cluster selects one user with the highest throughput, assuming no interference. Then sequentially, each cluster activates one more user that generates the highest sum throughput of the entire system. The newly activated user is cooperatively served with other users in the same cluster with the proposed cellular BD precoding, and acts as co-channel interference to other clusters. This process is performed from cluster 1 to cluster N , until the sum throughput starts to decrease.

5.4.3 Multi-mode Switching

Multi-mode switching is another interesting topic in the cellular MIMO context to determine the number of streams of mobile users adaptively. A possible solution is to follow the greedy allocation approach. At a time instant, one more data stream is allocated to the optimal user that generates the highest sum throughput with other cells and clusters. This process is repeated until the sum throughput starts to decrease.

5.5 Conclusions

In this chapter, coordinated multi-cell MIMO with cellular BD is studied. The core idea is to apply BD across multiple collaborated base stations to balance the interference in the cellular network, while optimizing a certain performance metric. Novel BD precoder design is proposed to address the individual power constraint per BS. Future research topics of cooperative base station transmission in cellular MIMO networks are discussed under the cellular BD framework.

Chapter 6

Conclusions

MIMO multi-antenna technology can significantly improve the capacity and link robustness of wireless communication. In this dissertation, the application of MIMO antenna systems in a multiuser environment is studied. The merits of this dissertation are to provide novel physical layer MIMO transmission techniques in the single-cell broadcast channel and in the multi-cell channel as a means to improve the spectral efficiency and signal quality of future wireless networks. Various signal processing algorithms are proposed to address the interference inherent in a multiuser MIMO system, to offer high capacity, enhance the ability to mitigate interference, and improve the robustness against channel fading.

Transmit precoding with selection diversity. Transmit precoding for the single-cell MIMO broadcast channel is studied. Advance transmit selection diversity techniques are proposed to use extra transmit antennas, beyond the minimum required for interference cancellation, to improve the diversity performance of all users. The proposed techniques can lead to significant diversity gain and error performance improvements, which translate to enhanced robustness against fading. Efficient antenna selection algorithms are proposed, which greatly reduce the computational complexity.

Joint user and antenna selection for MIMO broadcast channel. Multi-mode switching is investigated for MIMO broadcast channel to adaptively adjust the number of streams of mobile users, exploiting multi-mode switching diversity and enhancing the spectral efficiency. Joint user and antenna selection, as a suboptimal multi-mode switching scheme, is investigated due to its various advantages in practical operation. To avoid the computational complexity of brute-force search, several low-complexity user and receive an-

tenna selection algorithms are proposed to substantially reduce the computational burden, making multiuser multi-mode technique a practical scheme for spectral efficiency improvement in a multiuser MIMO system.

Power Control for Uplink Cellular MIMO. Power control is proposed as an interference-management tool for the uplink of a cellular spatial multiplexing system, to minimize the transmit power and mutual interference subject to a given QoS specification. Novel multi-dimensional power control techniques are proposed which balance the transmission of all users to achieve a fixed SINR threshold. The proposed work incorporates several prior power control schemes as special cases.

Multi-cell Block Diagonalization. Coordinated multi-cell MIMO with cellular BD is introduced. BD for single-cell broadcast channel is generalized to the multi-cell environment to enable collaboration across base stations in transmitting to multiple cells. Enhanced BD precoder design is introduced to address the individual resource constraint per base station. Future research topics on cooperative base station transmission for cellular MIMO are discussed.

The proposed work has novelty in the design of multiuser MIMO communication system, and can be used for future multiuser MIMO communication systems for better throughput and signal quality. For example, the IEEE 802.16/WiMAX standard, defined as the Worldwide Interoperability for Microwave Access, is an emerging standard for enabling the delivery of last mile wireless broadband access as an alternative to cable and DSL. MIMO plays a core role in the standard to meet the high data rate and link robustness requirement. During the last two years in my Ph.D. study, a collaborative project has been carried out between AT&T Laboratories and WNCG to investigate MIMO techniques in the fixed and mobile WiMAX standards. A MATLAB-based link level simulator is developed to evaluate performance of various MIMO techniques, such as open-loop MIMO spatial multiplexing, space-time codes, closed-loop MIMO linear precoding, code-book based

limited-feedback MIMO. Two publications have appeared and been submitted to the *IEEE Communications Magazine* to demonstrate the spectral efficiency improvement enabled by MIMO. The proposed multi-user techniques in this dissertation can be applied in future WiMAX standards (e.g., 802.16m) to incorporate SDMA transmission mode, providing further improved data rate and link robustness.

Appendix

For simplicity of notation, denote

$$\mathbf{z}_k = \sum_{j \neq k} \sqrt{\frac{P_j d_{k,j}^{-\rho} \chi_{k,j}}{P_k d_{k,k}^{-\rho} \chi_{k,k}}} \mathbf{H}_{k,j} \mathbf{x}_j, \quad \mathbf{R}_{\mathbf{z}_k} = E(\mathbf{z}_k \mathbf{z}_k^\dagger) = \sum_{j \neq k} \frac{P_j d_{k,j}^{-\rho} \chi_{k,j}}{P_k d_{k,k}^{-\rho} \chi_{k,k}} \mathbf{H}_{k,j} \mathbf{H}_{k,j}^\dagger, \quad (1)$$

$$\tilde{\mathbf{n}}_k = \sqrt{\frac{N_t}{P_k d_{k,k}^{-\rho} \chi_{k,k}}} \mathbf{n}_k, \quad \mathbf{R}_{\tilde{\mathbf{n}}_k} = E(\tilde{\mathbf{n}}_k \tilde{\mathbf{n}}_k^\dagger) = \frac{N_t \sigma_n^2}{P_k d_{k,k}^{-\rho} \chi_{k,k}}. \quad (2)$$

The estimate $\hat{\mathbf{x}}_k$ is given as $\hat{\mathbf{x}}_k = \mathbf{G}_k \mathbf{y}_k$ and the estimation error matrix with the MMSE receiver is given as [10]

$$\Sigma_{\mathbf{x}_k} = \left(\mathbf{H}_{k,k}^\dagger (\mathbf{R}_{\mathbf{z}_k} + \mathbf{R}_{\tilde{\mathbf{n}}_k})^{-1} \mathbf{H}_{k,k} + \mathbf{I} \right)^{-1}. \quad (3)$$

The minimum post-processing SINR of the k th user is bounded as

$$\begin{aligned} \gamma_{k,\min} &= \min_{1 \leq i \leq N_t} \gamma_{k,i} \\ &= \frac{1}{\max_i \left\{ \left(\mathbf{H}_{k,k}^\dagger (\mathbf{R}_{\mathbf{z}_k} + \mathbf{R}_{\tilde{\mathbf{n}}_k})^{-1} \mathbf{H}_{k,k} + \mathbf{I} \right)^{-1} \right\}^{(i,i)}} - 1 \end{aligned} \quad (4)$$

$$= \frac{1}{\max_{\mathbf{z}=\mathbf{e}_i, i=1, \dots, N_t} \mathbf{z}^\dagger \left(\mathbf{H}_{k,k}^\dagger (\mathbf{R}_{\mathbf{z}_k} + \mathbf{R}_{\tilde{\mathbf{n}}_k})^{-1} \mathbf{H}_{k,k} + \mathbf{I} \right)^{-1} \mathbf{z}} - 1 \quad (5)$$

$$\geq \frac{1}{\max_{\|\mathbf{z}\|_F^2=1} \mathbf{z}^\dagger \left(\mathbf{H}_{k,k}^\dagger (\mathbf{R}_{\mathbf{z}_k} + \mathbf{R}_{\tilde{\mathbf{n}}_k})^{-1} \mathbf{H}_{k,k} + \mathbf{I} \right)^{-1} \mathbf{z}} - 1 \quad (6)$$

$$\begin{aligned} &= \frac{1}{\mu_{\max} \left(\left(\mathbf{H}_{k,k}^\dagger (\mathbf{R}_{\mathbf{z}_k} + \mathbf{R}_{\tilde{\mathbf{n}}_k})^{-1} \mathbf{H}_{k,k} + \mathbf{I} \right)^{-1} \right)} - 1 \\ &= \mu_{\min} \left(\mathbf{H}_{k,k}^\dagger (\mathbf{R}_{\mathbf{z}_k} + \mathbf{R}_{\tilde{\mathbf{n}}_k})^{-1} \mathbf{H}_{k,k} + \mathbf{I} \right) - 1 \\ &= \mu_{\min} \left(\mathbf{H}_{k,k}^\dagger (\mathbf{R}_{\mathbf{z}_k} + \mathbf{R}_{\tilde{\mathbf{n}}_k})^{-1} \mathbf{H}_{k,k} \right) + \mu_{\min}(\mathbf{I}) - 1 \\ &= \frac{1}{\mu_{\max} \left(\left(\mathbf{H}_{k,k}^\dagger \mathbf{H}_{k,k} \right)^{-1} \mathbf{H}_{k,k}^\dagger (\mathbf{R}_{\mathbf{z}_k} + \mathbf{R}_{\tilde{\mathbf{n}}_k}) \mathbf{H}_{k,k} \left(\mathbf{H}_{k,k}^\dagger \mathbf{H}_{k,k} \right)^{-1} \right)} + 1 - 1 \\ &= \frac{P_k d_{k,k}^{-\rho} \chi_{k,k}}{\mu_{\max} \left(\sum_{j \neq k} P_j d_{k,j}^{-\rho} \chi_{k,j} \mathbf{\Omega}_{k,j,1} + N_t \sigma_n^2 \mathbf{\Omega}_{k,j,2} \right)}. \end{aligned} \quad (7)$$

The factor -1 in step (4) is to remove the estimation bias [65], and \mathbf{e}_i in (5) denotes the i th column of a $N_t \times N_t$ identity matrix. Step (6) follows the Rayleigh-Ritz theorem [47], which has widely used in deriving a SNR bound for MIMO systems [63, 71]

Bibliography

- [1] A. Agrawal, J. G. Andrews, J. M. Cioffi, and T. Meng, "Iterative power control for imperfect successive interference cancellation," *IEEE Trans. on Wireless Communications*, vol. 4, no. 3, pp. 878–884, May 2005.
- [2] M. Airy, A. Forenza, and R. W. Heath, Jr., "Nested linear/lattice codes for structured multiterminal binning," in *Proc., IEEE Globecom*, vol. 6, Dallas, TX, Nov. 2004, pp. 3942–3946.
- [3] M. Airy, S. Shakkottai, and R. W. Heath Jr., "Spatially greedy scheduling in multi-user MIMO wireless systems," in *Proc., IEEE Asilomar Conf. on Signal, Systems, and Computers*, vol. 1, Pacific Grove, CA, USA, Nov. 2003, pp. 982–986.
- [4] S. M. Alamouti, "A simple transmit diversity technique for wireless communications," *IEEE Journal on Sel. Areas in Communications*, vol. 16, no. 8, pp. 1451–1458, Oct. 1998.
- [5] J. G. Andrews, "Interference Cancellation for Cellular Systems: A Contemporary Overview," *IEEE Communications Magazine*, vol. 12, no. 2, pp. 19–29, Apr. 2005.
- [6] D. Asztely, "On antenna arrays in mobile communication systems: fast fading and gsm base station algorithms," Tech. Report IR-S3-SB-9611, Royal Inst. of Tech., Stockholm, Sweden, Mar. 1996.
- [7] M. Bengtsson, "A pragmatic approach to multi-user spatial multiplexing," in *Proc. IEEE Sensor Array and Multichannel Signal Processing Workshop.*, Aug. 2002, pp. 130–134.
- [8] R. S. Blum, J. H. Winters, and N. R. Sollenberger, "On the capacity of cellular systems with MIMO," *IEEE Communications Letters*, vol. 6, pp. 242–244, June 2002.
- [9] A. Bourdoux and N. Khaled, "Joint TX-RX optimization for MIMO-SDMA based on a space constraint," in *Proc., IEEE Veh. Technology Conf.*, vol. 48, no. 3, Mar. 2002, pp. 611–627.
- [10] S. Boyd, "Course Note - EE 363," *Stanford University, Stanford, CA*, 2003.
- [11] D. R. Brown, "Resource allocation for cooperative transmission in wireless networks with orthogonal users," *Proc., IEEE Asilomar Conf. on Signal, Systems, and Computers*, vol. 2, pp. 1473–1477, Nov. 2004.

- [12] G. Caire and S. Shamai, "On the achievable throughput of a multiantenna Gaussian broadcast channel," *IEEE Trans. on Info. Theory*, vol. 49, no. 7, pp. 1691–1706, July 2003.
- [13] S. Catreux, P. F. Driessen, and L. J. Greenstein, "Simulation results for an interference-limited multiple-input multiple-output cellular systems," *IEEE Communications Letters*, vol. 4, pp. 334–336, Nov. 2000.
- [14] R. Chen, J. G. Andrews, and R. W. Heath, Jr, "Multiuser space-time block coded MIMO system with downlink precoding," in *Proc., IEEE Intl. Conf. on Communications*, vol. 5, Paris, France, June 2004, pp. 2689–2693.
- [15] R. Chen, J. G. Andrews, R. W. Heath, Jr., and A. Ghosh, "Uplink power control for MIMO cellular systems," in *Proc., IEEE Globecom*, San Francisco, CA, 2006.
- [16] —, "Uplink power control for multi-cellular MIMO spatial multiplexing systems," *IEEE Trans. on Wireless Communications*, accepted 2006.
- [17] R. Chen, R. W. Heath, Jr., and J. G. Andrews, "Transmit selection diversity for multiuser spatial multiplexing wireless systems," in *Proc., IEEE Globecom*, vol. 4, Dallas, TX, Nov.29-Dec.3 2004, pp. 2625–2629.
- [18] —, "Transmit selection diversity for unitary precoded multiuser spatial multiplexing systems with linear receivers," *IEEE Trans. on Signal Processing*, vol. 55, no. 3, Mar. 2007.
- [19] R. Chen, Z. Shen, J. G. Andrews, and R. W. Heath, Jr., "Low-complexity joint user and antenna selection for multiuser MIMO communication systems with block diagonalization," in *Proc., IEEE International Conf. on Acoustics, Speech, and Sig. Processing*, accepted, 2006.
- [20] —, "Multimode transmission for multiuser MIMO systems with block diagonalization," *IEEE Trans. on Signal Processing*, submitted 2006.
- [21] D. Chizhik, G. J. Foschini, M. J. Gans, and R. A. Valenzuela, "Keyholes, correlations, and capacities of multielement transmit and receive antennas," *IEEE Trans. on Wireless Communications*, vol. 1, no. 2, pp. 361–368, Apr. 2002.
- [22] R. L. Choi and R. D. Murch, "A transmit processing technique for multiuser MIMO systems using a decomposition approach," *IEEE Trans. on Wireless Communications*, vol. 3, no. 1, pp. 20–24, Jan. 2004.
- [23] W. Choi and J. G. Andrews, "The capacity gain from base station cooperative scheduling in MIMO DPC cellular system," in *Proc., IEEE Intl. Symposium on Information Theory*.

- [24] —, “Base station cooperatively scheduled transmission in a cellular MIMO TDMA system,” in *Proc., IEEE Conf. on Inform. Sci. and Systems*, Seattle, WA, June 2006.
- [25] —, “Spatial multiplexing in cellular MIMO-CDMA systems with linear receivers: outage probability and capacity,” *IEEE Trans. on Wireless Communications*, accepted 2006.
- [26] P. S. Chow, J. M. Cioffi, and J. A. C. Bingham, “A practical discrete multi-tone transceiver loading algorithm for data transmission over spectrally shaped channels,” *IEEE Trans. on Communications*, vol. 43, no. 2, pp. 773–775, Feb. 1995.
- [27] D. Coppersmith and S. Winograd, “Matrix multiplication via arithmetic progressions,” *Jour. Symbolic Comput.*, vol. 9, pp. 251–280, Mar. 1990.
- [28] M. Costa, “Writing on dirty paper,” *IEEE Trans. on Info. Theory*, vol. 29, no. 3, pp. 439–441, May 1983.
- [29] H. Dai, A. F. Molisch, and H. V. Poor, “Downlink capacity of interference-limited MIMO systems with joint detection,” *IEEE Trans. on Wireless Communications*, vol. 3, no. 2, pp. 442–453, Mar. 2004.
- [30] H. Dai and H. V. Poor, “Asymptotic spectral efficiency of multicell MIMO systems with frequency-flat fading,” *IEEE Trans. on Signal Processing*, vol. 5, no. 11, pp. 2976–2988, Nov. 2003.
- [31] A. Forenza, D. J. Love, and R. W. Heath, Jr., “Simulation of the spatial covariance matrix,” in *IEEE 802.11N Channel Model Special Committee*, IEEE doc. 802.11-03/821r0, Albuquerque, NM, USA, Nov. 2003.
- [32] A. Forenza, M. R. McKay, R. W. Heath, Jr., and I. B. Collings, “Switching between OSTBC and spatial multiplexing with linear receivers in spatially correlated MIMO channels,” in *Proc., IEEE Veh. Technology Conf.*, vol. 3, May 2006, pp. 1387–1391.
- [33] G. J. Foschini, “Layered space-time architecture for wireless communication in a fading environment when using multiple antennas,” *Bell Labs Technical Journal*, vol. 1, no. 2, pp. 41–59, Autumn 1996.
- [34] G. J. Foschini and Z. Miljanic, “A simple distributed autonomous power control algorithm and its convergence,” *IEEE Trans. on Veh. Technology*, vol. 42, no. 4, pp. 641–646, Nov. 1993.
- [35] A. Ghosh, J. G. Andrews, R. Chen, and D. R. Wolter, “Broadband wireless access with wimax/802.16: Current performance benchmarks and future potential,” *IEEE Communications Magazine*, vol. 43, no. 2, pp. 129–136, Feb. 2005.

- [36] A. Goldsmith, *Wireless Communications*. Cambridge, UK: Cambridge Univ. Press, 2005.
- [37] G. H. Golub and C. F. V. Loan, *Matrix Computations*, 3rd ed. Johns Hopkins Univ., 1996.
- [38] D. A. Gore and A. J. Paulraj, "MIMO antenna subset selection for space-time coding," *IEEE Trans. on Signal Processing*, vol. 50, no. 10, pp. 2580–2588, Oct. 2002.
- [39] A. Gorokhov, D. A. Gore, and A. J. Paulraj, "Receive antenna selection for MIMO flat-fading channels: theory and algorithms," *IEEE Trans. on Info. Theory*, vol. 49, no. 10, pp. 2687–2696, Oct. 2003.
- [40] —, "Receive antenna selection for MIMO spatial multiplexing: theory and algorithms," *IEEE Trans. on Signal Processing*, vol. 51, no. 11, pp. 2796–2807, Nov. 2003.
- [41] A. Grant, S. Hanly, J. Evans, and R. Muller, "Distributed decoding for Wyner cellular systems," in *Australian Communication Theory Workshop*, Newcastle, Australia, Feb. 2004.
- [42] P. S. H. Sampath and A. J. Paulraj, "Redundant filterbank precoders and equalizers. ii: Blind channel estimation, synchronization, and direct equalization," *IEEE Trans. on Signal Processing*, vol. 49, no. 12, pp. 2198–2206, Dec. 2001.
- [43] B. Hassibi, "An efficient square-root algorithm for BLAST," *IEEE Trans. on Signal Processing*, submitted, 2005.
- [44] J. D. Herdtner and E. K. P. Chong, "Analysis of a class of distributed asynchronous power control algorithms for cellular wireless systems," *IEEE Journal on Sel. Areas in Communications*, vol. 18, no. 3, pp. 436–446, Mar. 2000.
- [45] B. M. Hochwald, C. Peel, and A. L. Swindlehurst, "A vector perturbation technique for near-capacity multiantenna multiuser communication - Part II: Perturbation," *IEEE Trans. on Communications*, vol. 51, no. 3, pp. 537–544, Mar. 2005.
- [46] Z. Hong, K. Liu, R. W. Heath, Jr., and A. Sayeed, "Spatial multiplexing in correlated fading via the virtual channel representation," *IEEE Journal on Sel. Areas in Communications*, vol. 21, no. 5, pp. 856–866, June 2003.
- [47] R. A. Horn and C. R. Johnson, *Matrix Analysis*. Cambridge, U.K.: Cambridge Univ. Press.

- [48] A. A. Hutter, E. de Carvalho, and J. M. Cioffi, "On the impact of channel estimation for multiple antenna diversity reception in mobile OFDM system," in *Proc., IEEE Asilomar Conf. on Signal, Systems, and Computers*, vol. 2, Nov. 2000, pp. 1820–1824.
- [49] S. Jafar, G. Foschini, and A. Goldsmith, "PhantomNet: Exploring optimal multicellular multiple antenna systems," in *Proc., IEEE Veh. Technology Conf.*, Sept. 2002, pp. 24–28.
- [50] N. Jindal and A. Goldsmith, "Dirty paper coding vs. TDMA for MIMO broadcast channels," *IEEE Trans. on Info. Theory*, vol. 51, May 2004.
- [51] N. Jindal, W. Rhee, S. Vishwanath, S. A. Jafar, and A. Goldsmith, "Sum-power iterative water-filling for multi-antenna Gaussian broadcast channels," *IEEE Trans. on Info. Theory*, vol. 51, no. 4, pp. 1570–1580, Jan. 2005.
- [52] M. K. Karakayali, G. J. Foschini, and R. A. Valenzuela, "Network coordination for spectrally efficient communications in cellular systems," *IEEE Communications Magazine*, vol. 13, no. 4, pp. 56–61, Aug. 2006.
- [53] J. P. Kermoal, L. Schumacher, K. I. Pedersen, P. E. Mogensen, and F. Frederiksen, "A stochastic MIMO radio channel model with experimental validation," *IEEE Journal on Sel. Areas in Communications*, vol. 20, no. 6, pp. 1211–1226, Aug. 2002.
- [54] D. Kim, "On the convergence of fixed-step power control algorithms with binary feedback for mobile communication systems," *IEEE Trans. on Communications*, vol. 49, no. 2, pp. 249–252, Feb. 2001.
- [55] C. Li, W. Hsu, B. Krishnamachari, and A. Helmy, "A local metric for geographic routing with power control in wireless networks," Sept. 2005.
- [56] D. J. Love and R. W. Heath, Jr., "Multimode precoding for MIMO wireless systems: Part I," *IEEE Trans. on Signal Processing*, vol. 53, no. 10, pp. 3674 – 3687, Oct. 2005.
- [57] M. R. McKay, I. B. Collings, A. Forenza, and R. W. Heath, Jr., "A throughput-based adaptive MIMO-BICM approach for spatially-correlated channels," in *Proc., IEEE Intl. Conf. on Communications*, June 2006.
- [58] F. Meshkati, M. Chiang, H. V. Poor, and S. C. Schwartz, "A game-theoretic approach to energy-efficient power control in multicarrier CDMA systems," *IEEE Journal on Sel. Areas in Communications*, vol. 24, no. 6, pp. 1115–1129, June 2006.

- [59] F. Meshkati, D. Guo, H. V. Poor, and S. C. Schwartz, “A unified approach to energy-efficient power control in large CDMA systems,” *IEEE Trans. on Wireless Communications*, submitted 2005.
- [60] F. Meshkati, H. V. Poor, S. C. Schwartz, and N. B. Mandayam, “An energy-efficient approach to power control and receiver design in wireless data networks,” *IEEE Trans. on Communications*, vol. 53, no. 11, pp. 1885–1894, Nov. 2005.
- [61] A. F. Molisch and M. Z. Win, “MIMO systems with antenna selection,” *IEEE Microwave Magazine*, vol. 50, no. 1, pp. 46–56, Mar. 2004.
- [62] A. F. Naguib, N. Seshadri, and A. R. Calderbank, “Applications of space-time block codes and interference suppression for high capacity and high data rate wireless systems,” in in *Proc. IEEE Asil. Conf. Sig. Sys. and Comp.*, Nov. 1998, pp. 1803–1810.
- [63] R. Narasimhan, “Spatial multiplexing with transmit antenna and constellation selection for correlated MIMO fading channels,” *IEEE Trans. on Signal Processing*, vol. 51, no. 11, pp. 2829–2838, Nov. 2003.
- [64] Z. Pan, K. K. Wong, and T. S. Ng, “Generalized multiuser orthogonal space-division multiplexing,” *IEEE Trans. on Wireless Communications*, vol. 3, no. 6, pp. 1969–1973, Nov. 2004.
- [65] A. Paulraj, “Course Note - EE 492m,” *Stanford University, Stanford, CA*, 2003.
- [66] C. Peel, B. M. Hochwald, and A. L. Swindlehurst, “A vector perturbation technique for near-capacity multiantenna multiuser communication - Part I: Channel inversion and regularization,” *IEEE Trans. on Communications*, vol. 51, no. 1, pp. 195–202, Jan. 2005.
- [67] R. W. Heath, Jr., M. Airy, and A. J. Paulraj, “Multiuser diversity for MIMO wireless systems with linear receivers,” in *Proc., IEEE Asilomar Conf. on Signal, Systems, and Computers*, vol. 2, Pacific Grove, CA, USA, Nov. 2001, pp. 1194–1199.
- [68] R. W. Heath, Jr. and D. J. Love, “Multimode precoding for MIMO wireless systems: Part II,” *IEEE Trans. on Signal Processing*, vol. 53, no. 8, pp. 3042 – 3056, Aug. 2005.
- [69] R. W. Heath, Jr. and A. J. Paulraj, “Linear dispersion codes for MIMO systems based on frame theory,” *IEEE Trans. on Signal Processing*, vol. 50, no. 10, pp. 2429 – 2441, Oct. 2002.
- [70] —, “Switching between diversity and multiplexing in MIMO systems,” *IEEE Trans. on Communications*, vol. 53, no. 6, pp. 962–968, June 2005.

- [71] R. W. Heath, Jr., S. Sandhu, and A. J. Paulraj, "Antenna selection for spatial multiplexing systems with linear receivers," *IEEE Communications Letters*, vol. 5, no. 4, pp. 142–144, Apr. 2001.
- [72] H. Sampath and A. J. Paulraj, "Linear precoding for space-time coded systems with known fading correlations," *IEEE Trans. on Info. Theory*, vol. 48, no. 3, pp. 611–627, Mar. 2002.
- [73] S. Sanayei and A. Nosratinia, "Antenna selection in MIMO systems," *IEEE Communications Magazine*, vol. 42, no. 10, pp. 68–73, Oct. 2004.
- [74] C. U. Saraydar, N. B. Mandayam, and D. J. Goodman, "Pricing and power control in a multicell wireless data network," *IEEE Journal on Sel. Areas in Communications*, vol. 19, no. 10, pp. 1883–1892, Oct. 2001.
- [75] —, "Efficient power control via pricing in wireless data networks," *IEEE Trans. on Communications*, vol. 50, no. 2, pp. 291–303, Feb. 2002.
- [76] A. Scaglione, G. Giannakis, and S. Barbarossa, "Redundant filterbank precoders and equalizers. I: Unification and optimal designs," *IEEE Trans. on Signal Processing*, vol. 47, no. 7, pp. 1988–2006, July 2001.
- [77] —, "Redundant filterbank precoders and equalizers. II: Blind channel estimation, synchronization, and direct equalization," *IEEE Trans. on Signal Processing*, vol. 47, no. 7, pp. 2007–2022, July 2001.
- [78] A. Scaglione, P. Stoica, S. Barbarossa, and G. Giannakis, "Optimal designs for space-time linear precoders and decoders," *IEEE Trans. on Info. Theory*, vol. 50, no. 5, pp. 1051–1064, May 2002.
- [79] S. Shamai and B. Zaidel, "Enhancing the cellular downlink capacity via co-processing at the transmitting end," in *Proc., IEEE Veh. Technology Conf.*, May 2001, pp. 1745–1749.
- [80] S. Shamai(Shitz) and A. D. Wyner, "Information theoretic considerations for symmetric cellular multiple access fading channels: Part I," *IEEE Trans. on Info. Theory*, vol. 43, pp. 1877–1894, Nov. 1997.
- [81] —, "Information theoretic considerations for symmetric cellular multiple access fading channels: Part II," *IEEE Trans. on Info. Theory*, vol. 43, pp. 1895–1911, Nov. 1997.
- [82] S. Shamai(Shitz) and B. M. Zaidel, "Enhancing the cellular downlink capacity via co-processing at the transmitting end," in *Proc., IEEE Veh. Technology Conf.*, vol. 3, Rhodes, Greece, May 6 - 9 2001, pp. 1745–1749.

- [83] M. Sharif and B. Hassibi, "A comparison of time-sharing, DPC, and beamforming for MIMO broadcast channels with many users," *IEEE Trans. on Communications*, vol. 55, no. 1, Jan. 2007.
- [84] Z. Shen, R. Chen, J. G. Andrews, R. W. Heath, Jr., and B. L. Evans, "Low complexity user selection algorithms for multiuser MIMO systems with block diagonalization," *IEEE Trans. on Signal Processing*, vol. 54, no. 9, pp. 2658–2663, Sept. 2006.
- [85] —, "Sum capacity of multiuser MIMO broadcast channels with block diagonalization," *IEEE Trans. on Wireless Communications*, accepted 2006.
- [86] O. Somekh and S. Shamai(Shitz), "Shannon theoretic approach to a Gaussian cellular multiple-access channel with fading," *IEEE Trans. on Info. Theory*, vol. 46, no. 4, pp. 1401–1425, July 2000.
- [87] O. Somekh, O. Simeone, Y. Bar-Ness, and A. M. Haimovich, "Distributed multi-cell zero-forcing beamforming in cellular downlink channels," in *Proc., IEEE Globecom*, San Francisco, CA, Nov. 27-Dec. 1, 2006.
- [88] O. Somekh, B. M. Zaidel, and S. Shamai(Shitz), "Sum rate characterization of joint multiple cell-site processing," *IEEE Trans. on Info. Theory*, submitted, 2005.
- [89] Q. H. Spencer, A. L. Swindlehurst, and M. Haardt, "Zero-forcing methods for downlink spatial multiplexing in multi-user MIMO channels," *IEEE Trans. on Signal Processing*, vol. 52, no. 2, pp. 461–471, Feb. 2004.
- [90] A. Stamoulis, N. AL-Dhahir, and A. R. Calderbank, "Further results on interference cancellation and space-time block codes," in *Proc., IEEE Asilomar Conf. on Signal, Systems, and Computers*, Nov. 2001, pp. 257–261.
- [91] V. Tarokh, H. Jafarkhani, and A. R. Calderbank, "Space-time block codes from orthogonal design," *IEEE Trans. on Info. Theory*, vol. 45, no. 5, pp. 1456–1467, July 1999.
- [92] V. Tarokh, N. Seshadri, and A. R. Calderbank, "Space-time codes for high data rate wireless communication: performance criterion and code construction," *IEEE Trans. on Info. Theory*, vol. 44, no. 2, pp. 744–765, Mar. 1998.
- [93] R. Valenzuela, "Fundamental limits and evolution of broadband wireless access networks," in *2005 Texas Wireless Symposium, Austin*, Austin, TX, Nov. 2005.
- [94] S. Vishwanath, N. Jindal, and A. Goldsmith, "Duality, achievable rates and sum-rate capacity of Gaussian MIMO broadcast channel," *IEEE Trans. on Info. Theory*, vol. 49, no. 10, pp. 2658–2668, Oct. 2003.

- [95] P. Viswanath and D. N. C. Tse, “Sum capacity of the vector Gaussian broadcast channel and uplink-downlink duality,” *IEEE Trans. on Info. Theory*, vol. 49, no. 8, pp. 1912–1921, Aug. 2003.
- [96] H. Viswanathan, S. Venkatesan, and H. Huang, “Downlink capacity evaluation of cellular networks with known-interference cancellation,” *IEEE Journal on Sel. Areas in Communications*, vol. 21, no. 5, pp. 802–811, June 2003.
- [97] H. Weingarten, Y. Steinberg, and S. Shamai (Shitz), “The capacity region of the Gaussian MIMO broadcast channel,” in *Proc., IEEE Intl. Symposium on Information Theory*, June 2004, p. 174.
- [98] K. K. Wong, R. D. Murch, and K. B. Letaief, “A joint-channel diagonalization for multiuser MIMO antenna systems,” *IEEE Trans. on Wireless Communications*, vol. 2, no. 4, pp. 773–786, July 2003.
- [99] A. D. Wyner, “Shannon theoretic approach to a Gaussian cellular multiple-access channel,” *IEEE Trans. on Info. Theory*, vol. 40, pp. 1713–1727, Nov. 1994.
- [100] M. Xiao, N. B. Shroff, and E. K. P. Chong, “A utility-based power control scheme in wireless cellular systems,” *IEEE/ACM Trans. on Networking*, vol. 11, no. 2, pp. 210–221, Apr. 2003.
- [101] R. D. Yates, “A framework for uplink power control in cellular radio system,” *IEEE Journal on Sel. Areas in Communications*, vol. 13, no. 7, pp. 1341–1347, Sept. 1995.
- [102] T. Yoo and A. Goldsmith, “Optimality of zero-forcing beamforming with multiuser diversity,” in *Proc., IEEE Intl. Conf. on Communications*, 2005.
- [103] W. Yu and J. M. Cioffi, “Trellis precoding for the broadcast channel,” in *Proc., IEEE Globecom*, San Antonio, TX, Nov. 2001, pp. 1344–1348.
- [104] ———, “Sum capacity of Gaussian vector broadcast channels,” *IEEE Trans. on Info. Theory*, vol. 50, no. 9, pp. 1875–1892, Sept. 2004.
- [105] W. Yu, G. Ginis, and J. M. Cioffi, “Distributed multiuser power control for digital subscriber line,” *IEEE Journal on Sel. Areas in Communications*, vol. 20, no. 5, pp. 1105–1115, June 2002.
- [106] W. Yu, W. Rhee, S. Boyd, and J. Cioffi, “Iterative water-filling for Gaussian vector multiple-access channels,” *IEEE Trans. on Info. Theory*, vol. 50, no. 1, pp. 145–152, Jan. 2004.
- [107] R. Zamir, S. Shamai, and U. Erez, “Nested linear/lattice codes for structured multiterminal binning,” in *Proc., IEEE Intl. Conf. on Communications*, vol. 5, Paris, France, June 2004, pp. 2689–2693.

- [108] H. Zhang, H. Dai, and Q. Zhou, “Base station cooperation for multiuser MIMO: Joint transmission and BS selection,” in *Proc., IEEE Conf. on Inform. Sci. and Systems*, Princeton University, March 17-19, 2004.
- [109] L. Zheng and D. Tse, “Diversity and multiplexing: A fundamental tradeoff in multiple antenna channels,” *IEEE Trans. on Info. Theory*, vol. 49, no. 5, pp. 1073–1096, May 2003.
- [110] X. Zhu and R. D. Murch, “Performance analysis of maximum likelihood detection in a MIMO antenna system,” *IEEE Communications Letters*, vol. 50, no. 2, pp. 187–191, Feb. 2002.

Vita

Runhua Chen received the B.S. in electrical engineering from Tsinghua University, China, in 2000, and the M.Phil. in electrical engineering from The Hong Kong University of Science and Technology (HKUST) in 2002. Since 2003 he has been pursuing his Ph.D. degree at the department of Electrical and Computer Engineering, The University of Texas at Austin.

In the summer of 2004 and 2005 he interned at the SBC Laboratories, Inc. (now AT&T Laboratories, Inc.), where he was actively involved in the investigation of high-speed fixed wireless systems based on WiMAX/802.16. In the summer of 2006 he interned at the DSPS R&D Center, Texas Instruments, where he investigated link adaptation for MIMO spatial multiplexing systems in 3GPP LTE. His research interests include physical layer transmission techniques for MIMO-OFDM, multiuser MIMO precoding, power control and cooperative MIMO systems.

Permanent address: 1801 S. Lakeshore Blvd 293
Austin, Texas 78741-1266

This dissertation was typeset with \LaTeX^\dagger by the author.

[†] \LaTeX is a document preparation system developed by Leslie Lamport as a special version of Donald Knuth's \TeX Program.